UNIVERSIDAD AUTÓNOMA DE BARCELONA

Departamento de Ciencia Animal y de los Alimentos

Facultad de Veterinaria

CENTRO DE INVESTIGACIÓN EN AGRIGENÓMICA

Departamento de Genética Animal

GENETIC BACKGROUND OF HEREDITARY CUTANEOUS HYALURONOSIS AND FAMILIAL SHAR PEI FEVER

Verónica Lucía Martínez Díaz

Ph.D Thesis

November 2014

La Dra. **Laura Altet Sanahujes,** Directora Científica en Vetgenomics S.L.

Y

El Dr. **Lluis Ferrer i Caubet,** catedrático del Departamento de Medicina y Cirugía Animal de la Universidad Autónoma de Barcelona

CERTIFICAN:

Que **Verónica Lucía Martínez Díaz** ha realizado bajo su dirección el trabajo de investigación titulado "Genetic Background of Hereditary Cutaneous Hyaluronosis and Familial Shar Pei Fever" para obtener el grado de doctor por la Universidad Autónoma de Barcelona.

Que este trabajo se ha llevado a cabo en el Departamento de Ciencia Animal y de los Alimentos de la Facultad de Veterinaria de la Universidad Autónoma de Barcelona.

Bellaterra, 30 de Septiembre de 2014

Dra. Laura Altet Sanahujes Dr. Lluís Ferrer i Caubet

“Cuando el misterio es demasiado impresionante,

es imposible desobedecer”

- El Principito -

CONTENTS

SUMMARY

Shar Pei dogs have a breed defined wrinkled skin phenotype (now known as Hereditary Cutaneous Hyaluronosis-HCH) and a genetic disorder called Familial Shar Pei fever (FSF) which is thought to be caused by an excess in Hyaluronic Acid (HA). The genetic origin is described as a regulatory mutation (Copy number variation) located upstream of the HA synthesizing gene (*HAS2*) in chromosome 13. A transgenic mouse model with increased copies of HAS2 was constructed to emulate and confirm the phenotype described in Shar Peis. We successfully obtained 5 transgenic founder mice from which the colony was formed. A total of 80 F2 mice were included in the study: 40 Transgenic (TG) (20 adult and 20 young) and 40 wild type (WT) used as controls (20 adult and 20 young). Phenotype *in vivo* analysis included visual inspection of possible skin alterations (laxity, folds, wrinkles) and body temperature (microchip implant system). Copy number (CN) determination was performed using the comparative cycle threshold (CT) relative quantification method ($2^{-\Delta\Delta Ct}$) with RT-qPCR. *Post mortem* analysis included complete blood count, skin HAS2 expression [using the endogenous *HAS2* gene as a reference gene and *HAS2 construction* (transgene) as target], histology of parenchymal organs and skin and the determination of serum HA concentration. After CN determination, TG mice were divided into three groups: i) low CN: <20 copies, ii) medium CN; 21-69 copies and iii) High CN: >70 copies.

Even though we successfully created a transgenic mouse which expressed *HAS2,* over produced HA and that in some aspects resembled the phenotype of Shar Pei dogs, we couldn't emulate the Shar Peis characteristic wrinkled skin, nor did we have mice with febrile episodes. With all these results, it is difficult to sustain that the wrinkled skin phenotype and febrile disorder of the Shar Pei are only consequence of an increased synthesis of HA.

Results of the transgenic mice generated in this thesis corroborate that many questions regarding the genetic basis of HCH and FSF remained to be answered and different approaches to insight on these diseases had to be used. Therefore we analyzed other HA degradation pathways such as *HAS2as,* gene which regulates *HAS2* expression as well as HA degradation product routes (Toll Like Receptors 2 and 4) without any significant findings. We also reanalyzed data from the Illumina CanineSNP20 BeadChip (22.362 SNPs) to look for other regions involved in Shar Peis phenotypes. We have found two homozygosity regions in Shar Peis CFA 6 (40,691,228-51,293,708; CanFam2.0) and CF 13 (23,222,643-27,079,420; CanFam2.0). Our results denote a specific haplotype characteristic to Shar Pei dogs in CFA6 which includes 2 genes (*TNFR1* and *MEFV)* related to Familiar Mediterranean Fever in humans and a CNV. We believe that it is important to consider other genomic regions such as that in CFA 6 which harbors many candidate genes to further inquire into the genetic background of these diseases as well as to finally confirm if HCH and FSF are related sharing a common genetic background or if they are two separate entities.

RESUMEN

Los perros de raza Shar Pei tienen dos características fenotípicas propias de la raza que son las arrugas de la piel (ahora conocido como Hialuronosis Cutánea Hereditaria-HCH) y un desorden genético llamado Fiebre Familiar del Shar Pei (FSF) que se cree que es causada por un exceso de Ácido Hialurónico (HA). El origen genético se describe como una mutación reguladora (Variación Número de Copias- CNV) localizada *upstream* del gen que sintetiza HA (*HAS2)* en el cromosoma 13. Se construyó un modelo murino transgénico con mayor número de copias del *HAS2* para emular y confirmar el fenotipo descrito en Shar Peis. Obtuvimos de manera exitosa 5 ratones transgénicos fundadores los cuales sirvieron para formar la colonia. Un total de 80 ratones de la F2 fueron incluidos en el estudio; 40 transgénicos (TG) (20 adultos y 20 jóvenes) y 40 tipo salvaje utilizados como control (20 adultos y 20 jóvenes). El análisis del fenotipo *in vivo* incluyó la inspección visual de posibles alteraciones en la piel (laxitud, pliegues, arrugas) y temperatura corporal (sistema basado implantación de microchip). Se determinó el número de copias (CN) utilizando el método de cuantificación relativa ($2^{-\Delta\Delta Ct}$) con una RT-qPCR. El análisis *post mortem* incluyó hemograma completo, análisis de expresión de *HAS2* en piel [utilizando el *HAS2* murino endógeno como referencia y el *HAS2constructo* (transgen) como diana], histología de órganos parenquimatosos y piel además de la determinación de concentración de HA en suero sanguíneo. Después que se determinó el CN, los ratones TG fueron divididos en tres grupos: i) bajo CN: <20 copias, ii) medio CN: 21-69 copias y iii) alto CN: >70 copias.

Aunque de manera exitosa conseguimos crear un ratón transgénico que expresaba *HAS2*, sobre producía HA y que en algunos aspectos semejaba el fenotipo de los Shar Peis, no pudimos emular la piel arrugada característica del Shar Pei ni tuvimos ratones con episodios febriles. Con todos estos resultados, es difícil sustentar el hecho de que el fenotipo de las arrugas de la piel del Shar Pei y el desorden febril sean consecuencia única de un aumento en la síntesis de HA.

Los resultados obtenidos de los ratones transgénicos generados en esta tesis corroboran que quedan muchas preguntas respecto a las bases genéticas de HCH y FSF por contestar y que diferentes enfoques para averiguar el porqué de estas enfermedades son necesarios. Es por esta razón que analizamos otras vías de degradación de HA como la función del *HAS2as*, un gen que regula la expresión de *HAS2*, además de los Toll Like Receptors 2 y 4, sin encontrar cambios significativos. También reanalizamos datos de chip de Illumina, CanineSNP20 BeadChip (22.362 SNPs) para buscar regiones de homocigosis involucradas en el fenotipo del Shar Peis. Encontramos dos regiones de homocigosis en los CFA6 6 (40, 691, 228-51, 293, 708 CanFam2.0) y CFA 13 (23, 222, 643-27, 079, 420 CanFam2.0). Nuestros resultados indican un haplotipo específico característico de los Perros Shar Peis en el CFA6 el cual incluye dos genes (*TNFR1* y *MEFV)* relacionados con la Fiebre Familiar Mediterránea en humanos y un CNV. Creemos que es importante considerar otras regiones en el genoma como la región del CFA6, la cual alberga muchos genes candidatos, para continuar indagando sobre las bases genéticas de estas enfermedades además de finalmente intentar confirmar si la HCH y la FSF están relacionados al compartir el mismo fondo genético o si son dos entidades distintas.

LIST OF TABLES

LIST OF FIGURES

ABREVIATIONS

a.m	*Ante meridian*
AOSD	Adult onset Still´s disease
asRNA	Antisense RNA
AIDs	Auto Inflammatory Diseases
AS	Ankylosing spondylitis
ATG	Adult transgenic
AWT	Adult wild type
bp	Base pair
CAPS	Cryopyrin-Associated Periodic Syndromes
CBC	Complete Blood Count
CD44	Cluster of Differentiation 44
cDNA	Complementary Deoxyribunocleic acid
CFA	Chromosome
chr	Chromosome
CNV	Copy number variant
CSLM	Confocal scanning laser microscopy
Da	Dalton
DAMP	Damage associated molecular pattern
DIC	Disseminated intravascular coagulation
F0	Founder
F1	First generation
F1TR	Transmission rate in F1
F2	Second generation
F2TR	Transmission rate in F2
FCAS	Familial cold associated syndrome
FMF	Familial Mediterranean Fever
FSF	Familial Shar Pei Fever
GAGs	Glycosaminoglycans
GFP	Green fluorescent protein
GWAS	Genome wide association studies
H&E	Haematoxylin and eosin stain
HA	Hyaluronic Acid, Hyaluronan
HAS	Hyaluronan Synthases
HAS2	Hyaluronan Synthase 2
HAS2as	Hyaluronan Synthase 2 Antisense
HCH	Hereditary Cutaneous Hyaluronosis
HIDS	Hyperimmunoglobulinemia-D with Periodic Fever Syndrome
HRFS	Hereditary Recurrent Fever Syndromes
HMWHA	High Molecular Weight Hyaluronic Acid/Hyaluronan
HYALS	Hyaluronidases
IGF-1	Insulin-like growth factor 1
IL-1	Interleukin 1
IL-6	Interleukin 6
IL-1ß	Interleukin 1 beta
iNOS	Calcium-insensitive nitric oxide synthases
kb	Kilo base
LMWHA	Low Molecular Weight Hyaluronic Acid/Hyaluronan

LYVE-1	Lymphatic vessel endothelial hyaluronan receptor
m	*Meridian*
MAF	Minor allele frequency
MEFV	Mediterranean Fever gene
mL	Milliliter
mRNA	Messenger RNA
MWS	Muckle-Wells syndrome
NIH	National Institutes of Health
NF-κβ	Nuclear factor kappa-beta
NLRs	Cytoplasmic NOD-like receptors
NLRP3	NOD-like receptor family pyrin domain containing 3
NOMID	Neonatal onset multisystem inflammatory disease.
nsSNPs	Non- Synonymous Single Nucleotide Polymorphisms
O/N	Over Night
PAMPs	Pathogen-associated molecular patterns
PAPA	Pyogenic Arthritis with Pyoderma Grangrenosum and Acne
PFAPA	Periodic Fever with Aphthous Stomatitis, Pharyngitis and Cervical Adenopathy
p.m	*post meridian*
PRRs	Pattern Recognition receptors
qPCR	Real-Time Polymerase chain reaction
-RT	Reverse transcriptase minus controls
R^2	Coefficient of determination
RBC	Red Blood Cells
RIN	RNA Integrity number
RHAMM	Hyaluronan-mediated motility receptor
rpm	Revolutions per minute
RT-PCR	Reverse transcriptase polymerase chain reaction
RT-qPCR	Reverse transcriptase real time polymerase chain reaction
SAA	Serum amyloid A protein
SHS	Swollen hock syndrome
SNP	Single Nucleotide polymorphism
SPAID	Shar Pei Auto inflammatory Disease
STSS	Streptococcal Toxic Shock Syndrome
TG	Transgenic
TNF-α	Tumor necrosis factor alpha
TLRs	Toll Like Receptors
TLR2	Toll like receptor 2
TLR4	Toll like receptor 4
TRAPS	Tumor Necrosis Factor Receptor-Associated Periodic Syndrome
UTRs	Untranslated regions
WBC	White blood cells
YTG	Young transgenic
YWT	Young wild type

INTRODUCTION

The Shar Pei Breed

Origin and History

Various theories regarding the Shar Pei´s history exists and its history is very difficult to trace since many records were lost during the communist era. This breed is thought to come from the small village of Dali in the Guangdong province of southern China. The Shar Pei breed probably has existed since the Han Dynasty (200 B.C.-220 A.D.). Statues of "tomb dogs" showing a strong resemblance to the breed (brow wrinkles, curled tail, height and body type) have been discovered in various burial sites **(Figure 1)** as well as a 13th century Chinese manuscript that has been translated describing a wrinkled dog. No other corroborating written history of the ancestry of the Shar Pei breed has been really demonstrated (Redditt, 1992). Genetic studies have also demonstrated that the Shar Pei is one of the fourteen most ancient dog breeds and it is believed to have split from common ancestors earlier when comparing to other breeds (Parker *et.al.,* 2004). The Shar Peis were the working breed of peasant Chinese farmers, carrying out roles of guard dog, wild boar hunter, herding and family dog characteristics for which they were first bred. Because of its physical appearance; wrinkled skin, short and abrasive coat, sunken eyes and small ears, it is also commonly accepted that this dog was used and bred for fighting (Staff American Kennel Club, 1998).

Figure 1. Statues of "tomb dogs" from the Han Dynasty. Notice curled tail, wrinkled skin on neck and small ears which resembles current Shar Pei Dogs. ("Han Dynasty Dogs" n.d retrieved May 25, 2014 from https://www.flickr.com/photos/lauraelaine/galleries/72157624911486872/)

The original or "Traditional" Shar-Pei experienced two major periods of genes mixing explaining why currently two separate lines exist; Chinese (also known as *Traditional* or *Bonemouth*) **(Figure 2)** and American (also known as *Meatmouth*) **(Figure 3).** The first period of gene mixing or "The Grand Mixing" occurred in Hong Kong during the 18th-19th century, a period in which dog fights were a common way of entertainment. It was during this time, when the British established trade relationships with the South of China along the Pearl River delta, that breeding experiments aimed to create a dog with a fighting temperament were

carried out, giving origin to the “Chinese Fighting dog” crossbreeding local Shar Pei dogs with European fighting dogs. The Chinese Fighting dog had the Shar Pei´s harsh coat and wrinkled skin which offered it and advantage when fighting with other dogs since it could wriggle out of its opponent’s jaws during fighting and even turn its back to bite back. No care for the maintenance of the traditional purebred Shar Pei breed was given at this time (Ditto, 2006).

After the People´s Republic of China was established in 1949, the Communist party declared dogs a "symbol of decadence and a criminal extravagance at a time of food shortages" and declared dogs and other pets a luxury. Mao Tse Tung declared that pets should be a status of the privileged since only they could afford to pay such heavy taxes. This resulted in dog breeding and ownership being banned, leading to the almost extinction of many dog breeds, including the Chinese Fighting Dog (Ditto, 2006; McDonald Brearley, 1991; Redditt, 1992). Some traditional Shar Pei dogs remained on isolated British occupied villages such as Macau, Taiwan and Hong Kong. Dog fanciers attempted to preserve the last specimens of the Traditional Shar Pei breed by exportation of the breed to other parts of the world (Staff American Kennel Club, 1998).

Matgo Law, was one of the first Shar Pei enthusiasts to export Chinese Fighting dogs and Traditional Shar Peis to the United States. “Lucky”, son of sire: *Blue Mynah of Taileh* and dam: *Jones' Chow Chow* was the first Chinese fighting dog to have entered America in 1966 (“Chinese Shar-Pei,” n.d retrieved 25 May, 2014 from http://www.chinese-sharpei.com/history/time.htm; Redditt, 1989). “Lucky”, was registered at the ADBA (American Dog Breeders Association) as a Chinese Fighting Dog in 1970. Fourteen Chinese Fighting dogs were registered by 1971, and in 1973, Matgo Law, the leader of the “Save the Shar Pei” movement, wrote a letter that was published in the April 1973 issue of DOGS Magazine (Collins, 1982) inviting dog fanciers in the United States to help save the Shar Pei from extinction in China. The American fanciers renamed the breed as "Shar Pei" which literally means "sand-skin", referring to the two distinctive qualities of the coat: roughness and shortness. They also decided to form a national dog club and registry; the Chinese Shar Pei Club of America, Inc. (CSPCA), which held its first organizational meeting in 1974 formulating requirements of the American Shar Pei breed, which was officially recognized by the American Kennel Club in June 1992 (Staff American Kennel Club, 1998; William, 1982). Americans fancied the dog´s wrinkled skin, and mainly bred these dogs for this characteristic creating difference in the breed´s standard.

The “great meat mouth gene flush” was a period when large quantities of American Shar Peis (*Meatmouth*) were shipped back to Dali in order to "improve" the breed. In 1988 a breed standard was finalized and the breed was accepted in to the Miscellaneous Class of the American Kennel Club. In the early 1990s the Shar Pei Hong Kong Club formed an affiliation with the Hong Kong Kennel Club and breed standards for both the “*Bonemouth*” and “*Meatmouth*” Shar Pei dogs were created. It can be said that since then, two lines of the Shar Pei breed exist: Traditional (*Bonemouth*) and American (*Meatmouth*) (“Chinese Shar-Pei,” n.d retrieved 25 May, 2014 from http://www.chinese-sharpei.com/history/time.htm; Redditt, 1989).

Breed Standards

As mentioned before, two lines of the breed exist and each has its own standards: the Traditional standard also known as "*Bonemouth*" **(Figure 2),** and the American Standard **(Figure 3)** also known as "*Meatmouth*". Few characteristics are present in both standards **(Table 1)** which are a dark blue/purple tongue as well as solid coat colors like red or black. To date, because of uncontrolled breeding, a mix from both Traditional and American standards exists. A direct comparison from both breed types can be seen in **Figure 4**.

Figure 2. Example of Traditional Shar Peis. Notice small wrinkles on forehead, short bristly coat and "Roof Tile Mouth" (Pictures provided by Kikka Posti)

Figure 3. Example of American Shar Pei. Notice heavy wrinkling on head, neck and hind legs and well padded muzzle ("Chinese Shar Pei guide," n.d retrieved 25 May, 2014 from http://www.animalplanet.com/breed-selector/dog-breeds/non-sporting/chinese-shar-pei.html)

Figure 4. Comparison of American" and "Traditional Shar Pei ("Book Cover- El shar-pei de A.K. Nicholas- 1998 Editorial Hispano Europea. Retrieved May 25, 2014 from http://www.fnac.es/mp930124/Shar-pei-el)

Table 1. American and Traditional Shar Pei Breed Standards. ("American Kennel Club Breed Standards," n.d. retrieved May 25, 2014 from http://www.akc.org/breeds/chinese_shar_pei/breed_standard.cfm, and "Traditional Shar Pei," n.d, retrieved May 25, 2014 from http://www.hksharpei.com/index.cfm?id=199742&fuseaction=browse&pageid=154)

Standard stipulation	American Shar Pei (*Meatmouth*)	Traditional Shar Pei (*Bonemouth*)
Origin	U.S.A.	China (Dali-Canton)
Valid original standard	April 14, 1999	January 25, 1994
Utilization	Hunting and watchdog	Hunting and watchdog
Temperament	Calm independent, loyal, affectionate to his family	Active and agile. Calm, independent, loyal and affectionate to people
Height	44 to 51 cm at wither	48.3 to 58.4 cm at wither
Weight	Not specified	18 to 29.5 kg
Head	Rather large in proportion to body	The skull is round and big at the base, but flat and broad at the forehead
Tongue	Bluish-black is preferred. Pink spotted tongue permissible. Solid pink tongue highly undesirable	Bluish-black tongue and gum preferred, pink and spotted only permissible in lighter colored dogs
Back	Dips slightly behind withers; then it rises slightly over loin Croup rather flat	Very strong and straight, with very strong back bone
Tail	Thick and round at the root, tapering to a fine point. May be carried high and curved, carried in tight curl or curved over or to either side of the back	There are several types of tail. The most common are the curl (big or small), and double ring. The tail must be firm and tightly over the hip
Wrinkles	Folds of skin on body in mature dogs highly undesirable except on withers and base of tail, which show moderate wrinkling	In the adult dog pronounced wrinkles are only allowed over the forehead and withers
	Wrinkles on forehead and cheeks continuing to form dewlap	Wrinkles on the forehead must be apparent but must not obstruct the eyes
	The loose skin under the neck should not be excessive	The loose skin around the throat should not be excessive. Excessive skin around the body in adults is most undesirable
	Wrinkles over skull and withers	Slight fold of skin on withers
Coat/Hair	Short, harsh and bristly. The coat is straight and off standing on the body, but generally flat on the limbs. The coat may vary in length from 1cm to 2.5 cm. Brush coat preferred over horse coat	Short, hard, bristly and as straight as possible. Length must not be over 2.5cm long. Horse coat is preferred over brush coat
Muzzle	Broad from root to tip of nose with no suggestion of tapering. Lips and top of muzzle well padded. Bulge at the base of the nose permissible.	The shape of the mouth when viewed from top should either be in the shape of a roundish roof tile commonly known as "Roof Tile Mouth" or with a wide jaw in the shape of a toad's mouth, known as "Toad Mouth".
Ear	Very small, rather thick, equilaterally triangular in shape, slightly rounded at tip and set high on skull with tips pointing towards eyes. Wide apart and close to skull.	Small, thick, equilaterally triangular in shape, slightly rounded at tips. Tips pointing towards eyes and folded to the skull. Wide apart and close to skull.
Eyes	Dark, almond-shaped with a scowling expression. Lighter color permissible in dilute-colored dogs.	Medium sized, almond shaped. As dark as possible. Light colored eyes are undesirable.
Feet	Moderate size, compact, not splayed. Toes well knuckled. Hind feet free from dewclaws.	Moderate size, compact, well padded, toes well knuckled.
Forequarters	Pastern slightly sloping, strong and flexible.	Pasterns slightly sloping, strong and flexible.
Hindquarters	Muscular, strong, moderately angulated. Wrinkles on upper thighs, lower thighs, rear pasterns as well as the thickening of the skin on hocks undesirable. Hocks well let down.	Strong and muscular. Moderately angulated. Hocks well let down.
Color	All solid colors acceptable except white. Tail and rear part of thighs frequently of a lighter color. Darker shading down the back and on the ears permissible.	Solid colors black, blue black, black with a hint of rust brown, red, and fawn. Cream is acceptable but less desirable.

Breed related diseases

Most purebred dog breeds show a very high susceptibility to one or more genetic diseases due to founder effects, breeding practices and reproductive isolation (Cruz & Webster, 2008). Some health problems such as Familial Shar Pei Fever (FSF), entropion, brachicephalyc airway syndrome and dermatitis present in Shar Pei, could be a result of the strong selection for maintaining the heavy folder skin characteristic of this breed. Little did the breeders know that selecting for a desirable trait (skin folds) could have brought problems to the breed that they were trying to recuperate after de communist era. Shar Peis are also predisposed to other diseases which are shown in **Figure 5.**

Figure 5. Diseases related to the Shar Pei breed.

Hyaluronic Acid (HA)

Definition

Hyaluronan (HA) also known as hyaluronic acid or hyaluronate belongs to the family of glycosaminoglycans (GAGs) and was first isolated from the vitreous humor of bovine eyes in 1934 by Karl Meyer and John Palmer (Meyer & Palmer, 1934). HA, is primarily found in the extracellular and pericellular matrix. It is a high molecular weight GAG composed of multiple copies of the disaccharide N-acetyl-D-glucosamine and D-glucoronate connected by β-linkages that can reach 10^7 Daltons (Da) in molecular size (Necas *et.al.,* 2008). The HA polymer can be found in many shapes, sizes and configurations. It can be found in various physiological states, circulating freely, and associated to a specific tissue. HA can also bind to proteins (hyaladherins), and even to itself, with cell surface receptors or with other GAGs. HA can be detected in various tissues and body fluids as studied in higher animals **(Table 2)** (Laurent, T. C. & Fraser, 1986) with varying concentrations. A study carried out in rats indicates that the skin harbors almost 56% of total body HA (Reed *et.al.,* 1988) **(Table 3)**.

Table 2. Concentration of Hyaluronan in tissue and body fluids. (Laurent, T. C., & Fraser, 1986)

Tissue or fluid	Concentration (mg/L)
Rooster comb	7500
Human umbilical cord	4100
Human synovial fluid	1420-3600
Bovine nasal cartilage	1200
Human vitreous body	140-338
Human dermis	200
Rabbit brain	65
Rabbit muscle	27
Human thoracic lymph	8.5-18
Human urine	0.1-0.5
Human serum	0.01-0.1

Table 3. Distribution of Hyaluronan between different organs in the rat. (Reed *et.al.,* 1988)

Organ System	Total Hyaluronan (mg)	Percentage (%)
Whole rat	60.5	100
Skin	33.8	55.9
Muscles	4.69	7.8
Skeleton and supporting structures	16.2	26.8
Intestines and stomach	0.5	0.8
Remaining internal organs	5.25	8.7

Function

HA has many different functions (Necas *et.al.,* 2008; Stern, 2004a). HA promotes cell motility, regulates cell-cell and cell-matrix adhesion, promotes cell proliferation and suppresses cell differentiation; it participates in embryological development and morphogenesis, wound healing, repair and regeneration, (providing a framework for ingrowth of blood vessels and fibroblasts), and inflammation. HA levels increase in response to stress and in tumor progression and invasion. According to its molecular size, HA chains of different lengths have different effects on cell behavior and different roles in the inflammatory response **(Table 4)**. The degradation products of hyaluronan, oligosaccharides and low molecular weight hyaluronan (LMWHA), exhibit pro-angiogenic properties (Mio & Stern, 2002; Necas *et.al.*, 2008) and stimulate inflammatory responses such as up-regulation of cytokines, chemokines and adhesion molecules. These smaller fragments signal the production of Interleukin-1 (IL-1), Tumor Necrosis Factor alpha (TNF-α), Insulin-like growth factor (IGF-1) and calcium-insensitive nitric oxide synthases (iNOS) by macrophages which are pro-inflammatory substances as well. This is why LMWHA is recognized as a danger signal or Damage Associated Molecular Pattern (DAMP) by the pattern recognition receptors (PRRs) of the innate immunity. Short hyaluronan chains can also be generated by degradation of extracellular HA through the action of hyaluronidases or oxidants. In the other hand, High Molecular Weight Hyaluronan (HMWHA) has long hyaluronan chains and cause the opposite effect; inhibiting cell proliferation, supporting tissue integrity and provides anti-inflammatory and anti-angiogenic properties (Stern, 2003).

Table 4. HA size and key functions. (Stern, 2003)

Ha	Function
Low Molecular Weight HA (LMWHA) ~2 X 105 Da	Promotion of cell differentiation and proliferation Suppression of apoptosis Induction of inflammatory chemokines and cytokines Promotion of angiogenesis Transcription of metalloproteinase Up-regulation of heat shock factor-1 Stimulation of tumor neo vascularization
High Molecular Weight HA (HMWHA) ~2 X 106 Da	Promotion of cell quiescence Induction of apoptosis Anti-inflammatory effect Suppression of angiogenesis Immune suppression Promotion of tissue integrity Hydration of tissues

HA contains a large volume of water that expands the extracellular space, it hydrates tissues and in the dermis it is responsible for skin moisture. HA regulates water balance, osmotic pressure and acts as an ion exchange resin by filtering certain molecules to enhance the extracellular domain of cell surfaces (Henry & Duling, 1999). HA also works as a lubricant and

shock absorber in joints, and it is an important structural molecule of the vitreous of the eye, joint fluid, heart, Wharton´s jelly (umbilical cord) and skin (Stern, 2004a).

Synthesis

HA is synthesized by a class of integral membrane proteins called hyaluronan synthases (HAS), of which vertebrates have three types: HAS1, HAS2, and HAS3. Each of these isoforms resides at a different chromosome location suggesting that the *HAS* gene family may have arisen comparatively early in vertebrate evolution by sequential duplication of an ancestral *HAS* gene **(Figure 6)** (Spicer & Mcdonald, 1998). The first event duplicated an ancestral hyaluronan synthase gene to form two genes, which gave rise to the *Has1* and ancestral *Has2* lineages. The ancestral *Has2* gene subsequently duplicated to give rise to the *Has2* and *Has3* genes (Spicer & Mcdonald, 1998).

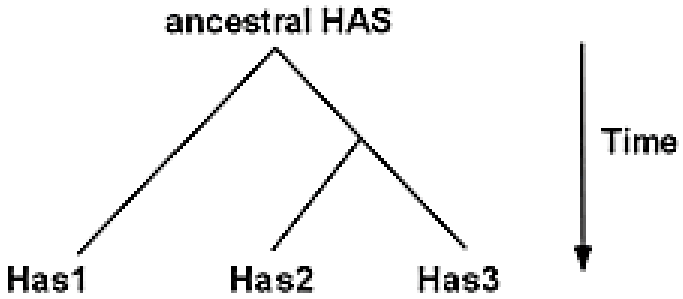

Figure 6. The evolution *HAS* genes. Vertebrate *HAS* gene family arose through two sequential gene duplication events (Andrew P Spicer & Mcdonald, 1998. retrieved May 25, 2014 from http://glycoforum.gr.jp/science/hyaluronan/HA07/HA07E.html)

Two of the main differences between the isoforms are the chain length of the hyaluronan molecules that they produce and the ease with which they can be released from the cell surface **(Figure7)** (Itano *et. al.*, 1999; Stern *et.al.,* 2006). When mammalian cells are stimulated by changes in their immediate environment (cytokines, extracellular matrix proximities), the HAS isoforms respond differently and appear to be under different control mechanisms **(Table 5)**.

Table 5. Role of HAS proteins. (Spicer & Mcdonald, 1998)

HAS	Activity	HA size	Level of synthesis	Possible function	Expressed in…
HAS1	least active	HMWHA ($2{\cdot}10^5$ – $2{\cdot}10^6$ Da)	Low constitutive synthesis	Background levels of HMWHA may have significant effects on tissue structure and volume. It also causes inhibition of cell proliferation.	Many cell types
HAS2	more active	HMWHA ($3{\cdot}10^5$ – >$2{\cdot}10^6$ Da)	Stress-induced synthesis (hypothetical)	HMWHA may have significant effects on tissue structure and volume. It is also involved in the response to stress, developmental and repair processes involving tissue expansion and growth.	During embryonic development; critical function (HAS2-deficient mice died during embryonic development) (Camenisch *et. al*, 2000; Zambrowicz *et.al.,* 1997)
HAS3	most active	LMWHA (<$2{\cdot}10^5$ – $3{\cdot}10^5$ Da) Short chains may be formed by degradation of extra cellular HA	-	LMWHA may contribute to the pericellular matrix or may interact with HA cell surface receptors, triggering of signal transduction cascades. It also stimulates cell proliferation, and is present in inflammatory responses.	Expressed late in embryonic development and in many adult tissues

HA synthesis, different to other GAGs, occurs in the inner face of the cell membrane, polymerizing and translocating at the same time it is being produced, instead of being synthesized by the Golgi enzymes and secreted by normal exocytotic mechanisms (Prehm, 1984).

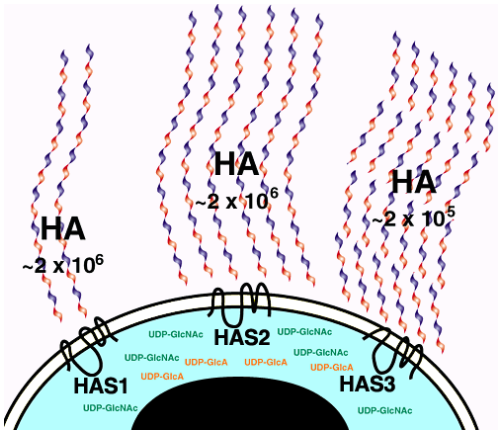

Figure 7. Regulation of hyaluronan amount and chain length by expression of a specific HAS protein. Has1 produces small amounts of HMWHA. Has2 produces significantly more HMWHA. Has3 is the most active of the hyaluronan synthases, yet produces LMWHA. (Spicer & Mcdonald, 1998 retrieved May 24, 2015 from http://glycoforum.gr.jp/science/hyaluronan/HA07/HA07E.html)

HA is present in both the dermis (primary source) where it constitutes ~0.5 mg/g wet tissue and the epidermis (secondary source) where it constitutes ~0.1 mg/g wet tissue *(Pienimaki et. al*, 2001; Toole, 1997). HA synthesis is usually balanced by catabolism, thereby maintaining a constant concentration in the tissue, but in the dermis, the cells actively synthesize more hyaluronan than they can catabolize (Hascall & Laurent, 1997).

HAS2as

Natural antisense RNAs (asRNA) are endogenous transcripts, which are complementary to mRNA sequences of known function (Vanhée-Brossollet & Vaquero, 1998). Natural asRNAs are capable of regulating prokaryotic and eukaryotic gene expression (Knee & Murphy, 1997). Natural antisense RNAs exert their regulatory effects at multiple levels, including transcription, RNA editing, post-transcription, and translation (Knee & Murphy, 1997; Tosic *et.al.,* 1990). By altering the expression of a particular gene, natural asRNAs regulate biological functions, such as development, viral infection, or adaptive responses.

A study by Chao & Spicer (Chao & Spicer, 2005), demonstrated that HAS2as mRNAs reduce HAS2 mRNA levels and HA biosynthesis in HAS2as-transfected cells. Suggesting that HAS2as is a novel and important mechanism in the regulation of HAS2 mRNA levels, HAS2-associated HA biosynthesis and HA-related biological functions *in vivo*.

Degradation

In mammals, the enzymatic degradation of HA results from the action of four types of enzymes: two hyaluronidases (HYAL1 and HYAL2), and two lysosomal enzymes β-glucuronidase, and β-N- acetylglucosaminidase (Stern, 2004a). Throughout the body, these enzymes are found in various forms, intracellularly and in serum. Hyaluronan is mainly degraded by the lymphatic system in lymph node sinuses and lymphatic vessels **(Figure 8)**.

Once it reaches the blood stream, 85-90% of HA is eliminated in the liver by receptor-facilitated uptake and catabolism in the hepatic sinusoidal endothelial cells. The kidneys are responsible for catabolism about 10% of total HA, but excrete 1-2% in urine (Fraser *et. al.*, 1997). In densely structured tissues like bone and cartilage, 20-30% of HA turnover occurs by metabolic degradation *in situ* concurrently with that of collagen and proteoglycans. The tissue half-life ranges from 1-3 days regardless its route of elimination.

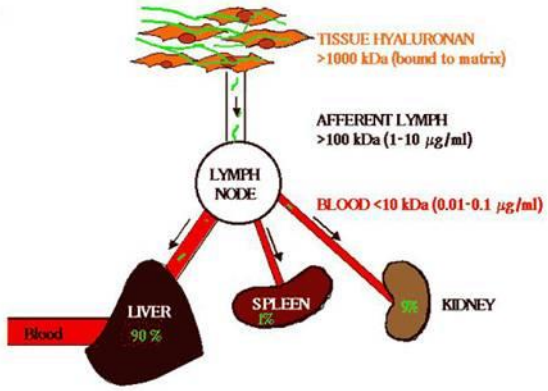

Figure 8. Hyaluronan and the lymphatic system. HMWHA (> 10^6 Da) complexed with proteoglycans in tissues, such as skin, is partly degraded to yield products of 10^5-10^6 Da which enter the afferent lymphatics for further degradation in the lymph nodes. The low molecular weight fragments are carried via efferent lymph to the portal blood and are terminally degraded in liver (90%), and to a lesser extent in spleen (1%) and kidney (9%). (David G. Jackson, 2004 retrieved May 25, 2014 from http://glycoforum.gr.jp/science/hyaluronan/HA28/HA28E.html)

In general, HYAL cleaves high molecular weight HA into smaller oligosaccharides while β- d -glucuronidase and β-N- acetylglucosaminidase further degrade the oligosaccharide fragments by removing non reducing terminal sugars (Leach & Schmidt, 2004) **(Figure 9)**.

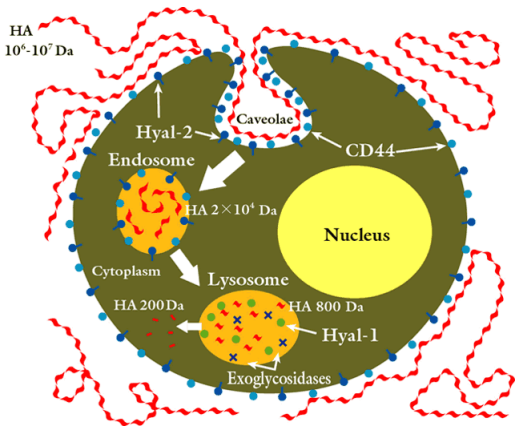

Figure 9. Hyaluronan degradation. (Stern, 2004 retrieved May 3, 2014 from http://www.glycoforum.gr.jp/science/hyaluronan/HA15a/HA15aE.html)

HA cell receptors and degradation products

Cluster of Differentiation 44 (CD44) is the major HA cell surface receptor. It mediates cellular events involved in cell growth and differentiation. It is also a primary mediator of the uptake and degradation of HA in many cells. It has important functions in cell migration during morphogenesis, angiogenesis, tumor invasion and metastasis. Lymphatic vessel endothelial hyaluronan receptor (LYVE-1) is an HA receptor confined to the lymphatic vessels and sinuses

which are the main sites of HA degradation. Hyaluronan-mediated motility receptor (RHAMM) seems to play a role in cellular responses to injury, chronic inflammation and cellular transformation as occurs in cancer states (Kaya *et.al.,* 2000).

Hyaluronan degradation products transduce their inflammatory signal through toll-like receptor 2 (TLR2) and toll-like receptor 4 (TLR4) in macrophages and dendritic cells, playing an important role in innate immunity (Termeer *et. al.*, 2002). It also interacts with cell surface receptors mentioned above such as CD44, LYVE-1 and RHAMM.

Inflammation

The immune system is divided into two categories: adaptive and innate. Adaptive immunity refers to antigen-specific immune response. The antigen first must be processed and recognized, and later on the adaptive immune system creates a specific response against that antigen. It also includes a "memory" that makes future responses against the antigen more efficient.

Innate immunity refers to nonspecific defense mechanisms that come into play immediately or within hours of an antigen's appearance in the body ("Immunity," 2014). These mechanisms include physical barriers such as the skin, chemicals in the blood, and immune system cells (macrophages, monocytes, neutrophils and dendritic cells) that attack foreign cells in the body by detecting signs of damage or invasion through PRRs (Iwasaki & Medzhitov, 2004).

The molecules recognized by a given PRRs are called pathogen-associated molecular patterns (PAMPs), and these include microbial pathogens (lipopolysaccharide, mannose), nucleic acids (bacterial or viral DNA/RNA), bacterial peptides (flagellin), peptidoglycans and lipoproteins and fungal glucans. PRRs also recognize DAMPs, which are associated with cellular stress and cell components released during cell damage as happens in HA degradation (Termeer *et. al.*, 2002).

Based on their function, PRRs are divided into signaling PRRs or endocytic PRRs. Signaling PRRs include large families of membrane-bound Toll-like receptors (TLRs) , C-type lecting receptors and cytoplasmic NOD- like receptors (NLRs) (Papadimitraki *et.al.,* 2007; Schnare *et. al.*, 2001; Takeda *et.al.,* 2003). Endocytic PRRs such as macrophages are those in charge of promoting attachment, engulfment and destruction of microorganisms by phagocytosis without the need of an intracellular signal.

HA in the inflammatory response

Hyaluronan and its binding proteins play a role in the pathogenesis of many diseases as well as in numerous experimental conditions. As we have commented before, depending on its size, HA play two different roles. HMWHA is anti-inflammatory and is recruited to sites of inflammation as an immune suppressor and building the matrices of connective tissue to aid in

the healing process. On the other hand, LMWHA is recognized as DAMP by the PRRs. LMWHA will induce inflammation by two distinct but cooperating routes **(Figure 10)**; (i) by binding to TLR2 or 4, LMWHA activates the Nuclear factor kappa-beta (NF-κB) pathway with an increased expression of Interleukin 1ß (IL-1ß) mRNA as a result and (ii) by binding to CD44 (HA-CD44 interactions are important in leukocyte homing and recruitment), LMWHA is endocytosed and further degraded by HYAL2 in the cytoplasm into a fragment size recognized by another receptor, NOD-like receptor family pyrin domain containing 3 (NLRP3), that will form the multiprotein complex referred to as the inflammasome (Olsson, 2012). The inflammasome is responsible for the transformation of pro-IL1ß into the mature form that is secreted from the cell.

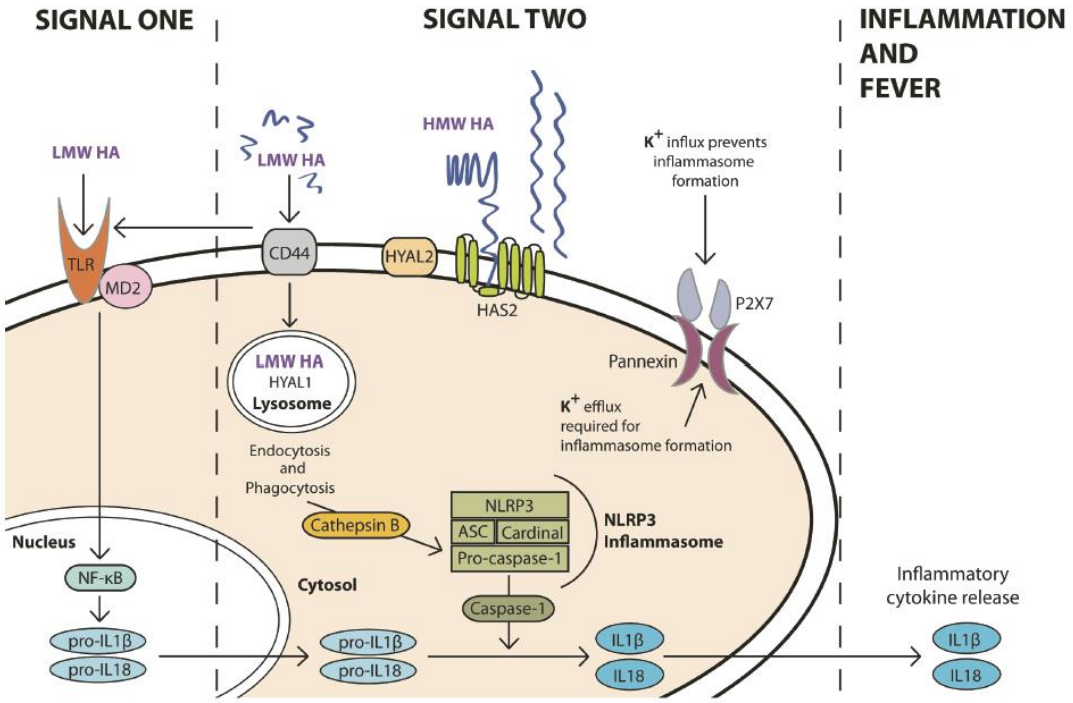

Figure 10. HA inflammation triggering routes. HA signals through two routes. In the first one, HA gets recognized DAMP by TLR2 and 4 activating the NF-κβ pathway and the increased production of pro-IL1β and IL-18 to the cytosol. In the second route, HA binds to CD44, becomes internalized and further degraded by HYAL2. HA is capable of triggering the formation of the inflammasome, which role is to cleave the pro-IL-1β into its active forms, which will get released by the cell (Olsson, 2012)

An example that HA-TLR interactions provide signals that initiate inflammatory responses, maintain epithelial cell integrity, and promote recovery from acute lung injury can be revised in a study carried out in 2011 by Jian and coworkers (Dianhua Jiang *et.al.,* 2011) which demonstrated that signaling of HA fragments requires both TLR4 and TLR2 (Scheibner *et. al.*, 2006) to stimulate inflammatory cells to produce inflammatory chemokines and cytokines. Disruption of HA-TLR interactions resulted in exaggerated injury in a noninfectious lung injury model **(Figure 11)**.

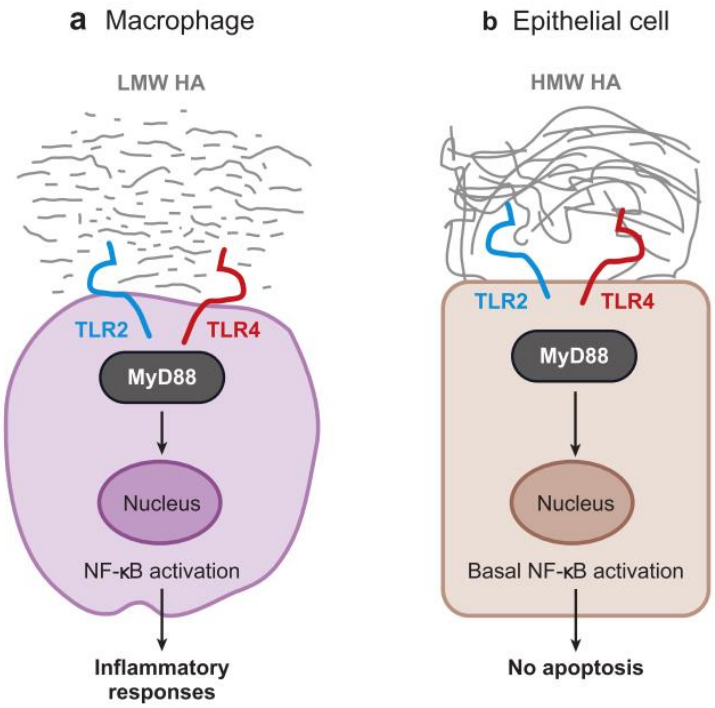

Figure 11. HA signals through TLR2 and TLR4. **(a)** LMWHA fragments generated during tissue injury signal through TLR2 and TLR4 and an adaptor molecule (MyD88) to stimulate chemokine/cytokine expression in macrophages, leading to inflammatory responses. **(b)** HMWHA on the cell surface or surrounding epithelial cells signals through to TLR2 and TLR4 and MyD88, providing cells with basal NF-κB activation. In turn, the tonic NF-κB activity prevents epithelial cells from undergoing apoptosis upon injury. Therefore, HMWHA on epithelial cells provides cells with a survival signal (Dianhua Jiang *et.al.,* 2006)

Auto inflammatory diseases

Auto Inflammatory Diseases (AIDs) (previously known as periodic or recurrent fever syndromes) are a group of disorders characterized by recurrent episodes of systemic and organ-specific unprovoked inflammation which are caused by errors in the innate immune system unlike autoimmune disorders which are caused by abnormalities of the adaptive immune system. Patients suffering from auto inflammatory diseases do not produce auto antibodies or antigen- specific T or B cells. They tend to suffer from fever episodes, joint pain, skin rashes, abdominal pains, and some can even develop secondary reactive amyloidosis caused by elevated levels of pro inflammatory cytokines and acute-phase proteins (such as C reactive protein and serum amyloid protein). Some AIDs are sub-classified into IL-1β activating diseases (or inflammasomopathies) based on accumulating evidence of successful anti-IL-1 therapy (Park *et.al.,* 2012).

In humans, AIDs include a category of diseases known as Hereditary Recurrent Fever Syndromes (HRFS). In this category we can find diseases such as Familial Mediterranean Fever (FMF), Tumor Necrosis Factor Receptor-Associated Periodic Syndrome (TRAPS), Hyperimmunoglobulinemia-D with Periodic Fever Syndrome (HIDS), and Cryopyrin-Associated Periodic Syndromes (CAPS). Other AIDs are Pyogenic Arthritis with Pyoderma Grangrenosum

and Acne (PAPA), Periodic Fever with Aphthous Stomatitis, Pharyngitis and Cervical Adenopathy (PFAPA), Behçet's disease and Idiopathic Pulmonary Fibrosis. Some AIDs have a genetic explanation since mutations on different genes are the cause for these diseases **(Table 6)**. The most common human genetic AID is FMF, which is caused by a mutation in the *MEFV* gene which encodes for the protein pyrin/marenostrin (Kastner *et.al.,* 2010). There are some auto inflammatory diseases (75%) that are not known to have a clear genetic cause, and it is believed that these diseases are multifactorial, and not only a gene mutation is responsible for the disease manifestation (Toplak *et, al.*, 2011).

Systemic amyloidosis is one of the most serious manifestations of the HFRS and is the result of the tissue deposition of misfolded fragments of serum amyloid A (SAA), one of the acute phase proteins produced by the liver in response to systemic inflammation.

Table 6. Human AID, symptoms, genes involved and suggested inflammation pathways. (Olsson, 2012) *(Note: Table has been updated with new genes involved in different human AIDs)*

Disease	Most common symptoms and disease onset	Involved genes and proposed mechanisms
Familial Mediterranean Fever (FMF)	Periodic fever (3-7 days), arthritis, serositis, amyloidosis, onset <20 years	*MEFV,* direct inflammasome mutations that results in IL-1β release
Hyper IgD syndrome (HIDS)	Periodic fever (3-7 days(, arthritis, skin lesions, amyloidosis, childhood onset	*MKV,* encodes a catalyzing enzyme for hormones needed in caspase-1-activation, which is part of the inflammasome
Cryopyrin-associated periodic syndromes (CAPS)*	Cold induced fevers, meningitis, cochlear inflammation, onset <5 years	*NLRP3,* direct inflammasome mutations that results in IL-1β release
PAPA syndrome	Pyogenic arthritis, Pyoderma granulosum, acne	*PSTPIP1,* disturbs the inhibitory effect of pyrin which is a part of the inflammasome, results in IL-1β release
Gout	Recurrent arthritis (mainly the metatarsal-phalangeal joint)	*Complex acquired,* alternative cleavage of pro-IL-1-β
TNF-associated periodic syndrome (TRAPS)	Periodic fever (1-6 weeks), rash, myalgia, serositis, amyloidosis, variable onset	*TNFRS1A,* shedding defect and/or protein misfolding
Ankylosing spondylitis (AS)	Chronic arthritis of spinal chord	*HLA-B27,* stress response following unfold protein and *TAP1*, Involved in the transport of antigens from the cytoplasm to the endoplasmic reticulum for association with MHC class I molecules
Blau syndrome	Arthritis, dermatitis, uveitis	*NOD2,* up-regulated NF-κβ activation
Chron´s disease	Intestinal inflammation	*NOD2 (complex),* NF-κβ activation
Systemic onset idiopathic juvenile arthritis	Long lasting arthritis, systemic symptoms, young onset < 16 years	*PRF,* Plays a key role in secretory granule-dependent cell death, and in defense against virus-infected or neoplastic cells.
Adult onset Still´s disease (AOSD)	Long lasting arthritis, systemic symptoms, adult onset	*IL18,* Augments natural killer cell activity in spleen cells and stimulates interferon gamma production in T-helper type I cells

* Including MWS=Muckle-Wells syndrome, FCAS=familial cold associated syndrome and NOMID=neonatal onset multisystem inflammatory disease.

A lot of effort is being put into finding the right model to better understand the AID phenotype. Animal models including knockout mice experiments for CAPS, gout (*NLRP3*) and mutations associated with FMF (*MEFV*) have been performed (Chae *et. al.,* 2011; Martinon *et.al.,* 2006).

Shar Pei breed as a model for Familial Mediterranean Fever and Cutaneous Mucinosis

Dog's evolutionary history constitutes one of the best tools we have to study different human diseases. Dogs have undergone two major bottleneck events; one that occurred at least 15,000 years ago with the domestication of the wolf (Vilà *et. al*, 1997) and second, a more recent event where different breeds were created **(Figure 12)**. These events have shaped the dog´s genome structure which is characterized by large haplotype blocks allowing an easier way to localize genes which are responsible for diseases using less sample size (Karlsson *et. al.*, 2007; Lindblad-Toh *et. al.*, 2005). In addition, the founder effect, breeding practices and reproductive isolation makes purebred dogs highly susceptible to one or more specific diseases (46% of genetic diseases in dogs are restricted to one specific breed).

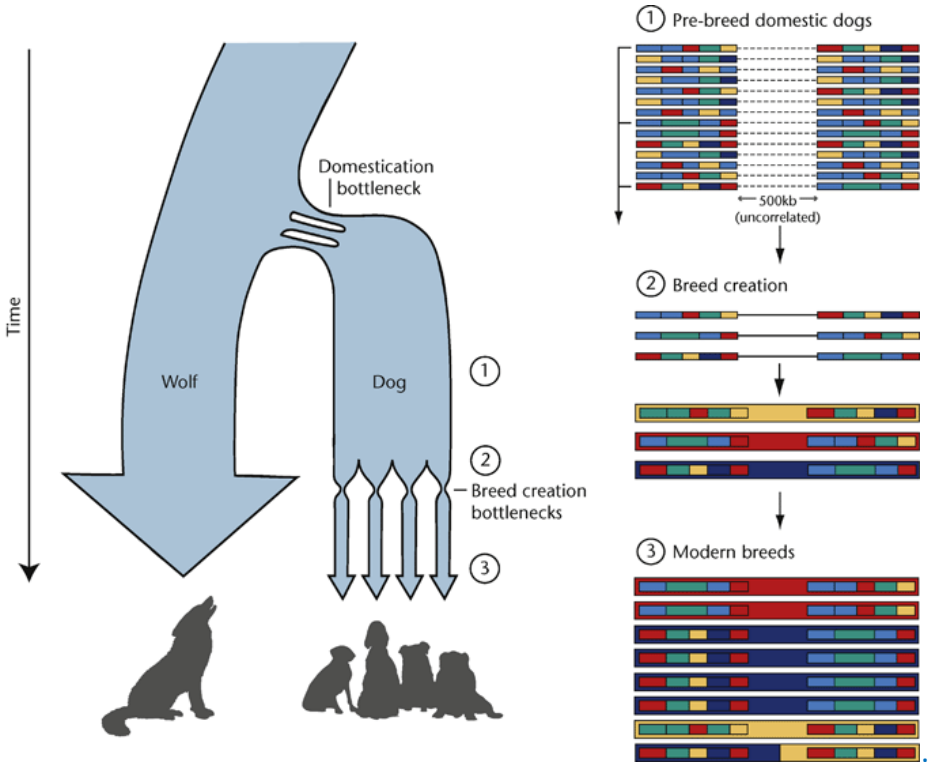

Figure 12. Genetic bottlenecks of dog domestication. (Lindblad-Toh *et. al*, 2005)

From all domestic animals, dogs have the highest level of health surveillance and the largest number of identified genetic disorders (Ostrander *et.al.,* 2000). Over 150 diseases of genetic origin have been compiled in the "*Canine Inherited Diseases in Dogs Database*" (http://idid.vet.cam.ac.uk/search.php) from Cambridge University (UK) and the Canadian Veterinary Medical Association´s "*Canine Inherited Disorders Database" (http://www.upei.ca/~cidd/intro.htm).*

More than 215 genetic diseases in dogs have been reported to be clinically similar to human diseases and at least 41 of these diseases involve mutations in the same gene products as in humans (Ostrander *et. al.*, 2000).

Taking into account (i) that symptoms are fairly similar to those shown in human patients; (ii) that dogs share the same environment as humans; (iii) that they live shorter lives and lastly (iv) their genetic architecture advantage; dogs make excellent models for finding underlying mutations of human diseases.

In the databases previously mentioned, Shar Peis are one of the dog breeds which accumulate more diseases of genetic origin; some of these diseases are very common such as Hereditary Cutaneous Hyaluronosis (HCH) and Familial Shar Pei Fever (FSF). This could be probably explained due to the breed´s history, since most current Shar Pei dogs are descendants from a small founding nucleus. Many studies have been made in order to understand both of these diseases and their possible relationship with human cutaneous mucinosis and Familial Mediterranean Fever.

Shar Peis unusual wrinkled and thickened skin has been considered to be the consequence of an abnormal deposition of mucin; this is why the disease entity is found in textbooks under the name of "cutaneous mucinosis". Lots of research has been done in order to comprehend, characterize and explain why the Shar Pei has its characteristic wrinkled skin phenotype (Beale *et.al.,* 1991; Edward *et.al.,* 2007; López *et.al.,* 1999; Madwell *et.al.,* 1992; von Bomhard & Kraft, 1998; Welle *et.al.,* 1999).

The first reported study on cutaneous mucinosis was carried out in 1986 by Dillberger and Altman where they reviewed cutaneous mucinosis in 7 different dogs of which 3 where Shar Pei and compared them to human cutaneous mucinosis (Dillberger & Altman, 1986).They suggested a genetic predisposition to focal mucinosis of the Shar Pei breed and proposed future studies to be carried out in this dog breed in order to understand the pathogenesis of cutaneous mucinosis in humans.

Mucinoses are a group of conditions caused by dermal fibroblasts producing abnormally large amounts of mucopolysaccharides. In 1995, Doliger and collaborators demonstrated that the main GAG involved in canine cutaneous mucinosis found in the skin of hypothyroid dogs was HA (Doliger *et. al*, 1995). In 2008, Zanna and coworkers confirmed Doliger´s work by stating that the main component of the mucin in Shar Peis with cutaneous mucinosis was also HA (Zanna *et. al*., 2008). Since then, the term Hereditary Cutaneous Hyaluronosis (HCH) is used to describe this skin phenomenon. The same study could not find a correlation between CD44 expression (responsible for HA uptake and catabolism) and HA deposition in the dermis as had

been previously found in studies with transgenic mice (Tammi *et.al.,* 2005). Abnormalities in CD44 expression seemed not to be the origin of HCH in Shar Pei dogs and the reduced degradation of HA due to decreased cell surface receptors is unlikely as found in other publications on human cutaneous mucinosis (Kaya *et.al.,* 2000; Kuroda *et.al.,* 2005). What they did find was a correlation of HA deposition in the dermis with elevated levels of HA in serum of Shar Pei dogs as was previously reported 2000 in a case where an infant was born with excessive skin folding in association with mucin deposition **(Figure 13)** similar to the Shar Pei wrinkled skin phenotype (Ramsden *et.al.,* 2000). Ramsden and collaborators measured serum HA concentration in 23 Shar Pei and 34 control dogs and found that the primary abnormality was excessively high levels of serum HA (5 times higher when compared to controls). They also measured serum HA concentration in the human patient and found that HA concentration in serum was markedly elevated as well. An increased activity of HAS in the patient´s cultured dermal fibroblast and normal HYAL activity in plasma suggested a disorder in HA metabolism, apparently an abnormal control of HA synthesis. Authors in both studies, Zanna *et.al.,* 2008 and Ramsden *et.al.,* 2000 (Ramsden *et.al.,* 2000; Zanna *et.al.,* 2008), proposed the Shar Peis to have some sort of genetic defect in the metabolism of HA and suggested further studies on HA metabolism in order to explain the etiopathogenesis of the disease.

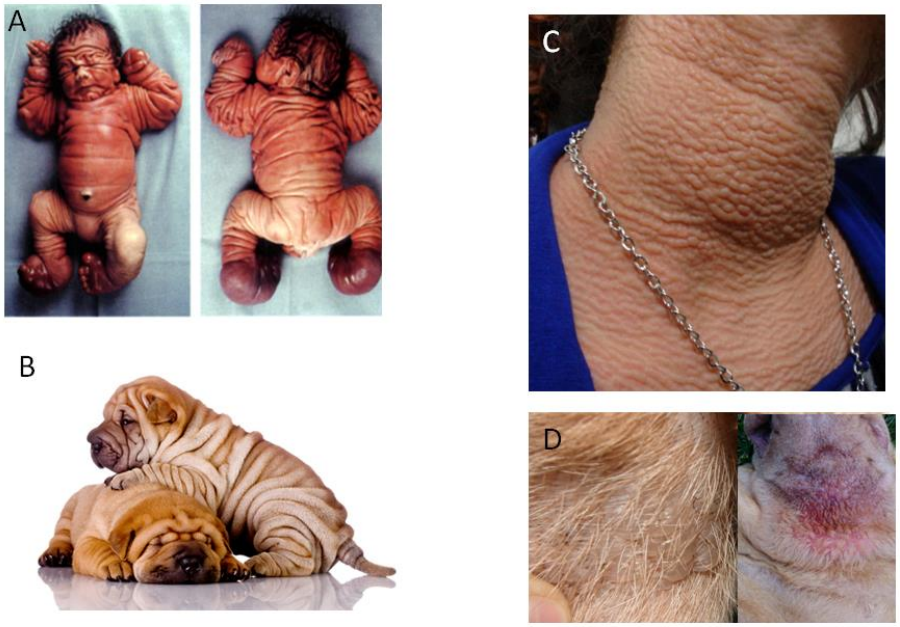

Figure 13. Human and Shar Pei cutaneous mucinosis. **A)** Generalized skin folding in 11 day old baby (Ramsden *et.al.,* 2000). **B)** Shar Pei puppies with generalized skin folding. **C)** Localized papular mucinosis on neck of 14 year old girl, retrieved May 20, 2014 from http://www.globalskinatlas.com/imagedetail.cfm?topLevelID=2257&imageID=5041&did=826.
D) Vesicular hyaluronosis on Neck of Shar Pei dog retrieved May 26, 2014 from Shar Pei Health Education Facebook group with the consent of owners and group administrator (https://www.facebook.com/groups/SharPeiHealthEducation/)

In humans, cutaneous mucinoses are mostly characterized by local thickening of the skin and not by a generalized or diffuse accumulation or skin folding such as the case described by

Ramsden and collaborators. A classification of human cutaneous mucinosis can be found in **Table 7.**

In dogs, HCH is characterized with an excessive amount of HA in the upper dermis. Abnormal HA deposition throughout the skin may be focal, multifocal or diffuse. HA is deposited in the skin in microscopic lakes, but it can also be seen as grossly evident vesicles and bullae, especially in skin folds around the head, chest and tibiotarsal joints (Gross *et.al.,* 2005). Almost all Shar Pei seem to be affected by hyaluronosis (Zanna *et.al.,* 2012), however the extent varies among individuals and adults exhibit less skin folds and hyaluronosis than puppies. HCH may occur as a primary condition, presumably due to hereditary or acquired metabolic or endocrine defects, or it can be seen as sub clinically histopathologic abnormality in association with other diseases. HCH may also occur secondarily in other dermatoses, such as hypothyroidism or in a variety of inflammatory skin diseases, including allergic and eosinophilic skin diseases, pyoderma and lupus erythematosus, as well as in mast cell tumors (Gross *et.al.,* 2005). Classification of canine cutaneous mucinosis or HCH can be found in **Figure 14**.

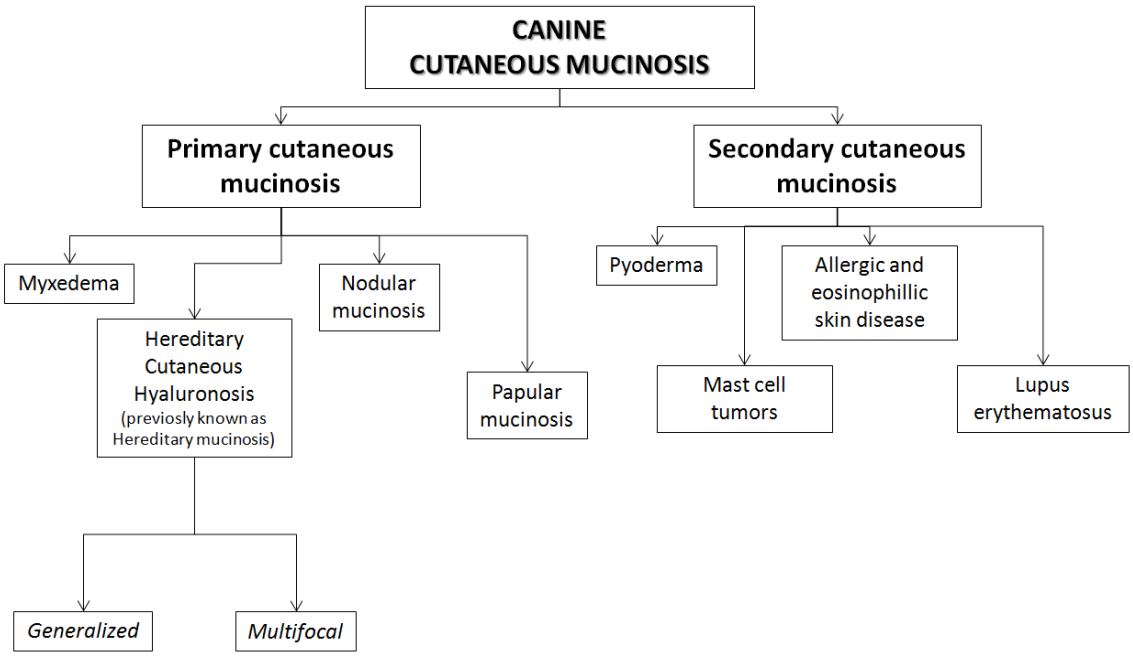

Figure 14. Classification of canine cutaneous mucinosis. (Gross *et.al.,* 2005)

Even though there are other wrinkled breeds (e.g. Neapolitan Mastiff, Pugs, Bull Mastiff), HCH is unique to the Shar-Pei manifesting several clinical signs such as thickening and puffing up of the skin without compromising cutaneous integrity and in more severe cases with vesicles and bullae that may rupture oozing out the viscous material (HA) (Gross *et.al.,* 2005; von Bomhard & Kraft, 1998). Shar Peis suffering HCH can also manifest lymphedema which is a condition where the hocks and thighs are swollen due to the pressure of HA on the lymph vessels which interfere with the return of lymph fluid back to the vascular system.

Table 7. Classification of human cutaneous mucinoses. (Rongioletti, 2006)

Human Cutaneous Mucinosis	
Primary Idiopathic Cutaneous Mucinosis (Lichen Myxedematosus)	
Subsets	***Subtypes***
Generalized popular form or scleromyxedema	No Subtypes
Localized popular form	Discrete popular form involving any site Acral persistent popular mucinosis involving only the extensor surface of the hands and wrists Papular mucinosis of infancy, a pediatric variant of the discrete form or the acral form of persistent popular mucinosis Nodular form
Atypical or intermediate form	Scleromyxedema without monoclonal gammopathy Localized forms with monoclonal gammopathy and/or systemic symptoms Localized forms with mixed features of the subtypes Not well-specified cases
Secondary Cutaneous Mucinosis	
Lupus erythematosus Dermatomyositits Granuloma annulare Scleroderma	

To insight in the mechanism underlying the increase of HA in the skin of the Shar Pei breed Zanna and coworkers performed another experiment with the main objective of identifying if the increase of HA in the skin was as a consequence of an excessive HA production or a problem with degradation (Zanna *et.al.,* 2009). They measured the transcription of the different isoenzymes involved in synthesis (HAS1, HAS2, HAS3) and degradation (HYAL1, HYAL2) in Shar Pei cultured dermal fibroblast by using reverse transcriptase polymerase chain reaction (RT-PCR) as well as detecting HA using confocal scanning laser microscopy (CSLM). For this study, researchers used skin biopsy from 13 healthy Shar Pei dogs all considered to be affected by cutaneous mucinosis as cases and skin biopsies from 4 non Shar Pei dogs. Histological evaluation confirmed that an excess of mucinous content was present in the skin of Shar Pei dogs when compared to controls. They suggested that primary cutaneous mucinosis in Shar Peis is a consequence of an increased synthesis of HA by dermal fibroblasts and found out that HAS2 was the most active of the three isoenzymes, showing an increased transcription in dermal fibroblasts of Shar Pei dogs when compared to other breeds. Regarding HYALs, no differences were detected between control and Shar Pei dogs. This finding suggested direct evidence that hereditary cutaneous mucinosis in the Shar Pei breed is a consequence of an increased synthesis of HA (Zanna *et.al.,* 2009).

To finally understand the phenotypic characteristics of HCH, Docampo and collaborators performed several experiments to compare Shar Pei to control dogs in order to further understand the etiopathogenesis of this disease. They confirmed that HA concentration in serum was higher in Shar Pei dogs as previously reported by Ramsden *et.al., (2000)* and Zanna *et.al.,* (2008) (Ramsden *et.al.,* 2000; Zanna *et.al.,* 2008). Morphologic differences of fibroblasts of Shar Pei dogs compared to controls showed that Shar Pei fibroblasts had a larger amount of HA and presented a high number of cell extensions compatible with high activity of HA synthesis and secretion as well as an increased number of dense particles corresponding to lysosomes. Shar Pei fibroblasts revealed surface protrusions projecting out of the cell membrane into the pericellular space, forming thicker connections with neighboring cells when compared to control dogs. RT-PCR and quantitative real time PCR confirmed that Shar Pei fibroblasts over express *HAS2* as previously demonstrated by Zanna *et.al.,* in 2008 (Zanna *et.al.,* 2008), and that HYALs were not differentially expressed between Shar Peis and controls suggesting that HA degradation is not involved in this disease. This lead researchers to think that the high content of HA in fibroblasts from Shar Pei dogs is a consequence of increased synthesis as confirmed with a western blot assay which demonstrated that a higher protein production was observed in Shar Pei dogs when compared to controls (Docampo *et.al.,* 2011).

At a genetic level, studies exploring selective sweeps generated by the drastic decrease of variation due to dog bottlenecks and artificial selection lead to the identification of a candidate region related to the wrinkled phenotype in Shar Pei dogs (Akey *et.al.,* 2010). This region, is located in chromosome 13 (CFA 13) and include the *HAS2* gene which was considered a strong candidate gene. To corroborate that it was indeed contributing to skin wrinkling, Akey *et.al.,* sequenced ≈3.7 kb of *HAS2* [including all exons, intron/exon boundaries, and untranslated regions (UTRs)] from 32 *Meatmouth* and 18 *Bonemouth* Shar Peis to observe the intrabreed phenotypic variation discovering 5 polymorphisms. Afterwards, authors sequenced all *HAS2* amplicons in a panel of 94 dogs from 20 different breeds and found that the most differentiated SNP (single nucleotide polymorphism) between Shar Pei and other breeds was a 2-bp indel ≈87bp 3' of intron 2, a deletion allele highly associated with the wrinkling phenotype. Resequencing of 50 Shar Pei dogs indicated that the strongest associations in the SNP data occurred upstream of the *HAS2* gene, suggesting that the casual polymorphism previously found lies 5´to *HAS2* gene (Akey *et.al.,* 2010).

In the meantime, Olsson and collaborators identified a selective sweep region which overlapped with the one previously found by Akey and collaborators (Akey *et.al.,* 2010), and they found that it had a strong association with susceptibility to Familial Shar Pei Fever. Olsson and collaborators further investigated the two unique features of the Shar Pei breed: the wrinkled skin phenotype and FSF, by performing a Genome Wide Association Study (GWAS) in Shar Peis extremely affected by these diseases They identified a reduction of heterozygosity which was 4 fold higher in CFA 5, CFA 6, CF 13, and CFA X when compared to control breeds and when performing a case-control GWAs of dogs suffering from FSF and correcting for stratification and multiple testing, they discovered a 10-fold reduction in heterozygosity in the 3.7 Mb region on canine CFA 13. Resequencing of 1.5Mb in the CFA 13 region (main focus in capturing *HAS2* region) revealed two duplications (14.3 kb and 16.1 kb) located 350Kb

upstream of the *HAS2* gene which was unique to Shar Pei since it occurred as single copy in other dog breeds **(Figure 15).**

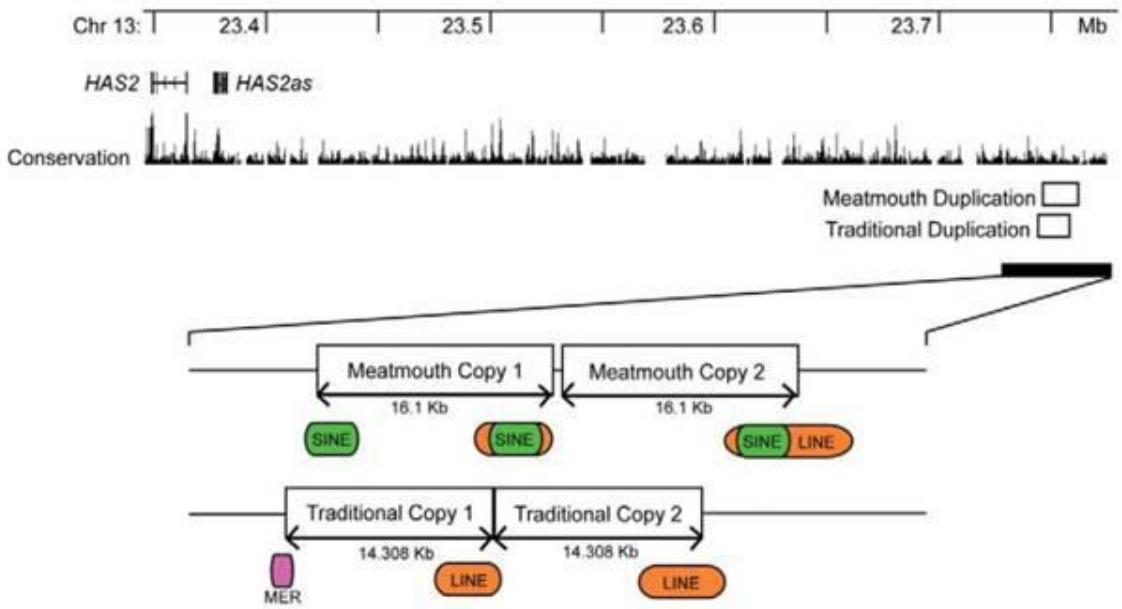

Figure 15. The ''Meatmouth'' duplication- 16.1 Kb fragment*:* CanFam 2.0 Chr13: 23,746,089–23,762,189) with individual copies separated by seven base pairs and the ''traditional'' duplication (14.3 Kb fragment: CanFam 2.0 Chr13: 23,743,906–23,758,214)

The Shar Pei´s characteristic skin phenotype and FSF was associated with a CNV (copy number variant) of the 16.1kb duplication which occurred principally in the *Meatmouth* Shar Pei (4-5 folds higher). Authors suggest that the region of the *Meatmouth* type duplication identified contains one or more regulatory elements that alter *HAS2* expression, proposing that as the duplication copy number increases, so does the copy number of potential enhancer elements leading to a higher expression of *HAS2* and elevated levels of HA in serum which results in de development of hyaluronosis. Even though Olsson *et a.,* discovered this mutation, authors recommend a reexamination of the genes found along the biosynthetic pathway such as those implicated in HA synthesis as well as to study regulators of HA to further elucidate on the knowledge of this disease and its relationship with other auto inflammatory disorders such as FSF (Olsson *et.al.,* 2011), since the absolute truth of the relationship between HCH and FSF has not been really defined.

The Shar Pei is the only dog breed that suffers from auto inflammation occurring spontaneously. Many dogs of this breed are affected by AID, resembling human Familial Mediterranean Fever by manifesting signs such as fevers, swollen joints, skin rash, and signs of systemic inflammation which include abdominal pain, hunched back and secondary amyloidosis **(Figure 16)**. A summary of similitude between FMF and FSF can be found in **table 8**.

Table 8. Similitude between FMF and FSF. (Olsson, 2012)

Familial Mediterranean Fever (FMF)	Familial Shar Pei Fever (FSF)
Early onset	Typically early onset
12-72 hour attacks of high fever Skin rash	12-36 hour attacks of high fever Skin rash
Abdominal pain	Abdominal Pain
Back pain	Back pain (hunched back)
Asymptomatic between attacks	Asymptomatic between attacks
Arthritis (ankle is most affected)	Arthritis (tibiotarsal joint/hock is most affected)
Some develop amyloidosis	40% of FSF patients develop AA amyloidosis (renal/hepatic)
Benefit from colchicine and IL-1β inhibitors	Benefit from colchicine and IL-1β inhibitors

In 1993, a survey indicated that 23% of Shar Pei dogs experienced fevers of unknown origin (Stojanov & Kastner, 2005). Clinical signs of FSF include episodic fevers, which is the most important and consistent clinical sign. Generally the fever is self-limiting and lasts between 12-36 hours with body temperature in the 40-41.5°C range. Another common clinical sign that is presented along with the fever is swelling of joints, usually the tibiotarsal joint. This is also known as the Swollen Hock Syndrome (SHS). Swelling can also be seen in the carpus joint or lips. Shar Peis with FSF are reluctant to move, they walk with a hunched back, have painful abdomen and some can even have mild vomiting and diarrhea (Bonagura & Twedt, 2009).

As we have commented before, the breakdown of LMWHA products have a proinflammatory role, and high levels of inflammatory proteins such as Interleukin-6 (IL-6) , IL-1β, acute phase reactant proteins, and SAA protein, among others are present on the Shar Peis with recurrent episodes of unknown fever (DiBartola *et.al.,* 1990; Rivas *et.al.,* 1992). Moreover, IL-6 is a pyrogenic cytokine which induces acute phase proteins which are precursors of the Serum amyloid A proteins (SAA) that accumulate extracelullarly in secondary amyloidosis (Lachmann *et.al.,* 2007; Röcken & Shakespeare, 2002).

Even though amyloidosis in the Shar Pei is generalized, about 5% of the FSF dogs will develop renal failure including renal amyloidosis (DiBartola *et.al.,* 1990; Lee *et.al.,*2007). The most reported cause of early death is due to kidney failure (Lee *et.al.,* 2007; Segev *et.al.,* 2012) followed by hepatic failure (Lee *et.al.,* 2007; Loeven, 1994). Renal amyloidosis in the Shar Pei is different from other breeds since the amyloid deposition in the Shar Pei accumulates in the medulla of the kidney instead of the cortex and the average onset of the disease is also lower in this breed (2-5 years of age) (Segev *et.al.,* 2012). Shar Peis seem to be more susceptible to immune-mediated kidney disease such as membranous glomerulonephritis and protein-losing glomerulopathies. They are also susceptible to disseminated intravascular coagulation (DIC), mesenteric, splenic and pulmonary embolism and Streptococcal Toxic Shock Syndrome (STSS)(Clements *et.al.*, 1995; Miller *et.al.,* 1996) .The diagnosis and classification of amyloid requires histological evidence. When amyloid is suspected, Congo red staining must be applied (Röcken & Shakespeare, 2002).

Familial Mediterranean Fever is the most common human auto inflammatory disease, caused by mutations in *MEFV*, a gene which encodes a 781–amino acid protein denoted pyrin [also known as marenostrin (The French FMF Consortium & Consortium, 1997)]. Pyrin is a protein normally present in the inflammasome, its normal function is to assist in controlling inflammation by deactivating the immune response, therefore, the mutated pyrin protein is thought to cause inappropriate activation of the inflammasome, leading to release of the pro-inflammatory cytokine IL-1β (Chae *et.al.,* 2008). Pyrin is expressed in dendritic cells, granulocytes, eosinophils, monocytes, and synovial and peritoneal fibroblasts. More than 80 *MEFV* mutations that cause FMF have been identified. Some mutations delete small amounts of DNA from the *MEFV* gene, leading to an abnormally small protein, but most *MEFV* mutations, change one of the amino acids used to make pyrin. The most common mutation replaces the amino acid methionine with the amino acid Valine at protein position 694 (written as Met694Val or M694V) (*MEFV - Mediterranean fever*, 2011).

The gene mutation variant may determine the clinical course of the disease in a particular individual. FMF is inherited in an autosomal recessive manner. There are 2 phenotypes for FMF: types 1 and 2. FMF type 1 is characterized by recurrent short episodes of inflammation and serositis, including fever, peritonitis, synovitis, pleuritis, and pericarditis. The symptoms and severity vary among affected individuals, sometimes even among members of the same family. Amyloidosis is the most severe complication leading to renal failure. FMF type 2 is characterized by amyloidosis as the first clinical manifestation of FMF in an asymptomatic individual (Ozen & Bilginer, 2014; Shohat & Halpern, 2011).

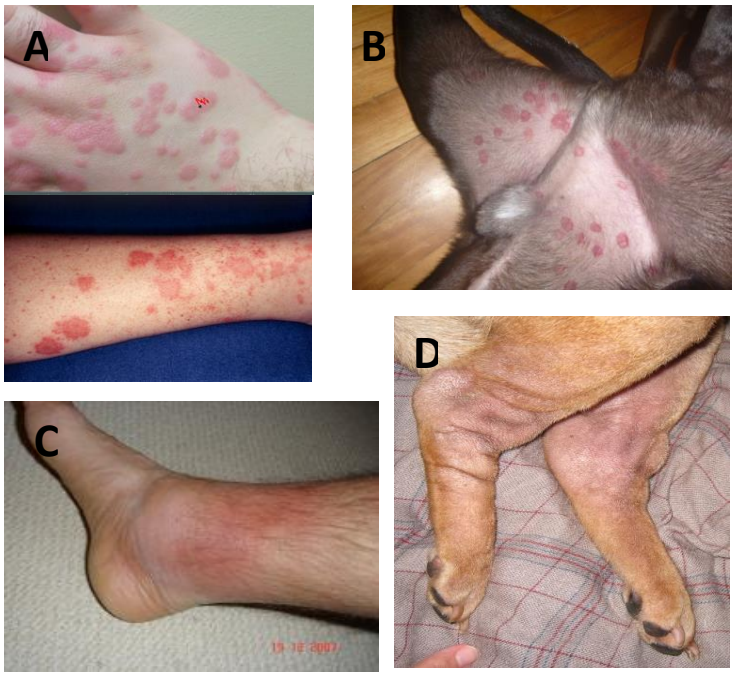

Figure 16. Arthritis and skin rash in FMF and FSF. Pictures **A** and **C** retrieved May 26, 2014 from http://www.amyloidosis.org.uk/fever-syndromes/the-inherited-fever-syndromes-information-on-each-syndrome/familial-mediterranean-fever-fmf/. Pictures **B** and **D** retrieved May 26, 2014 from Shar Pei Health Education Facebook group with the consent of owners and group administrator (https://www.facebook.com/groups/SharPeiHealthEducation/)

The canine equivalent of the *MEFV* gene was examined closely by Dr. Gary Johnson's group (University of Missouri) with the aid of Dr Daniel Kastner [National Institute of Arthritis and Musculoskeletal and Skin Disease, National Institutes of Health (NIH)], which were two of the international groups that discovered the mutations in the *MEFV* gene in humans. Unfortunately they couldn't find any mutations in this region of affected Shar Pei. Neither could they find mutations responsible *Tumor Necrosis Factor* or *TNFR1*-associated periodic syndromes (TRAPS) which as previously mentioned are other genes involved in human auto inflammatory diseases (Linda Tintle, Unpublished Data).

In 2013, Olsson and collaborators further investigated FSF, confirming a main risk locus and suggesting a modifier locus for amyloidosis as well as introducing a new terminology: SPAIDs (Shar Pei Auto Inflammatory Disorder). Using a GWAS on 255 Shar Pei genotyped with the Illumina Canine 170 K SNP chip they confirmed the region on chromosome 13 identified previously by selection mapping (Olsson *et.al.,* 2011) as well as locating a two peaks of differentiation on CFA 13 at ~22-23Mb for breed subtype (*Meatmouth*, *Bonemouth*) and vesicular hyaluronosis and the other at ~27-29 Mb with associations to fever, arthritis and amyloidosis. In addition to the amyloidosis peak on CFA 13 (at 27 Mb), the authors identified a new signal of association on CFA 14. Olsson *et.al.,* also performed a candidate gene expression study of 21 genes on both CFA 13 and CFA 14 using kidney tissue from Shar Peis affected and unaffected by renal amyloidosis, revealing 4 candidate genes (*AOAH*, *ELMO1*, *HAS2*, *IL6*) previously known to influence renal health and inflammation which showed significantly higher expression in affected Shar Peis (Olsson *et.al.,* 2013).

A more recent study by Metzger and Distl (Metzger & Distl, 2014) refused the association of FSF with the Meatmouth duplication previously discovered by Olsson and collaborators (Olsson *et.al.,* 2011). In this study, both Shar Pei susceptible to FSF and healthy Shar Pei showed an average CNV of almost 7 copies indicating that there was no significant association of CNV with FSF, but, they mentioned that the development of wrinkles could be shown to be significantly associated with FSF.

Even though lots of research has been made in order to understand the genetic basis of HCH and FSF, understanding the genetic background of these diseases is harder than it seems and further studies are much needed. In general, many genes are implicated in the inflammation-fever complex. It is interesting that studies including Shar Peis with fever and Hyaluronosis such as those performed by Akey *et.al.,* and Olsson *et.al.,* pointed to homozygosity regions on CFAs 5, 6, 13 and 14. Even though these studies focused mainly on the *HAS2* gene, other genes found on other chromosomic regions such as those on CFA6 are interesting, and mutations or regulatory alterations in these regions might help explain what causes the fever in Shar Peis, not just merely that the HAS2 gene or the CNV found in this region as previously mentioned by Olsson *et.al.,* (Akey *et.al.,* 2010; Olsson *et.al.,* 2011, 2013).

Few questions are still left to be answered regarding this topic such as: Is the HA over expression described in Shar Peis the definite cause of HCH and consequently the breakdown of excess HA the definite cause of FSF? Do all phenotypes described in the Shar Pei breed such as FSF, HCH, amyloidosis, share a common genetic background? Or are there other genes

located on other chromosomic regions different than CFA 13 involved in these complex diseases? Is the CNV discovered near the HAS2 gene in CFA13 the absolute cause of HAS2 over expression in this dog breed? But most importantly, why is it important to understand these diseases and the repercussion this has in the fields of biology, genetics and medicine?

Transgenic animal models

Genetically modified (transgenic) animal models, represent one of the best methodologies for understanding gene function in the context of disease susceptibility, progression and response to therapeutic intervention. There are several advantages when it comes to using transgenic animals for research, particularly the mouse (*Mus musculus*) which is the model organism of choice because of (i) the ability to perform very specific tests both physiologic and behavioral; (ii) their controlled laboratorial environment which aids in standardizing methods and completing a robust experiment; (iii) their short reproduction cycle and because they are easy to handle and economically advantageous when compared to other species (Waterston *et.al.,* 2002). Transgenic mice are generated to obtain information on gene function and regulation which helps to confirm the role of a disease mutation unraveling the underlying molecular and biochemical mechanisms (Houdebine, 2005) since low levels of genetic variation and a high frequency of the trait of interest are important when connecting genomic loci to a specific phenotype. A disadvantage when it comes to working with transgenic mice is that mutations studied in these models are induced, therefore not always mimicking the complexity that characterize complex diseases such as FSF or HCH. Even though these limitations exist, various studies using transgenic mice have been performed in order to try to understand the role of HA. Examples of these studies are that of Tammi and collaborators (Tammi *et.al.,* 2005) which studied CD44 expression and its relationship with HA uptake and catabolism. Knockout mice for Cryopyrin Associated Periodic Syndrome (CAPS), gout (NLRP3)(Martinon *et.al.,* 2006) and for mutations associated with FMF (*MEFV*) (Chae *et.al.,* 2011) have also been created.

OBJECTIVES

Develop of a transgenic mouse model with increased copies of HAS2 to emulate and confirm the phenotype described in Shar Pei dogs.

Gain insight in the genetic background of Familial Shar Pei Fever and of Hereditary Cutaneous Hyaluronosis in Shar Pei dogs.

MATERIAL & METHODS

Murine model

A mouse "Shar Pei"model overexpressing HAS2 was constructed to evaluate the effect of and HA overproduction.

All procedures were approved by the Comissió d'Ètica en Experimentació Animal i Humana of the UAB (Universitat Autònoma de Barcelona) with CEEAH No. 1964 (15-02-2013). Animal welfare was controlled daily; any reports of animal distress were recorded **(Annex 1)** and corrective actions to assure animal welfare was considered in each particular case.

Transgenic construction

The ROSA26p/HAS2 transgenic mice were created at the **CBATEG (Centre de Biotecnologia Animal i Teràpia Gènica** http://cbateg.uab.cat/). A chimera construction for the transgenic mice included three fundamental parts: i) a 0.8kb promoter of the mouse *rosa26* gene in order to have an ubiquitous and stable expression ii) and optimized sequence of the codifying region of the mouse HAS2 gene (see **Figure 20** for differences to endogenous murine HAS2), iii) a polyadenylation signal of Simian virus 40 PolyA (SV40).

The fragment of the promoter and the PolyA sequence were obtained from the same plasmid. This sequence incorporates the restriction targets *Bam*HI and *Eco*RI between the promoter and the PolyA sequence in order to clone the HAS2 gene. Additionally it incorporated *Sal*I and *Eco*RV targets at the extremes to obtain the fragment that were microinjected. The optimized mHAS2 sequence included the *Bam*HI and *Eco*RI targets at the extremes in order to being able to clone in the first plasmid **(Figure 17)**. Sequence of the construction can be found in **Annex 2.** Cloning was performed digesting both plasmids with the enzymes *Bam*HI and *Eco*RI to isolate the fragment of the coding DNA sequence (CDS) mHAS2 and the open plasmid rosa26-SV40PA. Once purified, they were ligated and transformed into bacteria and colonies were obtained with the chimeric plasmid. These colonies were analyzed and the positive clones were amplified and digested with *Sal*I. Later they were microinjected in one cell embryos. Six hundred thirty five microinjected embryos were transferred to the oviduct of 29 pseudo pregnant females. Born mice were genotyped by Southern Blot and later confirmed by Real-Time Polymerase chain reaction (qPCR).

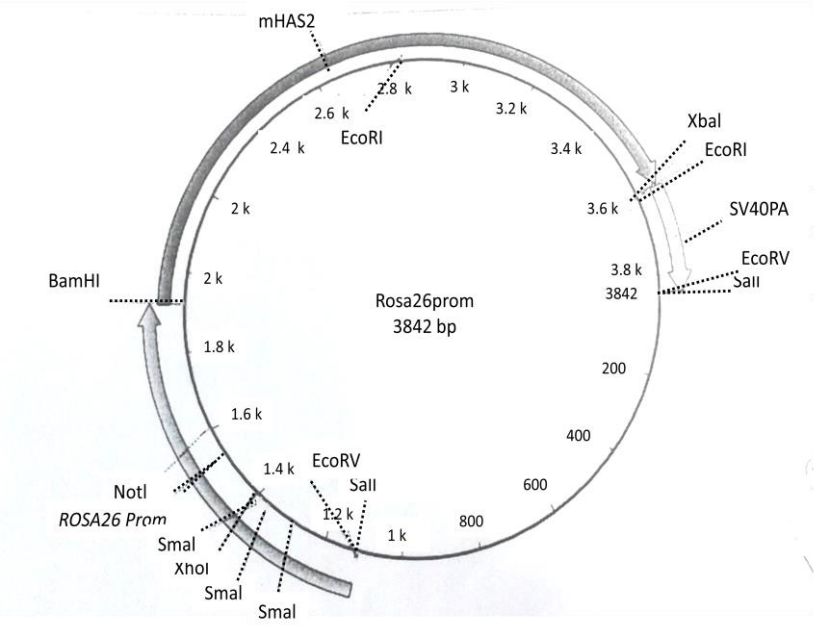

Figure 17. *HAS2* Transgene Plasmid.

Transgene "*in vitro*" expression was performed transfecting C2C12 cells with a plasmid that contained the construction (**Figure 18)**. As a control, a plasmid with GFP (Green fluorescent protein) was used. A Northern Blot with previous RNAse treatment analysis using the cDNA probe of the HAS2 gene was performed and served as confirmation of the "*in vitro*" expression of the ROSA26p/HAS2 transgene.

Cèl.lules: C2C12 (mioblasts murins)
Sonda: Fragment BglII/EcoRI cDNA HAS2

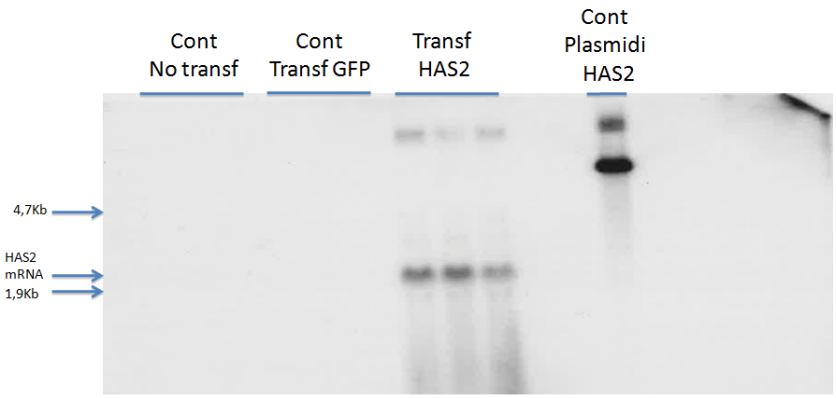

Figure 18. Northern Blot of expression of transgene ROSA26p/HAS2 in C2C12 cells.

Transgenic line

The HAS2 colony was formed from 5 transgenic founder mice; 3 males and 2 females which were crossbred with C57BL/6 partners. Male transgenic mice were bred in threesomes (2 females per male) and female transgenic mice had 1 male partner. Each founder mice represented a different transgenic line. Housing was performed at Servei d´Estabulari of the Universitat Autonoma de Barcelona (https://estabulari.uab.cat) under current legislation ensuring animal welfare. A total of 247 F1 mice were genotyped. Transgenic mice from each founder line were crossbred in order to obtain a homozygous F2. A F2 colony of 195 mice was obtained.

Phenotyping

In vivo analysis included the visual inspection of possible skin alterations (laxity, folds, and wrinkles), body temperature (microchip implant system) and weight **(Annex 3)**. *Post mortem* analysis included a complete blood count (CBC), HAS2 expression in skin tissue determined by reverse transcriptase real time polymerase chain reaction (RT-qPCR) using QuantStudio™ 12K Flex Real-Time PCR System (Life Technologies), and histology with Hematoxylin & Eosin (H&E) stain of parenchymal organs and skin as well as HA concentration in serum determined by Echelon® Biosciences HA Competitive K-1200 and Sandwich K-4800 ELISA kits. Animals were divided into four groups [young wild type (YWT), young transgenic (YTG), adult wild type (AWT) and adult transgenic (ATG)]. The age group was determined by the age of sexual maturity (6 weeks female, 8 weeks male).The final cohort included 20 animals in each group. Mice were identified by ear notches at wean age (3 weeks) with the use of an ear punch device using the Universal Mouse Numbering System **(Figure 19)**.

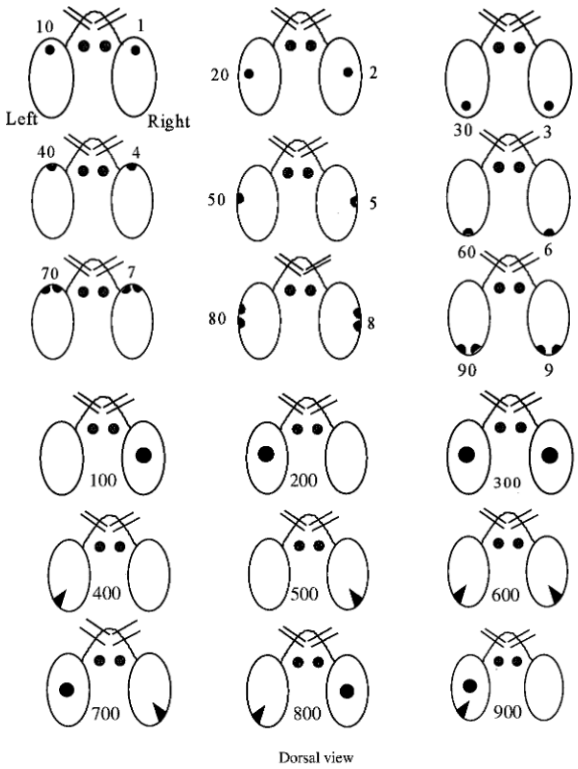

Figure 19. Universal Mouse Numbering system. (Dickie, 1966)

Microchip implant system and temperature recording

Body temperature was recorded using an implantable programmable temperature transponder TM IPTT-300 from Bio Medic Data Systems ("Lab Animal Identification - Bio Medic Data Systems » Products » Transponders » IPT-300," 2013). Microchips were injected gently into each mouse with a syringe-like pre-sterilized disposable needle at wean age (3 weeks old) under general gaseous anesthesia with isofluorane. Body temperature was recorded previous implantation and three times (a.m, m, p.m) a day until the mouse was sacrificed.

Tail biopsy

A 3-5mm tail biopsy was obtained in order to extract DNA for genotyping. This procedure was performed at wean age in order to reduce animal pain and assure a better DNA yield (Tien & Spicer, 2005). Mice were introduced in a contention box and anesthetized with isofluorane. Tail was cut with a scalpel and pressure was applied to stop hemorrhage. Mice were introduced to the cage when bleeding stopped.

Tail DNA isolation

Digestion buffer (700 µl) was added to each sample and incubated at 56°C over night (O/N). Digestion buffer is made with 1% proteinase K (Roche®) + 99% TESNA [100mM Tris pH= 8 (USB®; 5mM EDTA pH=8 (Sigma®), 0.2% SDS (Amresco®) and 200mM NaCl (Sigma®)]. Ten microliters (µl) RNAse at 10mg/mL where added to each sample to eliminate RNA and samples where incubated at 37°C for 1 hour. Following centrifugation for 10 minutes at 13000 revolutions per minute (rpm), supernatant was transferred to a new eppendorf which contained 700 µl of Phenol:Chloroform:Isoamyl alcohol (25:24:1) (USB®). Eppendorfs where stirred vigorously during 5 minutes to assure deproteinization and afterwards, centrifuged again for 10 minutes at 13000 rpm. The upper phase of the supernatant was transferred to a new eppendorf containing 700 µl of Chloroform:Isoamyl alcohol (24:1) (Panreac®) and stirred vigorously for 5 minutes. Following 15 minute centrifugation at 11000 rpm, upper phase of the supernatant was transferred to a new eppendorf containing 700 µl of Isopropanol + 15 µl of NaCl 5M for DNA precipitation. Samples were centrifuged for 15 minutes at 13000 rpm, supernatant was discarded and 300-400 µl of *Ethanol 70%* (Panreac®) where added. Samples where centrifuged again at 13000 rpm for 10 minutes, supernatant was removed and discarded and DNA pellet was allowed to air dry. DNA pellet was re suspended with 50-100 µl TE (depending on pellet size) and saved at 4°C O/N. DNA concentration was determined with the use of ND-1000 spectrophotometer (NanoDrop® Technologies,). A DNA yield of around 4-8 µg was obtained from a 3-5 mm tail biopsy.

Sacrifice, necropsy and parenchymal tissue sampling

Transgenic and Wild type mice were sacrificed at 6 weeks (young) or 10 weeks (adult) under gaseous anesthesia with isofluorane and exsanguination by intracardiac puncture in order to obtain the maximum volume of blood possible. Once blood was drawn, 0.3 mL were saved in a

0.5 mL EDTA tube for CBC and the remaining (approximately 0.6 mL) was allowed to clot and tubes were centrifuged at maximum speed during 20 minutes to obtain blood serum which was frozen at -20° until used for HA ELISA kits. Two skin samples of approximately 1 cm^2 were stored in cryotubes and frozen in liquid nitrogen immediately after the mouse´s death and later conserved at -80° until RNA extraction. General necropsy was performed and changes on parenchymal organs were recorded on the phenotyping record sheet **(Annex3)**. Samples from lung, heart, kidney, liver, and spleen were obtained and frozen in liquid nitrogen and later conserved at -80° in cryotubes. Mice were placed embedded in a stabilized and buffered *Formaldehyde* solution 3.7-4% pH 7 (Panreac®).

Hematology

CBC analyses were performed at **Servei d'Hematologia Clínica Veterinària (**http://www.uab.cat/web/serveis/servei-d-hematologia-clinica-veterinaria-1250721189599.html) on an automated hematology analyzer (Advia 120, Siemens Healthcare Diagnostics) using mouse-specific algorithms and parameters (Technicon H1E MultiSpecies Software, version 3.0, Siemens Healthcare Diagnostics). Parameters determined included white blood cell (WBC) count and differential, red blood cell (RBC) count, hemoglobin concentration, hematocrit, mean corpuscular volume, mean corpuscular hemoglobin, mean corpuscular hemoglobin concentration, platelet count, mean platelet volume, and reticulocyte count and percentage.

Histology

After a complete gross examination, samples of all parenchymal organs of each animal were collected and fixed in 10% buffered formalin, embedded in paraffin and routinely processed in 3µm sections for hematoxylin and eosin staining (H&E) at the **Unitat de Patologia Murina i Comparada (UPMiC)** (http://upmic.uab.cat/).

Skin RNA isolation and quality assessment

RNA isolation from skin tissue samples was performed using TRIzol® (Ambion - Life Technologies) as described by the W.M. Keck Foundation Biotechnology Microarray Resource Laboratory at Yale University (Foundation & Microarryay, n.d.). RNA was treated with TURBO DNA-free ™ Kit (Ambion - Life Technologies) following manufacturer's instructions. RNA was quantified using a NanoDrop ND-1000 spectrophotometer (NanoDrop® Technologies,) and its integrity was assessed by capillary electrophoresis using an Eukaryote Total RNA Nano 6000 Labchip on an Agilent 2100 Bioanalyzer (Agilent Technologies). RNA samples with an RNA integrity number (RIN) ≥ 7 were used for gene expression analysis.

Has2 expression analysis

Five hundred nanograms of murine skin RNA was reverse transcribed using the High-Capacity cDNA Archive Kit (Applied Biosystems) with random primers and following the manufacturer's instructions. Two assays were designed using Primer Express® software v2.0 (Applied

Biosystems) to target *HAS2* and *HAS2 construction* cDNA **(Table 9).** cDNA of mouse *HAS2* optimized gene was used with a sequence that differs from the endogenous gene giving a different mRNA even though they both translate on the same protein. Alignment of murine *HAS2* (Mus musculus hyaluronan synthase 2 (Has2), mRNA NCBI Reference Sequence: NM_008216.3 GenBankGraphics >gi|160358867|) and *HAS2 construction* can be seen in **Figure 20**.

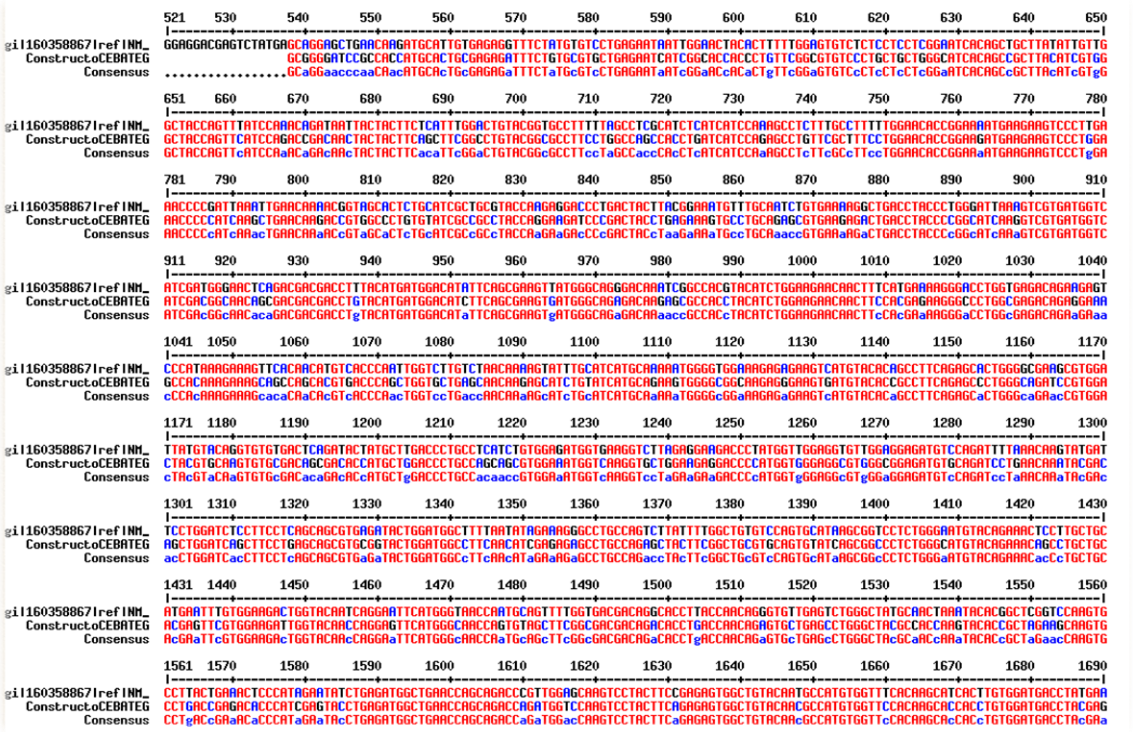

Figure 20: Alignment of 1169bp of Murine endogenous HAS2 and HAS2 construction. HAS2construction has a sequence that differs from the endogenous murine HAS2 giving a different mRNA even though it translates in the same protein.

The eukaryotic 18S RNA Pre-Developed TaqMan Assay Reagents (Life technologies) was used as an internal reference for DNA amplification to ensure (i) the proper PCR amplification of each sample and that (ii) negative results corresponded to true negative samples rather than to a problem with DNA loading, sample degradation or PCR inhibition.All samples were run in triplicate in a 15 µL reaction volume. HAS2 and HAS2 construction assays where run containing 1x SYBR® Select Master Mix (Life Technologies), 300nM of each primer and 2.5 µL of 1:100 diluted cDNA . The 18s Assay was run in triplicate in a 15 µL reaction volume using 2.5µL of 1:5 diluted cDNA. The PCRs were run in QuantStudio™ 12K Flex Real-Time PCR System (Life Technologies) using the following thermal cycling profile: 2 min at 50°C, 10 min at 95°C, and 40 cycles of 15 s at 95°C and 1 min at 60°C. PCR specificity assessment was performed by adding a dissociation curve analysis at the end of the run. Each amplification run contained water as negative control and reverse transcriptase minus controls (-RT) which is a mock reverse transcription containing all the RT-PCR reagents, except the reverse transcriptase, to ensure that is no genomic DNA contamination. The positive control for each mouse was the amplification of the endogenous murine *HAS2 gene*. Expression analyses was performed using Expression Suite software V1.0.3 (Applied Biosystems) by using the comparative cycle

threshold (CT) relative quantification method ($2^{-\Delta\Delta Ct}$) by using the endogenous murine *HAS2* gene as a reference gene and *HAS2 construction* (transgene) as target.

ELISA- HA serum concentration

Two different Enzyme-Linked Immuno- sorbent Assays (ELISAs) were used to determine HA concentration in murine blood serum using manufacturer´s instructions: (i) Echelon® Bioscience´s kits: Hyaluronic Acid Sandwich ELISA K-4800 (detects HA > 130kDa with a detection range of 12.5-3200ng/µL) and (ii) Hyaluronan Competitive ELISA Kit K -1200 (detects all sizes of HA, including LMWHA, from 6.4kDa and up- wards with a detection range of 50-1600ng/µL). Both ELISA were run in duplicates using 1:2 dilutions of serum samples. HA competitive ELISA standard curves were generated using non-linear regression analysis with GraphPad prism software using 4 point analysis for both kits.

Statistical Analysis

Statistical analysis to test the effect of temperature, HAS2 gene expression, CNV, and HA concentration in serum between the different transgenic mouse lines used where ANOVA and Tukey's HSD (Honestly Significant Difference) test to compare data between groups (transgenic/wild type, Young/adult) using R statistical package ("R Statistical Package," n.d.).

Genotyping and CNV analysis

Genotyping to determine if mice were transgenic or wild type was performed by real time PCR. Gene-specific Primers for qPCR were designed with Primer Express® software v2.0 (Applied Biosystems). Forward primer was common for both primer sets (Transgenics and Wildtypes) **(Table 9)** and was designed on the ROSA26 promoter. Two reverse primers were designed, one was designed at *ROSA26* gene (Mus musculus gene trap ROSA 26, Philippe Soriano (Gt(ROSA)26Sor), transcript variant 1, non-coding RNA NCBI Reference Sequence: NR_027008.)1), and the second one was designed using the *Has2 construction* sequence. This way, transgenic (TG) animals amplified both endogenous *ROSA26* primer set and *HAS2 construction* primer set, whereas wildtypes (WT) only amplified *ROSA26* primer set. Validation of the method was done comparing results by those obtained by southern blot in the first 118 F1 mice. Southern Blot was carried out at CBATEG (http://cbateg.uab.cat/) using the protocol in **Annex 4**.

Table 9. Primers used in this thesis.

Primer Name	Forward 5'-3'	Reverse 5'-3'	Concentration	Tm (°) *
ROSA26	TAAAGAAGAGGCTGTGCTTTGGG	CAGGCCCTCCGAGCGT	300nm	86.25
Constructo	TAAAGAAGAGGCTGTGCTTTGGG	ACCATGCACTGCGAGAGATTTC	300nm	84.56
HAS2	GGAGCTGAACAAGATGCATTGTG	AGCTGTGATTCCGAGGAGGAG	300nm	77.96
HAS2construct	ACTACGTGCAAGTGTGCGACA	GTTCAGGATCTGCACATCTCCG	300nm	86.92
Has2 (canine)	CTTCAGAGCACTGGGACGAAGT	TCTAAAACTTTCACCATCTCCACAGA	300nm	80.3

Has2as (canine)	ACTGGGTGGGTAATTCTTTCCA	GGAGGCAGAAAGCAACAACAG	300nm	78.3
G6PDH	CCGCGACGAGAAGGTCAA	GGGTCATCCAGGTACCCTTTG	300nm	85.2

Tm: Melting temperature.
* PCR performed with HT7900 (AB Life Technologies) and SYBR® Green Master Mix (Life Technologies)

qPCR was optimized by running a serial dilution template to generate a standard curve starting with 40ng of DNA and doing six 10-fold serial dilutions. The ROSA26 primer pair had a slope of 3.291, a coefficient of determination (R^2) of 0.999 and an efficiency of 101.35% whereas the Construct primer pair had a slope of 3.321 an R^2 of 0.995 and an efficiency of 100.08% **(Figure 18).** All samples were run in triplicate in a 20 µL reaction volume containing 1X SYBR® Green Master Mix (Life Technologies), 300nM of each primer and 40 ng of the genomic DNA. The PCR was run in the ABI Prism® 7900 HT Sequence Detection System (Applied Biosystems) using the following thermal cycling profile: 2 min at 50°C, 10 min at 95°C, and 40 cycles of 15 s at 95°C and 1 min at 60°C. PCR specificity assessment was performed by adding a dissociation curve analysis at the end of the run. Each amplification run contained water as negative template control and a 1:1000 dilution of the construction plasmid DNA and mouse genomic DNA as positive control. Results were observed in 7900HT SDS v2.4 software (Applied Biosystems,).

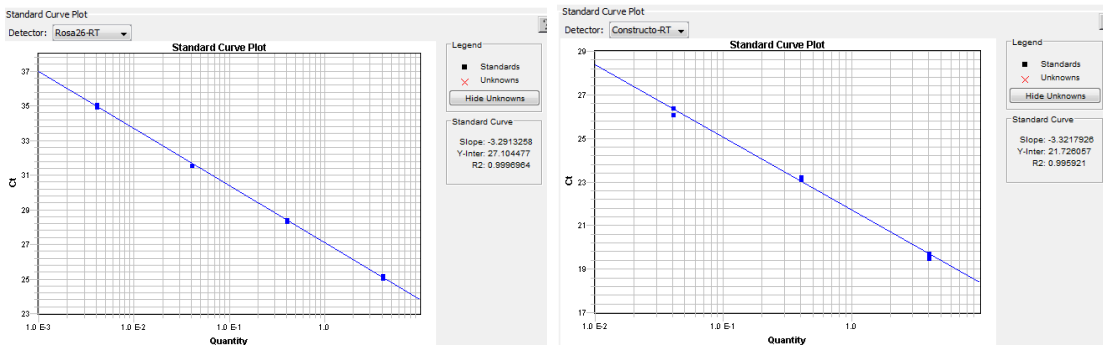

Figure 21. Standard curve of ROSA26 and Construct primers set.

Estimation of copy number was performed using the comparative cycle threshold (CT) relative quantification method ($2^{-\Delta\Delta Ct}$) (Livak & Schmittgen, 2001) in which a target gene (*Constructo*) is normalized to an endogenous control (ROSA26) and relative to a calibrator carrying one copy of the transgene [Founder 184 (F0184) which was previously determined by Southern blot analysis]. Transgenic mice were divided into 3 groups according to CNV estimation; i) Low: 1-20 copies, ii) Medium: 21-69 copies and iii) High: >70 copies.

Canine HAS2 and HAS2as analysis

Five hundred nanograms of canine skin RNA was reverse transcribed using the High-Capacity cDNA Archive Kit (Applied Biosystems Ref. 4368814) with random primers and following the manufacturer's instructions. HAS2 and HAS2as expression analysis was performed as described elsewhere (Olsson et al., 2011), except that all samples were run in triplicate instead of duplicates. Primer sets for HAS2 and HAS2as as well as internal control G6PDH can be found in **(Table 9).** HAS2 and HAS2as assays where run containing 1X of SYBR® Select Master Mix (Life Technologies), 300nM of each primer and 4 µL of 1:10 diluted cDNA. The PCR was run in the

ABI Prism® 7900 HT Sequence Detection System (Applied Biosystems) using the following thermal cycling profile: 2 min at 50°C, 10 min at 95°C, and 40 cycles of 15 s at 95°C and 1 min at 60°C. Results were analyzed in 7900HT SDS v2.4 software (Applied Biosystems). PCR specificity assessment was performed by adding a dissociation curve analysis at the end of the run. Each amplification run contained negative template controls as well as negative reverse transcription controls to assure there was no DNA contamination (RT-minus).

Shar Pei homozygosity regions

We used the raw data from the Illumina CanineSNP20 BeadChip which contained evenly spaced and validated 22.362 SNPs that were derived from CanFam2.0 assembly also used in another study (Olsson et al., 2011) to look for homozygosity regions in 37 Shar Peis compared to a non wrinkled dog breed (Ibizan hound). Analysis using 17,155 SNP was performed and minor Allele Frequency (MAF) in 10-SNPs sliding for each of the 17,155 SNPs was calculated. Regions of homozygosity were defined if shared across all Shar-Pei samples and PLINK software (Purcell et al., 2007) was used to draw a genome-wide graphic of the regions with a mayor variability lost (lowest MAF). The SNPs with an average MAF <5% were grouped in similar regions of the genome agreeing with the main signals. If there was only one SNP, the region was defined as the position of the SNP ±1M flanking bps (base pairs). A list of genes on these regions was obtained.

RESULTS & DISCUSION

As previously mentioned in the **Introduction** section, Hereditary Cutaneous Hyaluronosis (HCH) and Familial Shar Pei Fever (FSF) are two conditions which have been studied in several ways including phenotypic and genetic studies since they both resemble human diseases: cutaneous mucinosis and Familial Mediterranean Fever. A fully satisfactory explanation of pathogenesis of these complex diseases has not been found. Shar Peis have been used as models for these human diseases, but the complexity of HCH and FSF has not yet been resolved and authors who have researched these diseases always underline the need to reach a full understanding of these diseases before they can be considered useful model of the human counterparts.

In medical/veterinary research, simple model systems are needed to help understand the basics of certain diseases, the disease progression and the response to therapeutic interventions. Even though common experimental organisms include fruit flies, zebra fish, or yeast, some complex diseases require other organisms to be employed. In particular, mice have been the most used species in genetic studies, not only because their genomes resemble to that of humans (Austin et al., 2004), but because the advantages (availability, handling, reproductive rates, cost, etc.) that mice offer when compared to other species. In general, transgenic mice are generated to obtain information on gene function and regulation to help confirm the role of a specific gene in a particular disease; this is why we decided to create transgenic mice over expressing the *HAS2* gene. The expected results obtained in these experiments would help us to further understand the role of this gene on HCH and FSF, even though we are aware of the limitations that studies including transgenic mice suffer.

TRANSGENIC MICE MODEL

In the present thesis, a chimera construction which included the promoter of the mouse rosa26 gene, an optimized sequence of the codifying region of the mouse HAS2 gene as well as a polyadenilation signal, was made with the purpose to generate transgenic mice which over expressed *HAS2.* The purpose was the over production of HA in order to emulate the phenotype found in Shar Pei dogs (Docampo et al., 2011; Olsson et al., 2011; Giordana Zanna et al., 2009) and to evaluate the eventual effects of high HA production. In short, the transgenic model was designed to know if a HAS2 over expression could explain the phenotype observed in HCH and FSF.

After microinjection of 635 mice embryos with the chimera construction which had been transferred into the oviduct of 29 pseudo pregnant female, 222 mice were born of which 5 mice integrated the transgene: 3 males and 2 females. These mice were the founders (F0) which consequently were bred with C57BL/6 mice to generate the colony of five transgenic lines with different number of the HAS2 construction integrated **(Figure 22)**. Transgenic mice from each founder line were crossbred in order to obtain a homozygous F2. A total of 80 F2 mice were included in the study: 40 Transgenic (TG) [20 adult (ATG) and 20 young (YTG)] and 40 Wild Type (WT) used as controls [20 adult (AWT) and 20 young (YWT)].

Estimation of copy number was performed by quantitative real time PCR (qPCR), using the comparative cycle threshold (CT) relative quantification method ($2^{-\Delta\Delta Ct}$) (Livak & Schmittgen, 2001) in which a target gene (*Constructo*) is normalized to an endogenous control (ROSA26) and relative to a calibrator carrying one copy of the transgene. Difficulties in determining copy number in transgenic mice by qPCR has been reported in other studies (Ballester, Castelló, Ibáñez, Sánchez, & Folch, 2004). In our study we have obtained lines with more than 70 copies, but aware of technical limitation and that Ct values are outside the boundaries of our linear range we decided to divide the transgenic mice intro 3 groups according to CN estimation; i) Low: 1-20 copies (FO_184 and FO_194) ii) Medium: 21-69 copies (FO_221) and iii) High: >70 copies (FO_156 and FO_172).

We have obtained 2.25% of founder animals (5/222). The low rate obtained in our study could be explained by an insertional mutation. The insertion of an exogenous DNA in sequences of the active transcriptional genome might interrupt the normal expression of an endogenous gene, which might lead to embrionary death (Bialek, Chan, & Yee, 2000; Friedman, Adir, Crenshaw, Ryan, & Rosenfeld, 2000).

The F0_184 line was the only line which had 50% of transmission rate (50% of TG and 50% of WT mice) with an equal amount of copies among littermates, indicating a single stable site of transgene integration in the founder mouse. The remaining lines corresponding to founders 156, 194, 172, and 221 had discrepancies between copy number between founder and first generation (F1) which had higher copies of the transgene. This could probably be explained by late integration of the transgene in the genome of the founder (mosaicism) (Haruyama, Cho, & Kulkarni, 2009). Pronuclear microinjection can generate mosaic embryos of the transgene depending on the moment in which the exogenous DNA is integrated in the animal´s genome. If transgenic integration occurs after the first cell division, the animal will be a mosaic for the transgene, therefore only a portion of its cells will carry the transgene (Wilkie, Brinster, & Palmiter, 1986). In 1993, Whitelaw and collaborators determined that the majority of founder transgenic mice came from mosaic embryos (Whitelaw, Springbett, Webster, & Clark, 1993), others mention that about 10-20% of founders are mosaic for the transgene due to late transgene integration during embryogenesis (Haruyama et al., 2009). Transmission rates in F1 and F2 (second generation) for each line can be observed in **Figure 22.** The F2 generation usually shows normal Mendelian segregation and the copy number in this generation is much more stable (Willem Voncken, 2011).

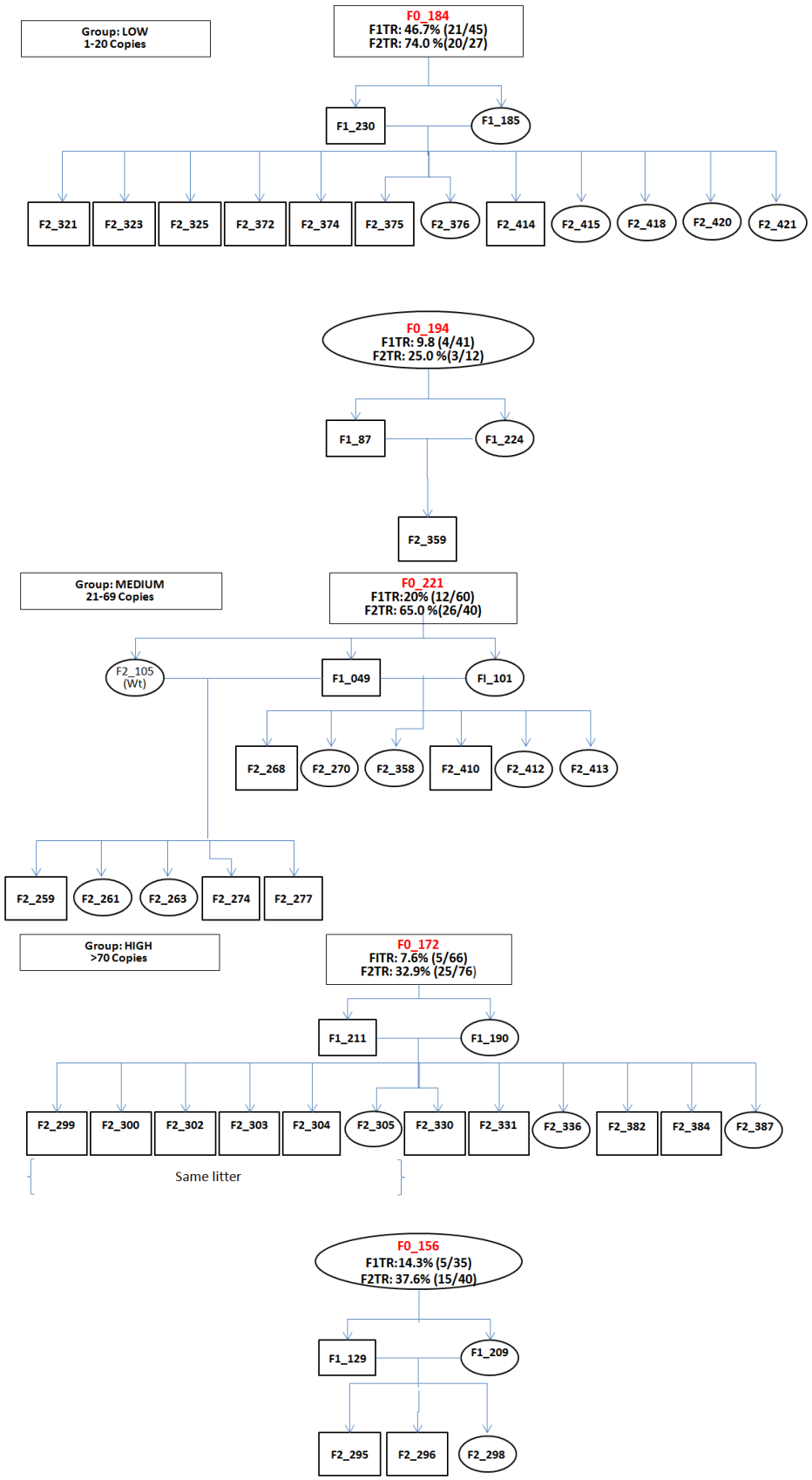

Figure 22. Pedigree and transmission rate in the 5 transgenic lines. F1TR: Transmission rate in F1. F2TR: Transmission rate in F2. WT mice are not represented in the pedigree.

HAS2 expression analyses was also performed by the ($2^{-\Delta\Delta Ct}$) quantification method using the endogenous murine *HAS2* gene as a reference gene and the *HAS2 construction* (transgene) as target. We decided to use skin as the tissue of choice to explore HAS2 expression since it was the tissue in which a *HAS2* over expression was documented in Shar Peis with HCM (Docampo et al., 2011; Giordana Zanna et al., 2009). As expected, endogenous murine *HAS2* was expressed similarly in all samples (WT and TG) and the optimized HAS2 of the chimera construction (*HAS2constructo)* was only expressed in all transgenic mice from the 5 different founder lines. Our overall results indicate that expression of the *HAS2* transgene does not directly depend on the number of integrated copies as can be seen in **Figure 24.** In our murine model, mice belonging to the "low copy number" group had a higher expression (double) of the transgene when compared to mice belonging to the "high copy number" (**Figure 23)**. Several mouse studies report a decrease in the level of expression per copy as copy number increases (Garrick, Fiering, Martin, & Whitelaw, 1998).

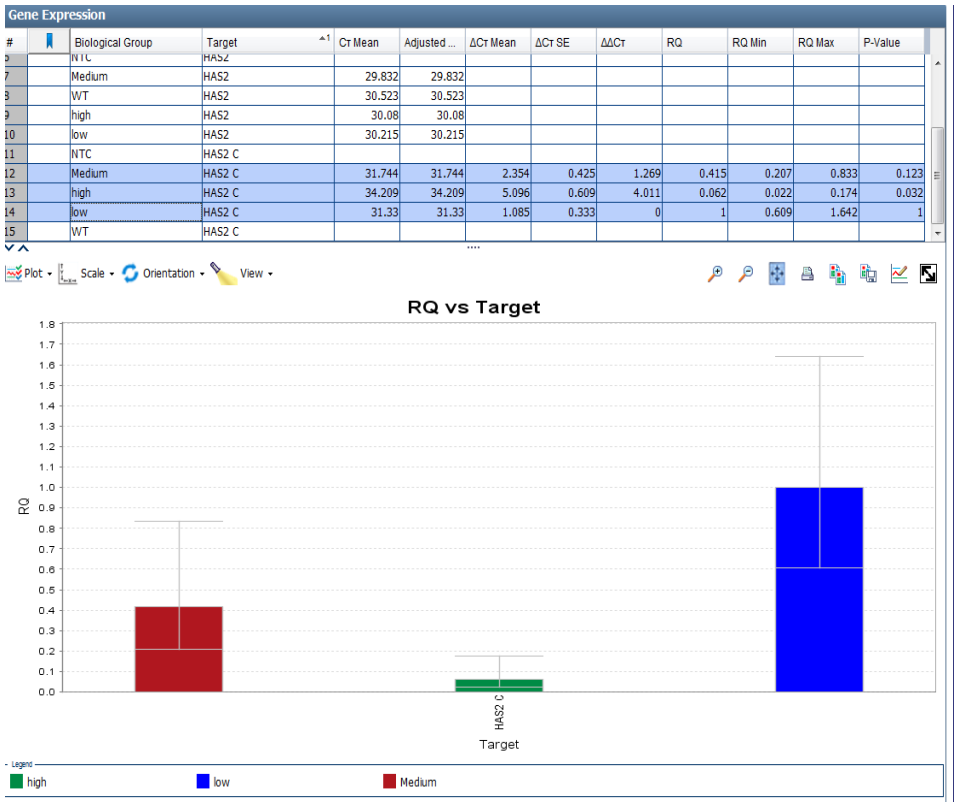

Figure 23. HAS2 construction expression. Notice that transgenic mice belonging to the "low copy number group" had higher expression of the transgene in skin sample.

It could be explained by (i) the site of integration, we believe that the localization of the transgene insertion is key in regulation/expression of the HAS2 gene; and/or (II) the transgene size since it has been generally observed that for large transgenes there is a more consistent correlation than for small constructs (PICCIOTTO & WICKMAN, 1998) (our transgene had a size of 2.7kb, which is considered small).

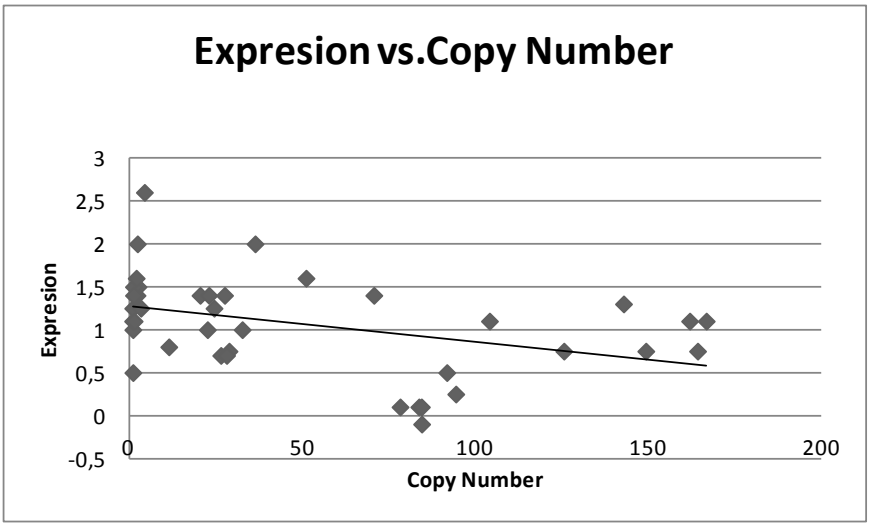

Figure 24. HAS2 construction expression (skin) vs. Copy Number correlation plot. Only transgenic mice [adult (n=20) and young (n-20)] where plotted. *HAS2construc* expression was measured by using the comparative cycle threshold (CT) relative quantification method ($2^{-\Delta\Delta Ct}$) by using the endogenous murine *HAS2* gene as a reference gene and *HAS2 construction* (transgene) as target. Values in Y axis correspond to ΔC and values in X axis correspond to CN.

Two different Enzyme-Linked Immunosorbent Assays (ELISAs) were used to determine HA concentration in murine blood serum. We used serum HA concentration to confirm that we had successfully obtained transgenic mice with increased copies of *HAS2*, which had actually translated into a protein.

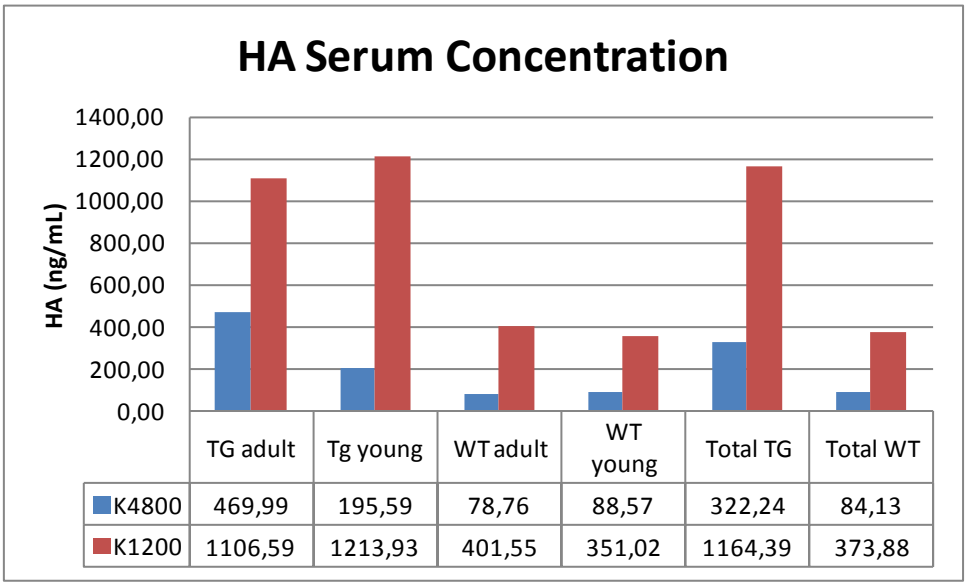

	TG adult	Tg young	WT adult	WT young	Total TG	Total WT
K4800	469,99	195,59	78,76	88,57	322,24	84,13
K1200	1106,59	1213,93	401,55	351,02	1164,39	373,88

Figure 25. HA serum concentration determined by two ELISA assays. Hyaluronic Acid Sandwich ELISA "K4800" (detects HA > 130kDa with a detection range of 12.5-3200ng/µL) and Hyaluronan Competitive ELISA Kit "K1200" (detects all sizes of HA, from 6.4kDa and up- wards with a detection range of 50-1600ng/µL). Assay K1200 is better in detecting LMWHA.

Overall results indicate that transgenic mice had higher concentrations of HA in serum when compared to wild type mice when using both assays **(Figure25)**. Statistical significance using Tukey´s Honestly Significant Difference test was obtained when comparing mice from different groups (ATG, YTG, AWT, and YWT) by using both ELISA assays (p-value: $1.96E^{-6}$ for assay K1200 and p-value: $5.23E^{-5}$ for assay K4800)**.** Absolute values of HA concentration in serum can be found in **Annex 5**.

Even though we successfully created a transgenic mouse which expressed *HAS2,* over produced HA and that in some aspects resembled the phenotype of Shar Pei dogs, we couldn't emulate the Shar Peis characteristic wrinkled skin, nor did we have mice with febrile episodes.

Previous studies mentioned that Shar Pei dogs, especially the "American Shar Pei" had high concentrations of mucin in dermal tissues (G Zanna et al., 2008; Giordana Zanna, Fondevila, Ferrer, & Espada, 2012). The aim of our transgenic model was to obtain a "wrinkled" mouse, simulating the wrinkled skin phenotype of Shar Pei dogs. Necropsy of all the animals included in the study did not reveal any macroscopic lesions. Regarding histopathologic analysis, only 3 mice demonstrated abnormal deposits of mucin in several organs. These animals were all transgenic adults from the F0_156 line. These mice belonged to the high copy number group, their HA concentration in serum was up to 2x higher when compared to other transgenic animals but did not present fever. Mucin depositions were found in heart (myocardium), lung, fore stomach (sub mucosa), peripheric nerves (peri and endoneurium) and skin (superficial dermis). A comparison between transgenic and wild type of different tissues can be seen in **Figure 25**.

Various animals (n= 12) presented general laxity of tissues, being the skin the most common tissue. Laxity was also found in uterus and stomach predominantly on transgenic adults (n= 8), and mice belonging to the F0_221 line. A study by Teixeira Gomes and collaborators reported that HA concentration and distribution in mouse uterine horns changed throughout the estrous cycle and was highest during the diestrous phase(Teixeira Gomes et al., 2009). It could be possible that these mice where in diestrous phase when sacrificied. No other significant findings were reported. Further information on histology of mice included in study can be found in **Annex 6**.

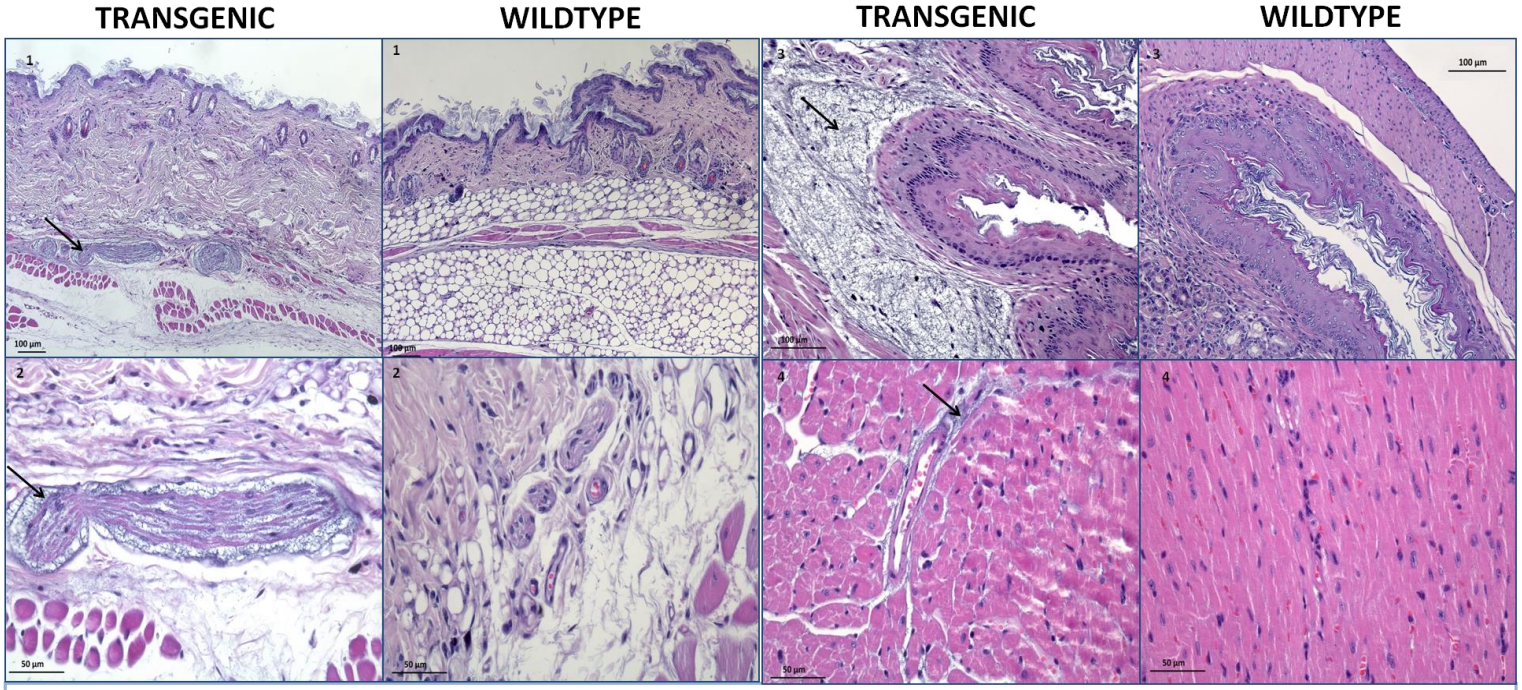

1. Skin
2. Small peripheral nerve in the skin
3. Forestomach (submucosa)
4. Myocardium: supporting tissue of blood vessels and cardiocytes

Black arrows indicate a basophilic substance (mucinous depositions.)

Figure 25. Histology of different tissues in transgenic and wild type mice.

Another phenotype characteristic of Shar Peis is that they suffer from unprovoked fever and inflammation with no underlying autoimmune or infectious cause. Shar Peis suffering FSF, usually have fever outbreaks occurring mostly at young age, but some continue with fever outbreaks until they are adults (Rivas, Tintle, Kimball, Scarlett, & Quimby, 1992). At the time when we first started our study, Olsson and collaborators (Olsson et al., 2011) proposed that a mutation near the *HAS2* gene predisposed Shar Pei dogs to periodic fever syndrome. We wanted to confirm this proposition in generating transgenic mice with increased copies of the *HAS2* gene, and thought that if more serum and tissue HA was produced, then they would probably suffer fever because of activation of other inflammatory routes by LMWHA degradation products (Wolf et al., 2001). We expected ATG and YTG mice to have higher body temperature, especially YTG mice since FSF and FMF are more common in younger patients. Temperature records where obtained 3 times a day (morning, midday, afternoon) for each mouse until the day of sacrifice with temperature records between 36.58°C-37.8°C, all of which were within normal physiological limits (mouse body temperature is 36.5- 38°C) (Zúñiga, Orellana, & Tur, 2008). According to our results, it is only possible to conclude that simply over expression of the *HAS2* gene and higher serum levels of HA do no cause fever in mice. These results, however, also suggest that the periodic fever of the Shar Pei dog has a different, o at least, a more complex pathogenesis. However, it is also possible that the fever is not related to changes in HA metabolism and that the CNV mutation near the *HAS2* gene previously described by Olsson and collaborators is not responsible for the fever episodes in this dog breed. A more recent study (Metzger & Distl, 2014) has refused the association between fever and the "*Meatmouth"* mutation as well suggesting the possibility of other genes implicated in these fever outbreaks.

Hematology was performed principally to further phenotipically characterize our transgenic mice. Only 5 animals (YWT) didn´t have any hematological alteration. In the red blood cell series only 19/80 mice (YWT: 6, AWT: 4, YTG: 8 and ATG: 1) had normal hematologic values. The most common alteration found in red blood series was hemoglobinemia. In the white cell count, 19/80 (YWT: 8, AWT: 4, YTG: 3 and ATG: 4) mice had no alteration, 35 mice (YWT: 10 AWT: 11, YTG: 10 and ATG: 4) presented leucopenia in which lymphocytes and neutrophils were the most common white cells to be diminished. Regarding platelets, 61/80 mice had normal platelet values and the most common alteration was thrombocytopenia which occurred in 16 mice (YWT: 3, AWT: 3, YTG: 7 and ATG: 3). Complete blood Count reports of mice included in the study can be found in **Annex 7**. In general, there was no significant difference when comparing transgenic and wild type mice and in TG animals, there was no significant correlation between hematologic findings, transgene copy number and transgene *HAS2* expression between mice from different lines or groups.

Therefore, our model demonstrates that transgenic mice with several functional copies of the *HAS2* and high serum levels of HA do not present the wrinkled phenotype of Shar Pei dogs, cutaneous hyaluronosis nor fever. With all these results, it is difficult to sustain that the wrinkled skin phenotype and the febrile disorder of the Shar Pei are only consequence of an increased synthesis of HA. It could be that we didn't get the desired wrinkled skin phenotype because the phenotype depends on the transgene integration site, even though we got HAS2

expression in skin. However it is possible that other factors or abnormalities are necessary to create the skin phenotype of Shar Pei dogs and the febrile disorder. It has been soundly demonstrated that Shar Peis dermal fibroblasts produce an excessive amount of HA and HYALs are not differentially expressed between Shar Pei or control dogs (Docampo et al., 2011; Giordana Zanna et al., 2009). One hypothesis could be that Shar Pei dogs might have problems with HA degradation and HA is accumulated in the skin of these dogs since their fibroblasts actively synthesize more HA than they can catabolize as explained Hascall & Laurent (Hascall & Torvard C. Laurent, 1997). The enzymatic degradation of HA results from the action of four types of enzymes: HYAL1, HYAL2, β- glucuronidase and β-N- acetylglucosaminidase (Stern, 2004). The latter two have not been studied in Shar Pei dogs, and perhaps these dogs have diminished enzymatic activity. Our transgenic mice over expressed *HAS2* but as Metzger & Distl (Metzger & Distl, 2014) comment, FSF is not associated with the "*Meatmouth*" duplication near *HAS2* as proposed by Olsson and collaborators (Olsson et al., 2011), and fevers in these dogs might well be explained by other genes in other genomic locations, for instance CFA6 were the canine *MEFV* gene is located.

Results of the transgenic mice generated in this thesis corroborate that many questions regarding the genetic basis of HCH and FSF remained to be answered and different approaches to insight on these diseases have to be used.

GENTIC BACKGROUND

A very recent study (Metzger & Distl, 2014) showed correlation between FSF and wrinkled phenotype but refused the Meatmouth duplication to be responsible for the FSF in Shar Peis as previously mentioned by Olsson et al. (Olsson et al., 2011). The strong wrinkled skin phenotype was supposed to have a predisposition for FSF as a result of HA accumulation that has been correlated with a higher activity of the HAS2. It all seems a true history but perhaps not all the explanation is HA overproduction but a problem with metabolism giving the possibility to think that other regions other than those CNV in CFA13 might be implicated. We tried several different approaches to help give light or open new pathways which might help explain the complexity of FSF and HCH.

By using dermal fibroblasts cultured from six *Meat mouth* Shar Pei, Olsson and collaborators studied the link between copy number and the expression of *HAS2* and *HAS2as* finding that the expression of both genes showed an increasing trend of expression with copy number. They suggested that a possible regulatory element for *HAS2* is located in the duplicated region in CFA 13 (Olsson et al., 2011); however the interpretation of the role of the *HAS2as* gene was not as clear. A study in another cell line (human osteosarcoma) demonstrated a regulatory function of the *HAS2as* regarding HAS2 expression which showed that HAS2 expression was reduced (Chao & Spicer, 2005). We wanted to investigate what occurred in non Shar Pei dogs regarding *HAS2* and *HAS2as* expression and see the role of the canine antisense mRNA. We found out that in non Shar Pei dogs, *HAS2as* was higher expressed when compared to *HAS2* as

occurred in Shar Pei dogs. Therefore we can conclude that *HAS2as* seems to regulate *HAS2* mRNA levels by the same way in all dogs regardless of the mutation described in Shar Pei, since no differences in the relation of the expression of these genes have been found between Shar Peis and other breeds.

As mentioned in the **Introduction**, the enzymatic degradation of HA results from the action of four types of enzymes: HYAL1, HYAL2, β- glucuronidase and β-N- acetylglucosaminidase (Stern, 2004) but only HYALs have been studied without any significant finding in Shar Pei dogs. HA degradation routes including HA cell receptors such as CD44, LYVE-1 and RHAMM have also been studied without any significant changes (Docampo et al., 2011; G Zanna et al., 2008; Giordana Zanna et al., 2009). Hyaluronan degradation products also transduce their inflammatory signal through TLR2 and TLR4 in macrophages and dendritic cells, playing an important role in innate immunity. In general, TLRs studies in humans are aimed to find the relationship between TLR polymorphism and susceptibility/resistance to disease as reviewed by Netea and collaborators (Netea, Wijmenga, & O'Neill, 2012) whereas in dogs, studies have focused on finding how genetic variants in TLRs are different among various dog breeds and if these genetic variants give further insight on a breed´s innate immune response to pathogens and their susceptibility/resistance to infections or autoimmune diseases. Therefore it was of great interest for us to see if we could find if Shar Peis had a significantly different TLR polymorphism, mainly focused on TLR2 and TLR4, which could help give further insight on HCH and FSF. Taking advantage of the data obtained from another study (Cuscó, Sánchez, Altet, Ferrer, & Francino, 2014), we analyzed 3 SNPs of TLR2 and 12 SNPs of TLR4 of which only one SNP of each TLR have a deleterious function. The other SNPs represent neutral substitutions. Frequencies of TLRs 2 and 4 polymorphisms were similar to those in other dog breeds included in the study and there wasn't a specific Shar Pei polymorphism. We found that Shar Peis were the only dog breed which shared the same Non- Synonymous Single Nucleotide Polymorphisms (nsSNPs) variation along with the wolf population in TLR2 (CFA15: 51464700; CanFam 3.1), although it didn't have an effect on the protein function. As Parker and collaborators reviewed, Shar Peis are one of the most ancient dog breeds (Parker et al., 2004), therefore this might help explain why this specific TLR was both found in the wolves population and Shar Pei dogs. Overall results indicate that no specific haplotype or SNP has been found in Shar Pei dogs that may suggest that a TLR signal could play a role in FSF.

To further explore other genomic regions, we used the raw data from the Illumina CanineSNP20 BeadChip using 37 Shar Peis derived from another study (Olsson et al., 2011) to look for homozygosity regions in Shar Peis compared to a non wrinkled dog breed (Ibizan hound). Analysis performed revealed 2 clear homozygosity regions on CFA 6 (40,691,228-51,293,708; CanFam2.0) and CF 13 (23,222,643-27,079,420; CanFam2.0) **(Figure 27)**. A complete list of all genes in these two regions can be found in **Annex 8,** but a list of possible candidate genes that might be related to FSF can be found in **Table 10.**

These regions overlap with regions found in other studies involving Shar Pei dogs ant their different phenotypic characteristics (**Table 11);** but curiously all efforts since to the moment has been focused in CFA13 and its CNV (Akey et al., 2010; Nicholas, Baker, Eichler, & Akey,

2011; Olsson et al., 2011; Vaysse et al., 2011). Homozygosity region in CFA 6 harbors the *MEFV* gene which is the gene responsible for Familiar Mediterranean Fever in humans. In the dog, the *MEFV* and *TNFR1* genes have been identified and cloned but no mutations related to the disease have been found (unpublished work). Conversely, our results denote an specific haplotype characteristic to Shar Pei dogs in CFA6 (**Figure 30)** which includes 2 genes (*TNFR1* and *MEFV)* and a CNV (Nicholas et al., 2011). Moreover, other candidate genes are included within these regions such as *OR2C1, NPRL3, ZNF200, CASP16, ZNF205, TNFRSF12A* and *HAGH* which in humans have been related to Familial Mediterranean Fever and Human CAPS (Cryopyrin-associated periodic syndromes).

We believe that it is important to consider other genomic regions such as that in CFA 6 which harbors many candidate genes since maybe they can further help to explain HCH and FSF. This is why we´ve decided to perform an ambitious approach by massive sequencing Shar Pei dogs with extreme phenotypes (wrinkles and fever) vs., traditional Shar Peis with no fever, as well as other dog breeds to further inquire into the genetic background of these diseases as well as to finally confirm if HCH and FSF are related sharing a common genetic background or if they are two separate entities.

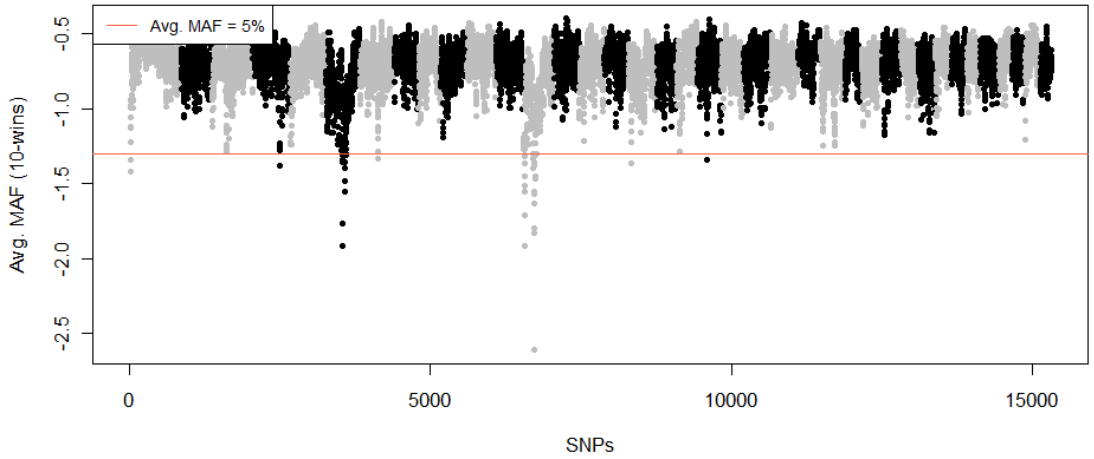

Figure 27. SNPs with average MAF <5% indicate strong signals in CFAs 6 and 13.

Table 11. Shar Pei Homozygosity regions in CFA 6 and CFA 13. Homozygosity region in CFA6 (Olsson et al., 2011)

	Our Study		**(Akey et al., 2010)**	**(Olsson et al., 2011)**		**(Vaysse et al., 2011)**		**(Nicholas et al., 2011)**	
CFA	Start	End		Start	End	Start	End	Start	End
6	40.691.228	51.293.708	44.693.880	*	*	40.695.686	411.096.221	40,876,217	40,974,223
13	23.222.643	27.079.420	26.415.740	23.743.906	23.762.189	23.845.380	24.150.791		

Table 10. List of Candidate Genes in chromosomes 6 and 13.

	CAN FAM 2		**CAN FAM 3**		EMSEMBLE	**Gene**	**Gene Name**	**Related Diseases**
chr6	40886307	40887619	37844712	37845650	ENSCAFG00000019302	**OR2C1**	**olfactory receptor, family 2, subfamily C, member 1**	**Familial mediterranean fever** and neuronitis.
chr6			40352963	40389489	ENSCAFG00000019696	NPRL3	Nitrogen permease regulator-like 3	Secondary hypertrophic osteoarthropathy, myoblastoma. Human CAPS (Cryopyrin-associated periodic syndromes) producing direct inflammasome mutations that results in IL-1β release.
chr6	41012203	41025333	37970548	37983737	ENSCAFG00000024473.2	**MEFV**	**Mediterranean Fever**	**Familial mediterranean fever**, serositis, hereditary periodic fever syndromes, muckle-wells syndrome, cold hypersensitivity, tumor necrosis factor receptor-associated periodic syndrome, renal amyloidosis, cinca syndrome, amyloidosis, brucellosis, psoriatic juvenile idiopathic arthritis , Behcet's disease, idiopathic recurrent pericarditis, Intermittent hydrarthrosis, polyarteritis nodosa, erysipelas.
chr6	41030049	41042812	37988373	38004294	ENSCAFG00000031888	**ZNF200**	**zinc finger protein 200**	**Familial mediterranean fever**,Fanconi's anemia and prostatitis.
chr6	41106459	41108818	38063599	38073992	ENSCAFG00000030711	**CASP16**	**caspase 16, apoptosis-related cysteine peptidase**	**Familial mediterranean fever.**
chr6	41113151	41133840	38085231	38093675	ENSCAFG00000023869	**ZNF205**	**zinc finger protein 205**	**Familial mediterranean fever,** intrahepatic cholangiocarcinoma, ataxia.
chr6	41208321	41209735	***38166719***	***38168133***	ENSCAFG00000023134	**TNFRSF12A**	**Canis lupus familiaris tumor necrosis factor receptor superfamily, member 12A**	Skeletal muscle regeneration, psoriatic arthritis, rheumatoid arthritis, multiple sclerosis, lupus, nephritis, kaposi's sarcoma, renal cell carcinoma, Multiple myeloma, prostate cancer, colon adenocarcinoma, hepatitis b, prostate cancer, atherosclerosis, hepatocellular carcinoma gingivitis ovarian cancer
chr6	42125683	42146748	39084527	39105592	ENSCAFG00000019490	**HAGH**	**Hydroxyacylglutathione Hydrolase**	Glyoxalase ii deficiency , **Familial mediterranean fever,** muscular dystrophy, thrombocytosis, bladder carcinoma, hepatitis b, hyperglycemia,, prostate cancer, breast cancer, prostatitis.
chr13	23348772	23364912	20311698	20327838	ENSCAFG00000029394	**HAS2**	**Hyaluronan synthase 2**	**Periodic Fever Syndrome,** Lipoblastoma arthropathy, rheumatoid arthritis, osteosarcoma, morquio syndrome b, arthritis, sly syndrome eye disease, mucopolysaccharidoses, osteoarthritis, prostate adenocarcinoma fibrosarcoma, hyperglycemia, multiple myeloma *atopic dermatitis,* diabetic nephropathy, peritonitis,endometrial carcinoma, aterosclerosis.

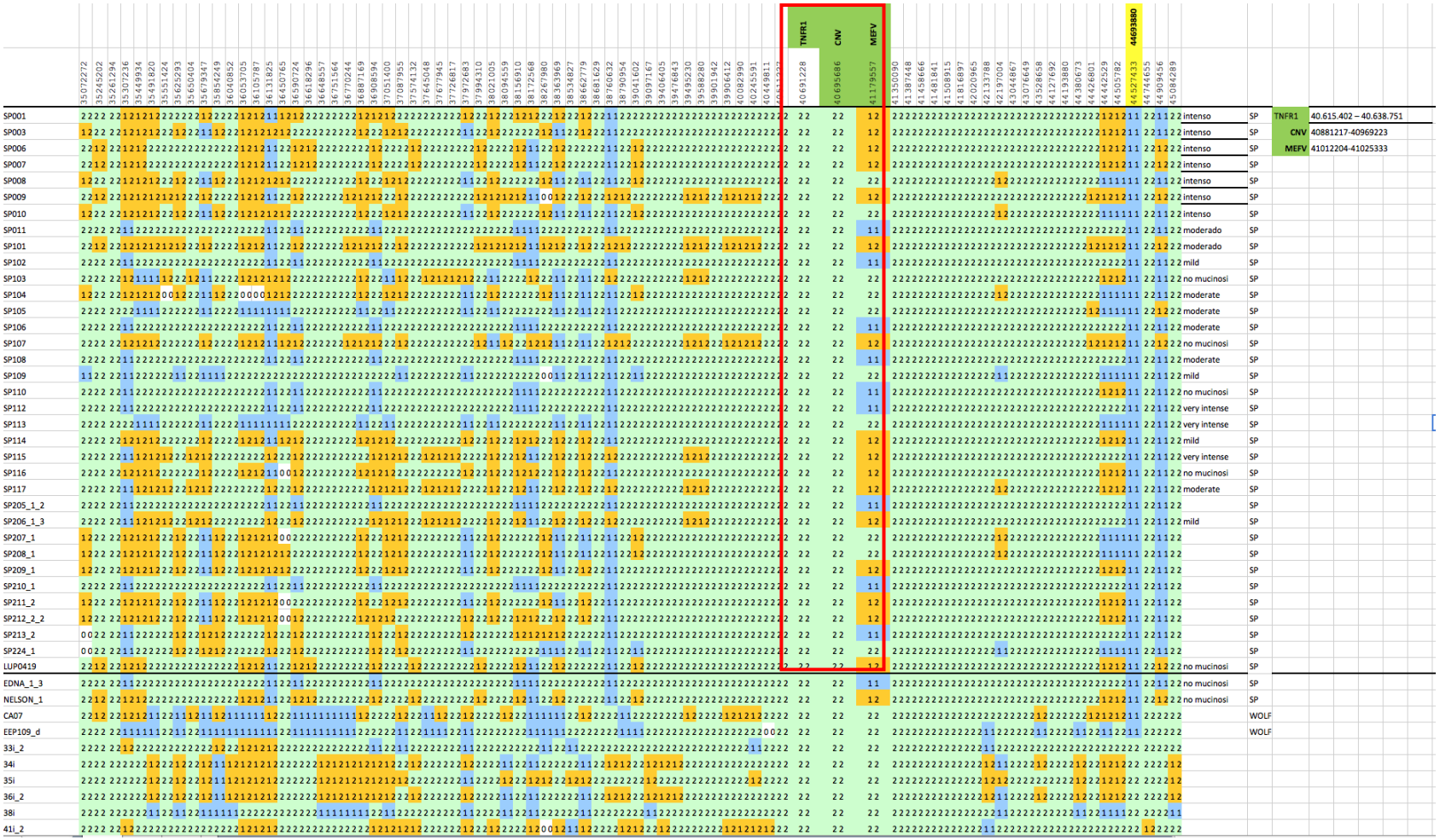

Figure 28. Homozygous haplotype in Shar Pei. First 37 lanes correspond to Shar Pei dogs, remaining lanes are controls (Ibizan Hound and wolf).

CONCLUSIONS

Even though we successfully created a transgenic mouse which expressed *HAS2,* over produced HA and that in some aspects resembled the phenotype of Shar Pei dogs, we couldn't emulate the Shar Peis characteristic wrinkled skin, nor did we have mice with febrile episodes. With all these results, it is difficult to sustain that the wrinkled skin phenotype and the febrile disorder of the Shar Pei are only consequence of an increased synthesis of HA and other factors or abnormalities are necessary to create the skin phenotype of Shar Pei dogs and the febrile disorder.

Our results denote an specific haplotype characteristic to Shar Pei dogs in CFA6 which is a candidate region to further analyze since it harbors many candidate genes such as *MEFV, OR2C1, NPRL3, ZNF200, CASP16, ZNF205, TNFRSF12A* and *HAGH* which in humans are related to Familial Mediterranean Fever and Human CAPS (Cryopyrin-associated periodic syndromes).

REFERENCES

Akey, J. M., Ruhe, A. L., Akey, D. T., Wong, A. K., Connelly, C. F., Madeoy, J., … Neff, M. W. (2010). Tracking footprints of artificial selection in the dog genome. *Proceedings of the National Academy of Sciences of the United States of America*, *107*(3), 1160–1165. doi:10.1073/pnas.0909918107

American Kennel Club Breed Standards. (n.d.). Retrieved May 24, 2014, from http://www.akc.org/breeds/chinese_shar_pei/breed_standard.cfm

Austin, C. P., Battey, J. F., Bradley, A., Bucan, M., Capecchi, M., Collins, F. S., … Zambrowicz, B. (2004). The knockout mouse project. *Nature Genetics*, *36*, 921–924. doi:10.1038/ng0904-921

Ballester, M., Castelló, A., Ibáñez, E., Sánchez, A., & Folch, J. M. (2004). Real-time quantitative PCR-based system for determining transgene copy number in transgenic animals. *BioTechniques*, *37*(4), 610–3. Retrieved from http://www.ncbi.nlm.nih.gov/pubmed/15517974

BEALE, K. M., CALDERWOOD-MAYS, M. B., & BUCHANAN, B. (1991). Papular and Plaque-like Mucinosis in a Puppy. *Veterinary Dermatology*, *2*(1), 29–36. doi:10.1111/j.1365-3164.1991.tb00107.x

Bialek, P., Chan, C. T., & Yee, S. P. (2000). Characterization of a novel insertional mouse mutation, kkt: A closely linked modifier of Pax1. *Developmental Biology*, *218*(2), 354–66. doi:10.1006/dbio.1999.9584

Björk, J., Kleinau, S., Tengblad, A., & Smedegård, G. (1989). Elevated levels of serum hyaluronate and correlation with disease activity in experimental models of arthritis. *Arthritis & Rheumatism*, *32*, 306–311.

Bonagura, J. ., & Twedt, D. . (Eds.). (2009). Shar Pei Fever Syndrome. In *kirk´s Current Veterinary Therapy* (XIV., pp. 1188–1195). St. Louis: Saunders Elsevier.

Camenisch, T. D., Spicer, A. P., Brehm-Gibson, T., Biesterfeldt, J., Augustine, M. L., Calabro, A., … McDonald, J. A. (2000). Disruption of hyaluronan synthase-2 abrogates normal cardiac morphogenesis and hyaluronan-mediated transformation of epithelium to mesenchyme. *The Journal of Clinical Investigation*, *106*, 349–360. doi:10.1172/JCI10272

Chae, J. J., Cho, Y. H., Lee, G. S., Cheng, J., Liu, P. P., Feigenbaum, L., … Kastner, D. L. (2011). Gain-of-Function Pyrin Mutations Induce NLRP3 Protein-Independent Interleukin-1?? Activation and Severe Autoinflammation in Mice. *Immunity*, *34*, 755–768. doi:10.1016/j.immuni.2011.02.020

Chae, J. J., Wood, G., Richard, K., Jaffe, H., Colburn, N. T., Masters, S. L., … Kastner, D. L. (2008). The familial Mediterranean fever protein, pyrin, is cleaved by caspase-1 and activates NF-kappaB through its N-terminal fragment. *Blood*, *112*(5), 1794–803. doi:10.1182/blood-2008-01-134932

Chandler, K. J., Chandler, R. L., Broeckelmann, E. M., Hou, Y., Southard-Smith, E. M., & Mortlock, D. P. (2007). Relevance of BAC transgene copy number in mice: transgene copy number variation across multiple transgenic lines and correlations with transgene integrity and expression. *Mammalian Genome : Official Journal of the International Mammalian Genome Society*, *18*(10), 693–708. doi:10.1007/s00335-007-9056-y

Chao, H., & Spicer, A. P. (2005). Natural antisense mRNAs to hyaluronan synthase 2 inhibit hyaluronan biosynthesis and cell proliferation. *The Journal of Biological Chemistry*, *280*(30), 27513–27522. doi:10.1074/jbc.M411544200

Chinese Shar-Pei. (n.d.). Retrieved May 25, 2014, from http://www.chinese-sharpei.com/history/time.htm

Clements, C. A., Rogers, K. S., Green, R. A., & Loy, J. K. (1995). Splenic vein thrombosis resulting in acute anemia: an unusual manifestation of nephrotic syndrome in a Chinese shar pei with reactive amyloidosis. *Journal of the American Animal Hospital Association*, *31*(5), 411–5. Retrieved from http://www.ncbi.nlm.nih.gov/pubmed/8542358

Collins, J. (1982). *History and Qualities of the Chinese Shar-Pei*. Dogworld.

Cruz, F., Vilá, C., & Webster, M. T. (2008). The legacy of domestication: Accumulation of deleterious mutations in the dog genome. *Molecular Biology and Evolution*, *25*, 2331–2336. doi:10.1093/molbev/msn177

Cuscó, A., Sánchez, A., Altet, L., Ferrer, L., & Francino, O. (2014). Non-synonymous genetic variation in exonic regions of canine Toll-like receptors. *Canine Genetics and Epidemiology*, *In press*.

David G. Jackson. (2004). The Lymphatic Endothelial Hyaluronan Receptor LYVE-1. Retrieved May 26, 2014, from http://glycoforum.gr.jp/science/hyaluronan/HA28/HA28E.html

DiBartola, S. P., Tarr, M. J., Webb, D. M., & Giger, U. (1990). Familial renal amyloidosis in Chinese Shar Pei dogs. *Journal of the American Veterinary Medical Association*, *197*(4), 483–487. Retrieved from http://www.ncbi.nlm.nih.gov/pubmed/2211293

Dickie, M. M. (1966). Keeping Records. In E. L. GREEN (Ed.), *Biology of the Laboratory Mouse* (2nd ed., pp. 522–537). NEW YORK 1966: DOVER PUBLICATIONS, INC. Retrieved from http://www.informatics.jax.org/greenbook/index.shtml

Dillberger, J. E., & Altman, N. H. Focal mucinosis in dogs: seven cases and review of cutaneous mucinoses of man and animals., 23 Veterinary pathology 132–139 (March 01, 1986). doi:10.1177/030098588602300205

Ditto, T. B. (2006). *Shar-Pei a Complete Pet Owners Manual* (2nd ed., pp. 6–9). Barron´s Educational Series Inc.

Docampo, M. J., Zanna, G., Fondevila, D., Cabrera, J., López-Iglesias, C., Carvalho, A., … Bassols, A. (2011). Increased HAS2-driven hyaluronic acid synthesis in shar-pei dogs with hereditary cutaneous hyaluronosis (mucinosis). *Veterinary Dermatology*, *22*(6), 535–45. doi:10.1111/j.1365-3164.2011.00986.x

Doliger, S., Delverdier, M., Moré, J., Longeart, L., Régnier, A., & Magnol, J. P. (1995). Histochemical study of cutaneous mucins in hypothyroid dogs. *Veterinary Pathology*, *32*, 628–634. doi:10.1177/030098589503200603

Edward, M., Fitzgerald, L., Thind, C., Leman, J., & Burden, A. D. (2007). Cutaneous mucinosis associated with dermatomyositis and nephrogenic fibrosing dermopathy: fibroblast hyaluronan synthesis and the effect of patient serum. *The British Journal of Dermatology*, *156*(3), 473–9. doi:10.1111/j.1365-2133.2006.07652.x

Foundation, K., & Microarryay, B. (n.d.). TRIZOL RNA Isolation Protocol, 5–7.

Fraser, J. R., Laurent, T. C., & Laurent, U. B. (1997). Hyaluronan: its nature, distribution, functions and turnover. *Journal of Internal Medicine*, *242*(1), 27–33.

Friedman, R. A., Adir, Y., Crenshaw, E. B., Ryan, A. F., & Rosenfeld, M. G. (2000). A transgenic insertional inner ear mutation on mouse chromosome 1. *The Laryngoscope*, *110*(4), 489–96. doi:10.1097/00005537-200004000-00001

Garrick, D., Fiering, S., Martin, D. I., & Whitelaw, E. (1998). Repeat-induced gene silencing in mammals. *Nature Genetics*, *18*(1), 56–9. doi:10.1038/ng0198-56

George, J., & Stern, R. (2004). Serum hyaluronan and hyaluronidase: Very early markers of toxic liver injury. *Clinica Chimica Acta*, *348*(1-2), 189–197. doi:10.1016/j.cccn.2004.05.018

Gross, T., Ihrke, P., Walder, E., & Affolter, V. (2005). Disease of the dermis: cutaneous mucinosis. In *Skin diseases of the dog and cat. Clinical and Histopathologic diagnosis.* (2ND ed., pp. 380–383). Oxford, UK: Blackwell Publishing.

Haruyama, N., Cho, A., & Kulkarni, A. B. (2009). Overview: engineering transgenic constructs and mice. *Current Protocols in Cell Biology / Editorial Board, Juan S. Bonifacino ... [et.al.,.]*, *Chapter 19*, Unit 19.10. doi:10.1002/0471143030.cb1910s42

Hascall, V. C., & Torvard C. Laurent. (1997). Hyaluronan: Structure and Physical properties. *Glycoforum*. Retrieved April 20, 2014, from http://glycoforum.gr.jp/science/hyaluronan/HA01/HA01E.html

Henry, C. B., & Duling, B. R. (1999). Permeation of the luminal capillary glycocalyx is determined by hyaluronan. *The American Journal of Physiology*, *277*, H508–H514.

Hogan, B., Beddington, R., Costantini, F., & Lacy, E. (1994). *Manipulating the mouse embryo. A laboratory manual* (2nd ed.). New York- United States: Cold Spring Harbor Laboratory Press.

Houdebine, L. M. (2005). Use of transgenic animals to improve human health and animal production. In *Reproduction in Domestic Animals* (Vol. 40, pp. 269–281). doi:10.1111/j.1439-0531.2005.00596.x

Immunity. (2014). *Wikipedia*. Retrieved May 25, 2014, from http://en.wikipedia.org/wiki/Immunity_(medical)

Itano, N., Sawai, T., Yoshida, M., Lenas, P., Yamada, Y., Imagawa, M., … Kimata, K. (1999). Three isoforms of mammalian hyaluronan synthases have distinct enzymatic properties. *The Journal of Biological Chemistry*, *274*(35), 25085–25092.

Iwasaki, A., & Medzhitov, R. (2004). Toll-like receptor control of the adaptive immune responses. *Nature Immunology*, *5*, 987–995. doi:10.1038/ni1112

Jiang, D., Liang, J., Li, Y., & Noble, P. W. (2006). The role of Toll-like receptors in non-infectious lung injury. *Cell Research*, *16*, 693–701. doi:10.1038/sj.cr.7310085

Jiang, D., Liang, J., & Noble, P. W. (2007). Hyaluronan in tissue injury and repair. *Annual Review of Cell and Developmental Biology*, *23*, 435–461. doi:10.1146/annurev.cellbio.23.090506.123337

Jiang, D., Liang, J., & Noble, P. W. (2011). Hyaluronan as an immune regulator in human diseases. *Physiological Reviews*, *91*(1), 221–264. doi:10.1152/physrev.00052.2009

Karlsson, E. K., Baranowska, I., Wade, C. M., Salmon Hillbertz, N. H. C., Zody, M. C., Anderson, N., … Lindblad-Toh, K. (2007). Efficient mapping of mendelian traits in dogs through genome-wide association. *Nature Genetics*, *39*(11), 1321–1328. doi:10.1038/ng.2007.10

Kastner, D. L., Aksentijevich, I., & Goldbach-Mansky, R. (2010). Autoinflammatory Disease Reloaded: A Clinical Perspective. *Cell*. doi:10.1016/j.cell.2010.03.002

Kaya, G., Augsburger, E., Stamenkovic, I., & Saurat, J. H. (2000). Decrease in epidermal CD44 expression as a potential mechanism for abnormal hyaluronate accumulation in

superficial dermis in lichen sclerosus et atrophicus. *The Journal of Investigative Dermatology*, *115*(6), 1054–1058.

Knee, R., & Murphy, P. R. (1997). Regulation of gene expression by natural antisense RNA transcripts. *Neurochemistry International*, *31*(3), 379–92. Retrieved from http://www.ncbi.nlm.nih.gov/pubmed/9246680

Kuroda, K., Fujimoto, N., & Tajima, S. (2005). Abnormal accumulation of inter-alpha-trypsin inhibitor and hyaluronic acid in lichen sclerosus. *Journal of Cutaneous Pathology*, *32*(2), 137–40. doi:10.1111/j.0303-6987.2005.00273.x

Lab Animal Identification - Bio Medic Data Systems » Products » Transponders » IPT-300. (2013). Retrieved June 26, 2014, from http://www.bmds.com/products/transponders/ipt-300

Lachmann, H. J., Goodman, H. J. B., Gilbertson, J. A., Gallimore, J. R., Sabin, C. A., Gillmore, J. D., & Hawkins, P. N. (2007). Natural history and outcome in systemic AA amyloidosis. *The New England Journal of Medicine*, *356*, 2361–2371. doi:10.1056/NEJMoa070265

Laurent, T. C., and Fraser, J. R. E. (1986). The properties and turnover of hyaluronan. In *Ciba Foundation Symposium Functions of Proteoglycans* (pp. 9–29). Wiley, Chichester, England.

Leach, J. B., & Schmidt, C. E. (2004). *Encyclopedia of Biomaterials and Biomedical Engineering* (pp. 779–789). New York: Marcel Dekker. doi:10.3109/9781420078039.135

Lee, S.-G., Moon, H.-S., Han, J.-H., Yoon, B.-I., & Hyun, C. (2007). Familiar renal amyloidosis in Shar Pei dog. *Korean J Vet Res*, *47*, 255–257.

Li, S., Hammer, R. E., George-Raizen, J. B., Meyers, K. C., & Garrard, W. T. (2000). High-level rearrangement and transcription of yeast artificial chromosome-based mouse Ig kappa transgenes containing distal regions of the contig. *Journal of Immunology (Baltimore, Md. : 1950)*, *164*, 812–824.

Lindblad-Toh, K., Wade, C. M., Mikkelsen, T. S., Karlsson, E. K., Jaffe, D. B., Kamal, M., … Lander, E. S. (2005). Genome sequence, comparative analysis and haplotype structure of the domestic dog. *Nature*, *438*(7069), 803–19. doi:10.1038/nature04338

Livak, K. J., & Schmittgen, T. D. (2001). Analysis of relative gene expression data using real-time quantitative PCR and the 2(-Delta Delta C(T)) Method. *Methods*, *25*(4), 402–8. doi:10.1006/meth.2001.1262

Loeven, K. O. Hepatic amyloidosis in two Chinese Shar Pei dogs., 204 Journal of the American Veterinary Medical Association 1212–1216 (1994).

López, A., Spracklin, D., McConkey, S., & Hanna, P. Cutaneous mucinosis and mastocytosis in a shar-pei., 40 The Canadian veterinary journal. La revue veterinaire canadienne 881–3 (December 1999). Retrieved from http://www.pubmedcentral.nih.gov/articlerender.fcgi?artid=1539873&tool=pmcentrez&rendertype=abstract

MADEWELL, B. R., AKITA, G. Y., & VOGEL, P. (1992). Cutaneous Mastocytosis and Mucinosis with Gross Deformity in a Shar pei Dog. *Veterinary Dermatology*, *3*(4-5), 171–175. doi:10.1111/j.1365-3164.1992.tb00167.x

Martinon, F., Pétrilli, V., Mayor, A., Tardivel, A., & Tschopp, J. (2006). Gout-associated uric acid crystals activate the NALP3 inflammasome. *Nature*, *440*, 237–241. doi:10.1038/nature04516

McDonald Brearley, J. (1991). *The Book of the Shar-Pei* (pp. 15–34). United States: TFH Publications Inc.

MEFV - Mediterranean fever. (2011). US National Library of Medicine, National Institutes of Health, Department of Health & Human Services. Retrieved from http://ghr.nlm.nih.gov/gene/MEFV

Metzger, J., & Distl, O. (2014). A study of Shar-Pei dogs refutes association of the “meatmouth” duplication near HAS2 with Familial Shar-Pei Fever. *Animal Genetics*, *45*(5), 763–4. doi:10.1111/age.12193

Meyer, K., & Palmer, J. W. (1934). The polysaccharide of the vitreous humor. *Journal of Biology and Chemistry*, *107*, 629–634.

Miller, C. W., Prescott, J. F., Mathews, K. A., Betschel, S. D., Yager, J. A., Guru, V., … Low, D. E. (1996). Streptococcal toxic shock syndrome in dogs. *Journal of the American Veterinary Medical Association*, *209*, 1421–1426.

Mio, K., & Stern, R. (2002). Inhibitors of the hyaluronidases. *Matrix Biology*. doi:10.1016/S0945-053X(01)00185-8

Necas, J., Bartosikova, L., Brauner, P., & Kolar, J. (2008). Hyaluronic acid (hyaluronan): a review, *2008*(8), 397–411.

Netea, M. G., Wijmenga, C., & O’Neill, L. a. (2012). Genetic variation in Toll-like receptors and disease susceptibility. *Nature Immunology*, *13*, 535–542. doi:10.1038/ni.2284

Nicholas, T. J., Baker, C., Eichler, E. E., & Akey, J. M. (2011). A high-resolution integrated map of copy number polymorphisms within and between breeds of the modern domesticated dog. *BMC Genomics*, *12*(1), 414. doi:10.1186/1471-2164-12-414

Olsson, M. (2012). *Uncovering a Novel Pathway for Autoinflammation With a Little Help from a Wrinkled Friend*.

Olsson, M. I. A. (2012). *Uncovering a Novel Pathway for Autoinflammation With a Little Help from a Wrinkled Friend*.

Olsson, M., Meadows, J. R. S., Truv??, K., Pielberg, G. R., Puppo, F., Mauceli, E., … Lindblad-Toh, K. (2011). A novel unstable duplication upstream of HAS2 predisposes to a breed-defining skin phenotype and a periodic fever syndrome in Chinese Shar-Pei dogs. *PLoS Genetics*, *7*(3), e1001332. doi:10.1371/journal.pgen.1001332

Olsson, M., Tintle, L., Kierczak, M., Perloski, M., Tonomura, N., Lundquist, A., … Meadows, J. R. S. (2013). Thorough Investigation of a Canine Autoinflammatory Disease (AID) Confirms One Main Risk Locus and Suggests a Modifier Locus for Amyloidosis. *PLoS ONE*, *8*. doi:10.1371/journal.pone.0075242

Ostrander, E. A., Galibert, F., & Patterson, D. F. (2000). Canine genetics comes of age. *Trends in Genetics*, *16*(3), 117–124. doi:10.1016/S0168-9525(99)01958-7

Ozen, S., & Bilginer, Y. (2014). A clinical guide to autoinflammatory diseases: familial Mediterranean fever and next-of-kin. *Nature Reviews. Rheumatology*, *10*(3), 135–47. doi:10.1038/nrrheum.2013.174

Papadimitraki, E. D., Bertsias, G. K., & Boumpas, D. T. (2007). Toll like receptors and autoimmunity: A critical appraisal. *Journal of Autoimmunity*. doi:10.1016/j.jaut.2007.09.001

Park, H., Bourla, A. B., Kastner, D. L., Colbert, R. A., & Siegel, R. M. (2012). Lighting the fires within: the cell biology of autoinflammatory diseases. *Nature Reviews Immunology*. doi:10.1038/nri3261

Parker, H. G., Kim, L. V, Sutter, N. B., Carlson, S., Lorentzen, T. D., Malek, T. B., … Kruglyak, L. (2004). Genetic structure of the purebred domestic dog. *Science (New York, N.Y.)*, *304*(5674), 1160–4. doi:10.1126/science.1097406

PICCIOTTO, M. R., & WICKMAN, K. (1998). Using Knockout and Transgenic Mice to Study Neurophysiology and Behavior. *Physiol Rev*, *78*(4), 1131–1163. Retrieved from http://physrev.physiology.org/content/78/4/1131

Pienimaki, J. P., Rilla, K., Fulop, C., Sironen, R. K., Karvinen, S., Pasonen, S., … Tammi, M. I. (2001). Epidermal growth factor activates hyaluronan synthase 2 in epidermal keratinocytes and increases pericellular and intracellular hyaluronan. *The Journal of Biological Chemistry*, *276*(23), 20428–20435. doi:10.1074/jbc.M007601200

Plevris, J. N., Haydon, G. H., Simpson, K. J., Dawkes, R., Ludlum, C. A., Harrison, D. J., & Hayes, P. C. (2000). Serum hyaluronan--a non-invasive test for diagnosing liver cirrhosis. *European Journal of Gastroenterology & Hepatology*, *12*, 1121–1127. doi:10.1097/00042737-200012100-00009

Prehm, P. (1984). Hyaluronate is synthesized at plasma membranes. *The Biochemical Journal*, *220*, 597–600.

Purcell, S., Neale, B., Todd-Brown, K., Thomas, L., Ferreira, M. A. R., Bender, D., … Sham, P. C. (2007). PLINK: a tool set for whole-genome association and population-based linkage analyses. *American Journal of Human Genetics*, *81*, 559–575. doi:10.1086/519795

R Statistical Package. (n.d.). Retrieved from http://www.r-project.org/

R??cken, C., & Shakespeare, A. (2002). Pathology, diagnosis and pathogenesis of AA amyloidosis. *Virchows Archiv*. doi:10.1007/s00428-001-0582-9

Ramsden, C. A., Bankier, A., Brown, T. J., Cowen, P. S., Frost, G. I., McCallum, D. D., … Fraser, J. R. (2000). A new disorder of hyaluronan metabolism associated with generalized folding and thickening of the skin. *The Journal of Pediatrics*, *136*(1), 62–8. Retrieved from http://www.ncbi.nlm.nih.gov/pubmed/10636976

Redditt, J. A. T. (1989). *Understanding the Chinese Shar-Pei* (19th ed., pp. 16–28). Arlington, VA, USA: Orient Publications Inc.

Redditt, J. A. T. (1992). The Chinese Shar pei. *American Kennel Club Gazette*, 109: 42–47.

Reed, R. K., Lilja, K., & Laurent, T. C. (1988). Hyaluronan in the rat with special reference to the skin. *Acta Physiologica Scandinavica*, *134*, 405–411. doi:10.1111/j.1748-1716.1988.tb08508.x

Rivas, A. L., Tintle, L., Kimball, E. S., Scarlett, J., & Quimby, F. W. (1992). A canine febrile disorder associated with elevated interleukin-6. *Clinical Immunology and Immunopathology*, *64*(1), 36–45. Retrieved from http://www.ncbi.nlm.nih.gov/pubmed/1606750

Rongioletti, F. (2006). Lichen myxedematosus (papular mucinosis): new concepts and perspectives for an old disease. *Seminars in Cutaneous Medicine and Surgery*, *25*(2), 100–4. doi:10.1016/j.sder.2006.04.001

Roy, C. N. (2010). Anemia of inflammation. *Hematology / the Education Program of the American Society of Hematology. American Society of Hematology. Education Program*, *2010*(1), 276–80. doi:10.1182/asheducation-2010.1.276

Scheibner, K. a., Lutz, M. a., Boodoo, S., Fenton, M. J., Powell, J. D., & Horton, M. R. (2006). Hyaluronan Fragments Act as an Endogenous Danger Signal by Engaging TLR2. *The Journal of Immunology*, *177*(2), 1272–1281. doi:10.4049/jimmunol.177.2.1272

Schnare, M., Barton, G. M., Holt, A. C., Takeda, K., Akira, S., & Medzhitov, R. (2001). Toll-like receptors control activation of adaptive immune responses. *Nature Immunology*, *2*, 947–950. doi:10.1038/ni712

Segev, G., Cowgill, L. D., Jessen, S., Berkowitz, A., Mohr, C. F., & Aroch, I. (2012). Renal Amyloidosis in Dogs: A Retrospective Study of 91 Cases with Comparison of the Disease between Shar-Pei and Non-Shar-Pei Dogs. *Journal of Veterinary Internal Medicine*, *26*, 259–268. doi:10.1111/j.1939-1676.2011.00878.x

Shohat, M., & Halpern, G. J. (2011). Familial Mediterranean fever--a review. *Genetics in Medicine : Official Journal of the American College of Medical Genetics*, *13*(6), 487–98. doi:10.1097/GIM.0b013e3182060456

Spicer, A. P., & Mcdonald, J. A. (1998). Eukaryotic Hyaluronan Synthases. *Glycoforum*. Retrieved May 25, 2014, from http://glycoforum.gr.jp/science/hyaluronan/HA07/HA07E.html

Staff American Kennel Club. (1998). *The Complete Dog Book* (19th ed., pp. 493–496). New York- United States: Howell Book House.

Stern, R. (2003). Devising a pathway for hyaluronan catabolism: are we there yet? *Glycobiology*, *13*(12), 105R–115R. doi:10.1093/glycob/cwg112

Stern, R. (2004a). Hyaluronan catabolism: a new metabolic pathway. *European Journal of Cell Biology*, *83*(7), 317–325.

Stern, R. (2004b). Update on the Mammalian Hyaluronidases. *Glycoforum*. Retrieved May 03, 2014, from http://www.glycoforum.gr.jp/science/hyaluronan/HA15a/HA15aE.html

Stern, R., Asari, A. A., & Sugahara, K. N. (2006). Hyaluronan fragments: An information-rich system. *European Journal of Cell Biology*, *85*, 699–715. doi:10.1016/j.ejcb.2006.05.009

Stojanov, S., & Kastner, D. L. (2005). Familial autoinflammatory diseases: genetics, pathogenesis and treatment. *Current Opinion in Rheumatology*, *17*, 586–599. doi:10.1097/bor.0000174210.78449.6b

Takeda, K., Kaisho, T., & Akira, S. (2003). Toll-like receptors. *Annual Review of Immunology*, *21*, 335–376. doi:10.1146/annurev.immunol.21.120601.141126

Tammi, R., Pasonen-Seppänen, S., Kolehmainen, E., & Tammi, M. (2005). Hyaluronan synthase induction and hyaluronan accumulation in mouse epidermis following skin injury. *The Journal of Investigative Dermatology*, *124*(5), 898–905. doi:10.1111/j.0022-202X.2005.23697.x

Teixeira Gomes, R. C., Verna, C., Nader, H. B., dos Santos Simões, R., Dreyfuss, J. L., Martins, J. R. M., … Soares, J. M. (2009). Concentration and distribution of hyaluronic acid in mouse uterus throughout the estrous cycle. *Fertility and Sterility*, *92*, 785–792. doi:10.1016/j.fertnstert.2008.07.005

Termeer, C., Benedix, F., Sleeman, J., Fieber, C., Voith, U., Ahrens, T., … Simon, J. C. (2002). Oligosaccharides of Hyaluronan activate dendritic cells via toll-like receptor 4. *The Journal of Experimental Medicine*, *195*(1), 99–111. Retrieved from http://www.pubmedcentral.nih.gov/articlerender.fcgi?artid=2196009&tool=pmcentrez&rendertype=abstract

The French FMF Consortium, & Consortium, T. F. F. (1997). A candidate gene for familial Mediterranean fever. *Nature Genetics*, *17*(1), 25–31. doi:10.1038/ng0997-25

Tien, J. Y. L., & Spicer, A. P. (2005). Three vertebrate hyaluronan synthases are expressed during mouse development in distinct spatial and temporal patterns. *Developmental Dynamics : An Official Publication of the American Association of Anatomists*, *233*(1), 130–141. doi:10.1002/dvdy.20328

Toole, B. P. (1997). Hyaluronan in morphogenesis. *Journal of Internal Medicine*, *242*(1), 35–40. doi:10.1006/scdb.2000.0244

Toplak, N., Frenkel, J., Ozen, S., De Benedetti, F., Hofer, M., Kone-Paut, I., … Gattorno, M. (2011). The Eurofever Registry for autoinflammatory diseases: results of the first 15 months of enrolment. *Pediatric Rheumatology*. doi:10.1186/1546-0096-9-S1-P303

Tosic, M., Roach, A., de Rivaz, J. C., Dolivo, M., & Matthieu, J. M. (1990). Post-transcriptional events are responsible for low expression of myelin basic protein in myelin deficient mice: role of natural antisense RNA. *The EMBO Journal*, *9*(2), 401–6. Retrieved from http://www.pubmedcentral.nih.gov/articlerender.fcgi?artid=551680&tool=pmcentrez&rendertype=abstract

Traditional Shar Pei. (n.d.). Retrieved March 25, 2014, from http://www.hkshar-pei.com/index.cfm?id=199742&fuseaction=browse&pageid=121

Vanhée-Brossollet, C., & Vaquero, C. (1998). Do natural antisense transcripts make sense in eukaryotes? *Gene*, *211*(1), 1–9. Retrieved from http://www.ncbi.nlm.nih.gov/pubmed/9573333

Vilà, C., Savolainen, P., Maldonado, J. E., Amorim, I. R., Rice, J. E., Honeycutt, R. L., … Wayne, R. K. (1997). Multiple and ancient origins of the domestic dog. *Science (New York, N.Y.)*, *276*, 1687–1689. doi:10.1126/science.276.5319.1687

Vlahu, C. A., Lemkes, B. A., Struijk, D. G., Koopman, M. G., Krediet, R. T., & Vink, H. (2012). Damage of the endothelial glycocalyx in dialysis patients. *Journal of the American Society of Nephrology : JASN*, *23*(11), 1900–8. doi:10.1681/ASN.2011121181

Von Bomhard, D., & Kraft, W. (1998). Idiopathic mucinosis cutis in Chinese Shar pei dogs: epidemiology, clinical features, histopathologic findings and treatment. *Tierarztliche Praxis. Ausgabe K, Kleintiere/Heimtiere*, *26*(3), 189–196. Retrieved from http://www.ncbi.nlm.nih.gov/pubmed/9646415

Waterston, R. H., Lindblad-Toh, K., Birney, E., Rogers, J., Abril, J. F., Agarwal, P., … Lander, E. S. (2002). Initial sequencing and comparative analysis of the mouse genome. *Nature*, *420*, 520–562. doi:10.1038/nature01262

Welle, M., Grimm, S., Suter, M., & von Tscharner, C. (1999). Mast cell density and subtypes in the skin of Shar Pei dogs with cutaneous mucinosis. *Zentralblatt Fur Veterinarmedizin. Reihe A*, *46*(5), 309–16. Retrieved from http://www.ncbi.nlm.nih.gov/pubmed/10445005

Whitelaw, C. B., Springbett, A. J., Webster, J., & Clark, J. (1993). The majority of G0 transgenic mice are derived from mosaic embryos. *Transgenic Research*, *2*(1), 29–32. Retrieved from http://www.ncbi.nlm.nih.gov/pubmed/8513336

Wilkie, T. M., Brinster, R. L., & Palmiter, R. D. (1986). Germline and somatic mosaicism in transgenic mice. *Developmental Biology*, *118*, 9–18. doi:10.1016/0012-1606(86)90068-0

Willem Voncken, J. (2011). *Transgenic Mouse Methods and Protocols*. (M. H. Hofker & J. van Deursen, Eds.) (2nd ed., p. 29). Humana Press. Retrieved from http://www.springer.com/life+sciences/animal+sciences/book/978-1-60761-973-4

William, M. (1982). *Chinese Shar Pei Stud Book Registry* (Vol. 3, pp. 47–48). Concord, CA, USA: CSPCA Inc.

Wolf, D., Schümann, J., Koerber, K., Kiemer, a K., Vollmar, a M., Sass, G., … Tiegs, G. (2001). Low-molecular-weight hyaluronic acid induces nuclear factor-kappaB-dependent resistance against tumor necrosis factor alpha-mediated liver injury in mice. *Hepatology (Baltimore, Md.)*, *34*(3), 535–547. doi:10.1053/jhep.2001.27218

Zambrowicz, B. P., Imamoto, a, Fiering, S., Herzenberg, L. a, Kerr, W. G., & Soriano, P. (1997). Disruption of overlapping transcripts in the ROSA beta geo 26 gene trap strain leads to widespread expression of beta-galactosidase in mouse embryos and hematopoietic cells.

Proceedings of the National Academy of Sciences of the United States of America, *94*(8), 3789–3794.

Zanna, G., Docampo, M. J., Fondevila, D., Bardagí, M., Bassols, A., & Ferrer, L. (2009). Hereditary cutaneous mucinosis in shar pei dogs is associated with increased hyaluronan synthase-2 mRNA transcription by cultured dermal fibroblasts. *Veterinary Dermatology*, *20*(5-6), 377–382. doi:10.1111/j.1365-3164.2009.00799.x

Zanna, G., Fondevila, D., Bardagí, M., Docampo, M. J., Bassols, a, & Ferrer, L. (2008). Cutaneous mucinosis in shar-pei dogs is due to hyaluronic acid deposition and is associated with high levels of hyaluronic acid in serum. *Veterinary Dermatology*, *19*(5), 314–318. doi:10.1111/j.1365-3164.2008.00703.x

Zanna, G., Fondevila, D., Ferrer, L., & Espada, Y. (2012). Evaluation of ultrasonography for measurement of skin thickness in Shar-Peis. *American Journal of Veterinary Research*, *73*(2), 220–226.

Zúñiga, J. ., Orellana, J. ., & Tur, J. . (2008). *Ciencia y Tecnología del Animal de Laboratorio*. (U. de Alcalá & S. E. para las C. del A. de L. (SECAL), Eds.) (pp. 151–153). Salamanca.

ANNEXES

ANNEX 1. Supervision of Animal welfare protocol.

SUPERVISION PROTOCOL

ID mouse: _____ **Ear notch:** _____**Mouse Line:** _____
Date of Birth: _____/_____/_____
Genotype: Tg No Tg **Sexo:** ♂ ♀
Fur color : _____ **Weight:** _____
Microchip Temperature: Yes No
Supervisor: _____

1. **Changes in body weight (0-3 points)**
   - ☐ No weight loss or growing adequaterly (0)
   - ☐ Weight loss <10% (1)
   - ☐ Weight loss between 10-20% (2)
   - ☐ Weight loss over >20% (3)
2. **Physical Appereance: (0-4 points)**

A: Fur
   - ☐ Normal (0)
   - ☐ Dirty or in bad shape (1)
   - ☐ Piloerection (2)

B: Secretions
   - ☐ Normal (0)
   - ☐ Nasal or ocular (1)
   - ☐ Nasal and ocular (2)

3. **Spontaneous behaviour (0-4 points)**
   - ☐ Normal (0)
   - ☐ Inactivity (1)
   - ☐ Abnormal posture (2)
   - ☐ Automutilation, abnormal vozalization, restlesness, stereotyped movements (3)
   - ☐ Changes in social behavior (animal is excluded by others) (4)
4. **Behavior response to handling (0-4 points)**
   - ☐ Normal (0)
   - ☐ Small changes (1)
   - ☐ Moderate changes (2)
   - ☐ Animal is aggressive or comatose (3)
   - ☐ Prostration, no response to stimuli (4)*
5. **Physiological Parameters (vital signs) (0-2)**
   - ☐ Normal (0)
   - ☐ Changes of 1-2 °C of temperature, increased respiratory or cardiac frequence (1)
   - ☐ Changes < o > 2°C of temperature and increased respiratory or cardiac frequence ror dispnea (2)

Corrective measures suggested according to punctuation:

0-3 Normal	9-12: Intense suffering**
4-8 Carefully supervise	> 12: Euthanasia (cervical dislocation)

* If the animal is in this state, cervical dislocation will be applied immediately.
** The animals that obtain this punctuation will be immediately sacrificed to prevent prolonged and unnecessary suffering.

ANNEX 2. *HAS2* Construction Sequence.

```
LOCUS       rosa26sv40PA            2743 bp                          23-FEB-2012
EMBL_ID     rosa26sv40PA            1084 bp DNA     linear
EMBL_ID     rosa26sv40PA            2743 bp CIRCULAR                 22-FEB-2012
UNIMARK     rosa26sv40PA annotations
            rosa26sv40PA

FEATURES             Location/Qualifiers
     misc_feature    7..12                                          /ugene_name="Opt Has2"
                     /db_xref="REBASE:01588"              misc_feature    2486..2491
                     /cut=1                                         /db_xref="REBASE:00993"
                     /ugene_name="SalI"                             /cut=1
     misc_feature    7..820                                         /ugene_name="EcoRI"
                     /ugene_name="Rosa26 Prom"            misc_feature    2486..2491
     misc_feature    815..820                                       /db_xref="REBASE:00993"
                     /db_xref="REBASE:00185"                        /cut=1
                     /cut=1                                         /ugene_name="EcoRI"
                     /ugene_name="BamHI"                  misc_feature    2486..2737
     misc_feature    815..820                                       /ugene_name="SV40PA"
                     /db_xref="REBASE:00185"              misc_feature    2732..2737
                     /cut=1                                         /db_xref="REBASE:01588"
                     /ugene_name="BamHI"                            /cut=1
                                                                    /ugene_name="SalI"

 misc_feature    815..2491
ORIGIN
        1 GATATCGTCG ACTAGATGAA GGAGAGCCTT TCTCTCTGGG CAAGAGCGGT GCAATGGTGT
       61 GTAAAGGTAG CTGAGAAGAC GAAAAGGGCA AGCATCTTCC TGCTACCAGG CTGGGGAGGC
      121 CCAGGCCCAC GACCCCGAGG AGAGGGAACG CAGGGAGACT GAGGTGACCC TTCTTTCCCC
      181 CGGGGCCCGG TCGTGTGGTT CGGTGTCTCT TTTCTGTTGG ACCCTTACCT TGACCCAGGC
      241 GCTGCCGGGG CCTGGGCCCG GGCTGCGGCG CACGGCACTC CCGGGAGGCA GCGAGACTCG
      301 AGTTAGGCCC AACGCGGCGC CACGGCGTTT CCTGGCCGGG AATGGCCCGT ACCCGTGAGG
      361 TGGGGGTGGG GGGCAGAAAA GGCGGAGCGA GCCCGAGGCG GGGAGGGGGA GGGCCAGGGG
      421 CGGAGGGGGC CGGCACTACT GTGTTGGCGG ACTGGCGGGA CTAGGGCTGC GTGAGTCTCT
      481 GAGCGCAGGC GGGCGGCGGC CGCCCCTCCC CCGGCGGCGG CAGCGGCGGC AGCGGCGGCA
      541 GCTCACTCAG CCCGCTGCCC GAGCGGAAAC GCCACTGACC GCACGGGGAT TCCCAGTGCC
      601 GGCGCCAGGG GCACGCGGGA CACGCCCCCT CCCGCCGCGC CATTGGCCTC TCCGCCCACC
      661 GCCCCACACT TATTGGCCGG TGCGCCGCCA ATCAGCGGAG GCTGCCGGGG CCGCCTAAAG
      721 AAGAGGCTGT GCTTTGGGGC TCCGGCTCCT CAGAGAGCCT CGGCTAGGTA GGGGATCGGG
      781 ACTCTGGCGG GAGGGCGGCT TGGTGCGTTT GCGGGGATCC GCCACCATGC ACTGCGAGAG
      841 ATTTCTGTGC GTGCTGAGAA TCATCGGCAC CACCCTGTTC GGCGTGTCCC TGCTGCTGGG
      901 CATCACAGCC GCTTACATCG TGGGCTACCA GTTCATCCAG ACCGACAACT ACTACTTCAG
      961 CTTCGGCCTG TACGGCGCCT TCCTGGCCAG CCACCTGATC ATCCAGAGCC TGTTCGCTTT
     1021 CCTGGAACAC CGGAAGATGA AGAAGTCCCT GGAAACCCCC ATCAAGCTGA ACAAGACCGT
     1081 GGCCCTGTGT ATCGCCGCCT ACCAGGAAGA TCCCGACTAC CTGAGAAAGT GCCTGCAGAG
     1141 CGTGAAGAGA CTGACCTACC CCGGCATCAA GGTCGTGATG GTCATCGACG GCAACAGCGA
     1201 CGACGACCTG TACATGATGG ACATCTTCAG CGAAGTGATG GGCAGAGACA AGAGCGCCAC
     1261 CTACATCTGG AAGAACAACT TCCACGAGAA GGGCCCTGGC GAGACAGAGG AAAGCCACAA
     1321 AGAAAGCAGC CAGCACGTGA CCCAGCTGGT GCTGAGCAAC AAGAGCATCT GTATCATGCA
     1381 GAAGTGGGGC GGCAAGAGGG AAGTGATGTA CACCGCCTTC AGAGCCCTGG GCAGATCCGT
     1441 GGACTACGTG CAAGTGTGCG ACAGCGACAC CATGCTGGAC CCTGCCAGCA GCGTGGAAAT
     1501 GGTCAAGGTG CTGGAAGAGG ACCCCATGGT GGGAGGCGTG GGCGGAGATG TGCAGATCCT
     1561 GAACAAATAC GACAGCTGGA TCAGCTTCCT GAGCAGCGTG CGGTACTGGA TGGCCTTCAA
     1621 CATCGAGAGA GCCTGCCAGA GCTACTTCGG CTGCGTGCAG TGTATCAGCG GCCCTCTGGG
     1681 CATGTACAGA AACAGCCTGC TGCACGAGTT CGTGGAAGAT TGGTACAACC AGGAGTTCAT
     1741 GGGCAACCAG TGTAGCTTCG GCGACGACAG ACACCTGACC AACAGAGTGC TGAGCCTGGG
     1801 CTACGCCACC AAGTACACCG CTAGAAGCAA GTGCCTGACC GAGACACCCA TCGAGTACCT
     1861 GAGATGGCTG AACCAGCAGA CCAGATGGTC CAAGTCCTAC TTCAGAGAGT GGCTGTACAA
     1921 CGCCATGTGG TTCCACAAGC ACCACCTGTG GATGACCTAC GAGGCCGTGA TTACCGGCTT
     1981 CTTCCCCTTC TTCCTGATCG CCACCGTGAT TCAGCTGTTC TACAGAGGCA AGATCTGGAA
     2041 CATCCTGCTG TTTCTGCTGA CCGTGCAGCT CGTGGGCCTG ATCAAGAGCA GCTTCGCCAG
     2101 CTGCCTGAGA GGCAACATTG TGATGGTGTT CATGAGCCTG TACTCCGTGC TGTACATGTC
     2161 ATCTCTGCTG CCCGCCAAGA TGTTCGCTAT CGCCACCATC AACAAGGCCG GCTGGGGCAC
     2221 CAGCGGCAGA AAGACCATCG TCGTGAACTT CATCGGCCTG ATCCCCGTGT CCGTGTGGTT
     2281 CACAATCCTG CTGGGCGGCG TGATCTTCAC CATCTACAAA GAGAGCAAGA AGCCCTTCAG
     2341 CGAGAGCAAG CAGACCGTGC TGATTGTGGG CACCCTGATC TACGCCTGCT ACTGGGTCAT
     2401 GCTGCTGACC CTGTACGTGG TGCTGATTAA CAAGTGCGGC AGAAGAAAGA AGGGCCAGCA
     2461 GTACGACATG GTGCTGGATG TCTGAGAATT CATCTAGATA ACTGATCATA ATCAGCCATA
     2521 CCACATTTGT AGAGGTTTTA CTTGCTTTAA AAAACCTCCC ACACCTCCCC CTGAACCTGA
     2581 AACATAAAAT GAATGCAATT GTTGTTGTTA ACTTGTTTAT TGCAGCTTAT AATGGTTACA
     2641 AATAAAGCAA TAGCATCACA AATTTCACAA ATAAAGCATT TTTTTCACTG CATTCTAGTT
     2701 GTGGTTTGTC CAAACTCATC AATGTATCTT AGTCGACGAT ATC
```

ANNEX 3. Phenotyping Record Sheet.

PHENOTYPING HAS2 MICE

Mouse ID: _____**Ear notch:** _____**Mouse Line:**_____
Date of Birth: _____/_____/_____**Date of Sacrifice**: _____/_____/_____
Age at sacrifice (days): _____
Genotype: ☐ Tg ☐ No Tg **Sex:** ♂ ♀ ☐**Fur color:** _____
Weight: _____**Temperature microchip:** Ye☐ No ☐
Sacrifice method: _____

IN VIVO ANALYSIS

1. **Visual inspection of possible skin alterations**

_____
_____
_____

POST-MORTEM ANALYSIS

2. **Total blood drawn (intra cardiac puncture):** _____ml EDTA _____ml (serum)
3. **Number of skin samples obtained:** _____ **4. Morphologic changes in necropsy**

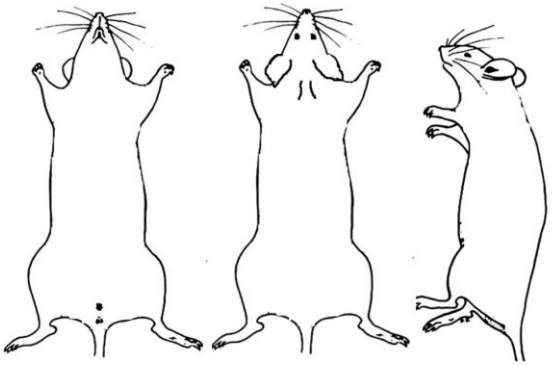

-
_____
_____
_____
_____
_____
_____
_____
_____

5. **Samples of other organs obtained:**

- ☐ **Lung**
- ☐ **Heart**
- ☐ **Kidney**
- ☐ **Liver**
- ☐ **Spleen**

6. **General observations:**

CBC: ☐Yes ☐No **Date sample is sent:** _____/_____/_____
Histology: ☐es ☐o **Date sample is sent:** _____/_____/_____
Serum: ☐Yes ☐ No

_____
_____
_____

ANNEX 4. Southern Blot protocol performed at CBATEG.

PROTOCOL DE SOUTHERN

A. OBJECTIU
El southern ens permet analitzar el genoma del ratolí i detectar així aquells que hagin integrat el transgén, per tant que siguin transgènics. Alhora, permet també detectar el nombre de còpies del transgén integrades.

B. ÀMBIT A QUI AFECTA
Afecta als tècnics de la UAT qualificats per fer biología molecular.

C. SEGURETAT
Manipulació de Bromur d'Etidi , producte cancerígen. Cal usar bata, guants i tenir precaució en la generació i eliminació dels residus contaminants.

Manipulació de fonts radiactives no encapsulades (P32). Cal treballar seguint les normes de Protecció Radiológica que tot ussuari de la Unitat ha de conèixer.

D. PROCEDIMENT
Un cop tenim el DNA de les cues aÏllat i quantificat:

D1.Montar digestions amb Enzims de Restricció.
X µl DNA (per 10 µg de DNA)
Y µl H_2O
1 µl Enzim de Restricció
3 µl Buffer (depen de l'enzim)
30 µl Volum total
Incubar O/N a 37ºC (mínim 4 hores)
10U d`enzim digereix 1 µg en 1 h.
Normalmente els buffers es presenten 10X

D2.Electroforesi en gel d'Agarosa.
- Preparar un gel d'Agarosa a l'1% (ref:seakem LE agarose, BMA 1kg)
- 1 g Agarosa / 100 ml TAE 1X (bullir en microones per disoldre)
- Afegir 0,5 µl BrEt / 10 ml TAE
- Deixar refredar una mica i abocar sobre llit/cubeta del sistema d'electroforesi. En el llit d'electroforesis se li posa cinta adhesiva (celo) als extrems i se li col·loquen les pintes.
- Deixar aixugar amb la pinta corresponent.
- Un cop sec, cobrir amb solució TAE 1X.
- Treure la pinta amb molt de compte per no trencar els pous.
- Afegir a cada mostra 3 µl de Buffer de càrrega 10X (Blue juice) i fer un pols en la microcentrífuga per fer baixar tota la mostra.
- Sembrar els pous amb les mostres i DNA marcador (Marker VII, X, 1 Kb…).
- Endollar la font amb els cables corresponents al sistema. Fer còrrer el gel a 60-90 Volts (primer més fort fins que el DNA surti dels pous). Comprobar el pas de corrent mirant que existexi Amperatge en la font.

Quan el DNA ha corregut el desitjat, parar la font, desconectar els cables i anar amb el gel+llit dins d'una safata a fer una foto amb llum U.V. per tenir constància de com ha corregut el DNA i veure si alguna mostra s'ha degradat.

D3.Tractament del gel

- Submergir el gel durant 10 minuts (màxim 15 minuts) en una *solució de HCl 0,25 M* en agitació. Serveix per despurinitzar el DNA i així trencar els troços més grans. (no deixar-ho més temps !!). El buffer de càrrega (blau) es torna grogós.
- Submergir el gel 15 minuts en una *solució d'alcali* en agitació. D'aquesta manera desnaturalitza el DNA separant les dues cadenes. (no deixar-ho més temps !!). El buffer de càrrega recupera la tonalitat blava.
- Submergir el gel entre 30 minuts en la *solució neutralizing* en agitació, s'hi pot deixar més temps (fins a 2 hores). D'aquesta manera s'atura l'acció de l'alcali.

D4.Transferència a membrana

- Utilitzar el sistema "turboblot" per fer la transferència.
- Solució de transferència: 10X SSC.
- Retallar un tros de membrana de Nylon de la mateixa mida que el gel a transferir i marcar-la en la part superior amb un bolígraf amb les dades corresponents (nom del constructe, data …) per identificar després la membrana.
- Posar la membrana en remull amb 10X SSC perque es vagi hidratant.
- Preparar els papers secants necesaris per fer el montatge de la trasferència.
- Montar la transferència seguint les instruccions del sistema "turboblot": Sobre la base de plàstic del sistema anirem posant per ordre de baix a dalt:
    - 1º. 10 papers absorvent gruixuts.
    - 2º. 3 papers absorvent prims.
- 3º. 1 paper absorvent prim hidratat amb 10X SSC.
    - 4º. La membrana de Nylon hidratada amb 10X SSC.
    - 5º. El gel d'agarosa. Vigilar que no quedin bombolles!.
    - 6º. 3 papers absorvents hidratats amb 10X SSC.
- Posar la part superior de plàstic del sistema. Hidratar més papers prims amb 10X SSC per montar un pont. Omplir amb la solució de transferència la peça superior de plàstic. Montar el pont amb els papers prims de manera que els extrems del pont quedin sumergits en la solució de transferència.
- Temps de transferència: 2hores (mínim) - 1 O/N.

D5.Marcatge de sondes

Aquest protocol está basat en el Kit "Ready·to·go" d'Amershan pharmacia biotech :

- En un epperndorf de rosca posar entre 15-40 μg de DNA en un volum total de 45 μl. Ajustar el volum amb aigua.
- Bullir la sonda 5 minuts per desnaturalitzar el DNA.
- Posar l'eppendor en gel (així evitem que es tornin a unir les dues cadenes de DNA).
- Resuspendre la sonda en el tub del kit que conté la resta dels elements per dur a terme la reacció ("boleta") :enzim, buffer i dNTPs.
- Anar a la cambra de radioactivitat i afegir 5 μl de dCTP* al tub.
- Deixar incubant el tub en un bany amb agitació suau a 37ºC entre 15-30 minuts.
- Passar la sonda per una columna de purificació Amersham Pharmacia per eliminar restes d'oligonucleotids i monocadenes.:

- Vortexar la columna per homogenitzar el contingut i trencar la punta.
- Posar la columna sobre un eppendorf i centrifugar 1 minut a 3000 rpm. Guardar el líquid resultant de la centrifugació.
- Posar la columna sobre un tub de rosca nou i posar-hi el volum total de la reacció.
- Centrifugar 2 minuts a 3000 rpm.
- Augmentar el volum final de la sonda amb 150 μl del líquid reservat anteriorment resultant de la primera centrifugació de la columna.

D6. Hibridació de la membrana
- Desmontar la transferència. Treure la membrana i posar-la al "stratalinker" per crear enllaços covalents entre el DNA i la membrana.
- Els següents passos es realitzaran a la cambra de radioactivitat :
- Posar la membrana en un tub d'hibridació. Si està seca afegir al tub uns 25 ml d'aigua per hidratar la membrana i després llençar l'aigua.
- Afegir 25 ml de *solució de prehibridació/hibridació* que prèviament haurem escalfat a 65ºC i repartir-la per tot el tub inclinant-lo cap als dos extrems.. Deixar-ho en el forn d'hibridació a 65 ºC durant una hora com a mínim. (periode de prehibridació)
- Bullir la sonda 5 minuts per desnaturalitzar el DNA.
- Treure el tub del forn d'hibridació i posar-hi la sonda mitjançant una pipeta de 200 μl fent que caigui al centre del tub, sobre el fons i no en la membrana.
- Tornar a posar el tub en el forn d'hibridació (sempre equilibrat) i deixar-ho com a mínim 6 hores a 65 ºC. Normalment ho deixem hibridant 1 O/N.

D7.Rentats de la membrana
- Treure el tub del forn d'hibridació. Llençar la solució de prehibridació/hibridació amb la sonda a la garrafa de residus radioactius líquids.
- Afegir al tub uns 25 μl de *solució de baixa astringència*, inclinar el tub cap als dos extrems agitant suaument i llençar aquest primer rentat a la garrafa de residus líquids.
- Afegir 25 μl més de solució de baixa astringència i deixar-ho al forn 20-30 minuts a 40ºC.
- Llençar la solució i comprovar amb el comptador Geiger-Müller el nivell de radiació emesa per la membrana i si és molt alt podem repetir un altre rentat de baixa astringència en les mateixes condicions o disminuint el temps de rentat.
- Posar a escalfar la *solució d'alta astringència* en un bany a 65 Cº.
- Canviar la solució de baixa astringència per la d'alta calenta i deixar-la durant 5-15 minuts a 65 Cº.
- Llençar la solució i treure la membrana del tub per comprovar amb el comptador Geiger que pels extrems no hi ha radioactivitat i que només es detecta en llocs concrets de la zona central de la membrana

D8.Exposició i revelat de la membrana
- Deixar la membrana sobre paper de poiata perque s'assequi i quedi només humida (aprofitar aquesta estona per rentar el tub d'hibridació amb sabó Daber i molta aigua).
- Amb l'ajuda d'unes pinces i una segelladora plastificar la membrana. La membrana és a punt per posar-la a exposar
- Posar la membrana plastificada en un cassette i en una cambra fosca afegir un film d'autorradiografia en contacte amb la membrana. Tancar el cassette i deixar-ho exposant-se a –80ºC mínim 1 O/N.
- Revelar la placa en la cambra fosca fent passar el film pel revelador. Si la intensitat de les bandes és baixa, es pot tornar a posar a exposar més temps (fins a 1 setmana).

Annex 5. HA serum concentration values in both assays.

Cross	Founder (Line)	ID plate	Group	K-4800	K-1200*
49	221	1*	ATG	218,28	1600,00
49	221	2	ATG	170,96	1180,09
129 X 209	156	3*	ATG	1213,00	1600,00
129 X 209	156	4*	ATG	1798,47	1600,00
129 X 209	156	5*	ATG	1565,58	1600,00
211 X 190	172	6	ATG	46,79	150,74
211 X 190	172	7	ATG	3,07	124,02
211 X 190	172	8	ATG	73,71	250,53
211 X 190	172	9	ATG	66,07	555,89
211 X 190	172	10	ATG	55,02	258,27
211 X 190	172	11	ATG	25,17	331,88
211 X 190	172	12	ATG	221,01	729,07
230 x 185	184	13	ATG	608,28	1938,04
230 x 185	184	14*	ATG	646,17	1600,00
230 x 185	184	15*	ATG	460,80	1600,00
49 X 101	221	16*	ATG	371,83	1600,00
49 X 101	221	17*	ATG	416,01	1600,00
87 x 224	194	18*	ATG	499,69	1600,00
49	221	19	YTG	55,85	211,39
49	221	20	YTG	156,60	635,66
49	221	21*	YTG	405,41	1600,00
211 X 190	172	22	YTG	36,90	184,83
211 X 190	172	23	YTG	95,21	729,07
211 X 190	172	24	YTG	36,63	308,07
211 X 190	172	25	YTG	8,43	149,96
211 X 190	172	26	YTG	63,77	513,12
230 x 185	184	27	YTG	431,38	3085,52
230 x 185	184	28	YTG	105,54	795,47
230 x 185	184	29	YTG	78,23	791,50
230 x 185	184	30	YTG	185,27	2354,27
230 x 185	184	31*	YTG	204,55	1600,00
230 x 185	184	32*	YTG	207,13	1600,00
230 x 185	184	33*	YTG	236,85	1600,00
230 x 185	184	34*	YTG	123,18	1600,00
230 x 185	184	35	YTG	186,70	905,56
49 X 101	221	36*	YTG	369,96	1600,00
49 X 101	221	37	YTG	622,99	2119,02
49 X 101	221	38	YTG	236,85	1509,07
49 X 101	221	39*	YTG	260,00	1600,00
49	221	***40***	AWT	53,90	489,35
49	221	***41***	AWT	66,07	433,95

87	194	***42***	AWT	68,12	471,45
168	172	***43***	AWT	110,89	331,76
168	172	***44***	AWT	106,63	161,63
168	172	***45***	AWT	98,36	218,96
168	172	***46***	AWT	129,94	578,27
168	172	***47***	AWT	21,57	392,57
168	172	***48***	AWT	86,83	910,67
168	172	***49***	AWT	74,20	386,86
129 X 209	156	***50***	AWT	32,98	512,30
211 X 190	172	***51***	AWT	349,80	99,70
230 x 185	184	***52***	AWT	41,17	275,70
257 H	156	***53***	AWT	80,95	105,99
257 H	156	***54***	AWT	25,86	204,10
257 H	156	***55***	AWT	3,35	916,76
257 H	156	***56***	AWT	3,35	221,99
257 H	156	***57***	AWT	20,78	481,44
49 X 101	221	***58***	AWT	121,63	435,93
49	221	***59***	YWT	12,91	362,80
49	221	***60***	YWT	132,48	406,37
87	194	***61***	YWT	174,20	75,34
87	194	***62***	YWT	54,49	132,85
87	194	***63***	YWT	69,27	393,82
211 X 190	172	***64***	YWT	3,35	463,82
212 X 190	172	***65***	YWT	3,35	0,00
230 x 185	184	***66***	YWT	91,45	125,78
230 x 185	184	***67***	YWT	19,45	166,91
232 x 185	184	***68***	YWT	576,69	606,88
253 X 209	156	***69***	YWT	39,46	447,05
257 H	156	***70***	YWT	27,22	1160,24
257 H	156	***71***	YWT	92,52	173,25
258 H	156	***72***	YWT	68,95	375,85
258 H	156	***73***	YWT	110,89	455,33
259 H	156	***74***	YWT	256,05	211,54
259 H	156	***75***	YWT	25,32	202,27
260 H	156	***76***	YWT	39,75	379,19
260 H	156	***77***	YWT	70,57	164,80
261 H	156	***78***	YWT	44,65	239,04
261 H	156	***79***	YWT	27,76	986,27
262 H	156	***80***	YWT	58,18	379,19
262 H	156	***81***	YWT	38,04	164,80

* Samples with HA concentration >1600 ng/mL

ANNEX 6. Histology Report of mice in Study.

Fundador	ID	Grupo	Histología
221	1	TG adulto	Piel inter escapular y cuello ventral: epidermis y dermis superficial replegada, disgregación de fibras de colágeno focal (rotura) de la dermis. Reacción a cuerpo extraño (fragmento de piel con células gigantes). Tejido conectivo entre tejido adiposo y músculo subcutáneo muy laxo. Infiltrado mixto intersticial. Vejiga: vacuolización marcada de las células superficiales del epitelio. Resto de órganos sin lesiones aparente (SLA).
221	2	TG adulto	Piel inter escapular: áreas de infiltrado linfocitario de difuso a perianexal, infiltrado intersticial de mastocitos y de algún polimorfo nuclear, foco de fibrosis. Disgregación focal de las fibras de colágeno. Tejido conectivo entre tejido adiposo y músculo subcutáneo muy laxo. Infiltrado focal de macrófagos, presencia de cuerpo extraño. Distensión de vasos linfáticos. Resto de órganos SLA.
156	3	TG adulto	Corazón, pulmón: Mucina intersticial y perivasculares focal y leve. Mucosa región esofágica (estómago): depósitos de Mucina. Riñón: Glomerulonefritis-glomeruloesclerosis multifocal; nefritis intersticial crónica. Material ligeramente basófilo (concreciones) en túbulos. Hidronefrosis. Hígado: microgranulomas asociados a necrosis aislada de hepatocitos Piel: infiltrado intersticial mono nuclear con mastocitos dispersos. MEC de la dermis superficial y laxo subcutáneo focalmente con escasa Mucina. Nervios periféricos: depósitos de Mucina endo- y epineuro.
156	4	TG adulto	Corazón: depósito focal leve Mucina. Piel: infiltrado intersticial mono nuclear con mastocitos dispersos. MEC de la dermis superficial y laxo subcutáneo focalmente con Mucina en el intersticio atrio-ventricular. Nervios periféricos: depósitos de Mucina endo y epineuro.
156	5	TG adulto	Corazón, pulmón: Mucina intersticial y perivasculares focal y leve. Riñón: glomeruloesclerosis focal. Nefritis intersticial focal leve. Material ligeramente basófilo (concreciones) y cilindros hialinos (perdida proteína) en algún túbulo renal. Vacuolización y fenómenos de reepitelización de células tubulares. Nervios periféricos: depósitos de Mucina endo- y epineuro. Piel: infiltrado intersticial mono nuclear con mastocitos dispersos. MEC de la dermis superficial y laxo subcutáneo focalmente con Mucina. Útero: mucosa de aspecto edematoso SNC: Material basófilo en meninges.
172	6	TG adulto	Riñón: engrosamiento membranas escasos glomérulos y túbulos; infiltrado mono nuclear focal leve asociado; material ligeramente acidófilo en el filtrado glomerular y túbulos. Hígado: microgranulomas necrosis aislada de hepatocitos. Piel del dorso: tejido subcutáneo extremadamente laxo.
172	7	TG adulto	Riñón: engrosamiento membranas escasos glomérulos y túbulos; infiltrado mono nuclear focal leve asociado; material ligeramente acidófilo en el filtrado glomerular y túbulos contorneados.
172	8	TG adulto	Pulmón: hemorragias alveolares y perivasculares focales. Riñón: engrosamiento membranas escasos glomérulos y túbulos; infiltrado mono nuclear focal leve asociado; material ligeramente acidófilo en el filtrado glomerular, túbulos y pelvis renal. Estómago: submucosa gástrica extremadamente laxa.
172	9	TG adulto	Estomago glandular: infiltrado inflamatorio mixto focal en la submucosa. Piel: infiltrado inflamatorio mono nuclear intersticial difuso leve en la zona del cuello
172	10	TG adulto	Riñón: material ligeramente acidófilo en el filtrado glomerular y túbulos contorneados.
172	11	TG adulto	Riñón: engrosamiento membranas escasos glomérulos y túbulos; infiltrado mono nuclear focal leve asociado; material ligeramente acidófilo en el filtrado glomerular y túbulos.

172	12	TG adulto	Riñón: engrosamiento membranas escasos glomérulos y túbulos; infiltrado mono nuclear focal leve asociado.
184	13	TG adulto	Corazón: metaplasia cartilaginosa nodular pared vena pulmonar y intramural arteria aorta focal. Riñón: engrosamiento de las membranas de diversos túbulos y de glomérulos con aumento de la celularidad; infiltrado intersticial mono nuclear asociado. Reepitelización tubular Cilindros hialinos en algunos túbulos. Tejido conectivo laxo subcutáneo y de relleno focalmente ligeramente basófilo.
184	14	TG adulto	Riñón: engrosamiento de las membranas de diversos túbulos y de glomérulos con aumento de la celularidad; infiltrado intersticial mono nuclear asociado. Reepitelización tubular Cilindros hialinos en algunos túbulos. Tejido conectivo laxo peri vascular, subepitelial y de relleno de diversas localizaciones aspecto vacuolizado y ligeramente basófilo (pulmón, reproductor, glándulas salivares, subcutáneo).
184	15	TG adulto	Riñón: engrosamiento de las membranas de diversos túbulos y de glomérulos con aumento de la celularidad; infiltrado intersticial mono nuclear asociado. Piel ventral cuello y dorso: focos dispersos de fibrosis subepidérmica e infiltrado mono nuclear de focal a intersticial leve.
221	16	TG adulto	Piel inter escapular: tejido conectivo subcutáneo bastante celular, infiltrado intersticial disperso leve mono nuclear y de mastocitosis. Piel cuello ventral: dermis delgada y focalmente laxa. Riñón: presencia de material granular, ligeramente acidófilo y cilindros hialinos en la luz de algunos túbulos renales. Infiltrado mono nuclear focal en el cortex. Vejiga: vacuolización de las células superficiales del epitelio. Resto de órganos SLA.
221	17	TG adulto	Piel ventral cuello: infiltrado mixto leve de intersticial a focal de la dermis superficial. Tejido conectivo subcutáneo muy laxo. Riñón: presencia de material granular ligeramente acidófilo, y cilindros hialinos en la luz de algunos túbulos renales. Infiltrado mono nuclear focal en el cortex. Vejiga: vacuolización de células superficiales del epitelio. Resto de órganos: SLA
194	18	TG adulto	Riñón: engrosamiento de las membranas de diversos túbulos y de glomérulos con aumento de la celularidad; infiltrado intersticial mono nuclear asociado. Piel ventral cuello y dorso: focos dispersos de fibrosis subepidérmica e infiltrado mono nuclear de focal a intersticial leve.
221	19	TG joven	Riñón: presencia de material fibrogranular ligeramente acidófilo en filtrado glomerular y tubos del cortex y medula. Infiltrado linfocitario focal leve. Vejiga: vacuolización de las células superficiales del epitelio. Resto de órganos SLA.
221	20	TG joven	Piel inter escapular: infiltrado intersticial a focal de mono nucleares en dermis profunda e hipodermis. Resto de órganos SLA.
221	21	TG joven	Piel cuello ventral: infiltrado intersticial focal de linfocitos, algunos polimorfo nucleares en la dermis profunda y subcutis. Vejiga: vacuolización de las células superficiales del epitelio. Resto de órganos SLA.
172	22	TG joven	Riñón: engrosamiento membranas escasos glomérulos y túbulos; infiltrado mono nuclear focal leve asociado; material ligeramente acidófilo en el filtrado glomerular y túbulos
172	23	TG joven	Riñón: material ligeramente acidófilo en algunos túbulos.
172	24	TG joven	Corazón: metaplasia condroide focal de la pared de la aorta. Riñón: engrosamiento de la membrana basal de algunos túbulos. Cilindros hialinos a la luz de algún túbulo. Vejiga: vacuolización de las células superficiales del epitelio. Estomago glandular: infiltrado inflamatorio mixto focal en la submucosa. Piel: infiltrado inflamatorio mono nuclear intersticial difuso leve. En la zona del cuello: infiltrado inflamatorio mono nuclear focalmente perianexal y foco de fibrosis en la hipodermis.

172	25	TG joven	Hígado: leve infiltrado inflamatorio mono nuclear alrededor de algún conducto biliar. Riñón: gotas hialinas en células mesangiales extra glomerulares. Engrosamiento de la membrana basal de algunos túbulos.
172	26	TG joven	Riñón: engrosamiento de la cápsula de Bowman de algunos glomérulos con aumento del número de células. Cilindros hialinos en algún túbulo. Estomago glandular: infiltrado inflamatorio mono nuclear multifocal leve en la parte profunda de la mucosa (asociado a degeneración de algunas células glandulares) y en la submucosa. Tráquea: dos focos de material granular basófilo d en la lamina propia. Piel: infiltrado inflamatorio mono nuclear intersticial difuso en la dermis. En la zona inter escapular; discretos focos de infiltrado mono nuclear y fibrosis en el panículo adiposo. En la zona del cuello: focos leve de material granular basófilo en la dermis profunda.
184	27	TG joven	Riñón: engrosamiento de la Cápsula de Bowman de algún glomérulo y membrana basal de algunos túbulos. Glomerulonefritis focal leve. Piel: infiltrado inflamatorio mono nuclear intersticial difuso leve.
184	28	TG joven	Riñón: engrosamiento de la cápsula de Bowman y algunos glomérulos y membrana basal de algunos túbulos. Dilatación focal de algún túbulo. Estomago glandular: infiltrado mixto y difuso en la parte profunda de la lámina propia y submucosa. Formas cristaloides hialinas en algunas células glandulares (hialinosis). Piel: infiltrado inflamatorio mono nuclear intersticial difuso y focalmente perianexal leve. En la zona del cuello se observa un foco de infiltrado inflamatorio mixto en el tejido adiposos adyacente a la musculatura esquelética con presencia de material granular basófilo.
184	29	TG joven	Hígado: microgranulomas asociados a necrosis aislada de hepatocitos. Riñón: engrosamiento de la membrana basal de algunos tubulosa asociados a un leve infiltrado inflamatorio mono nuclear. Estomago glandular: infiltrado inflamatorio mixto en la parte profunda de la lámina propia y submucosa. Formas cristaloides hialinas en algunas células glandulares (hialinosis). Piel: infiltrado inflamatorio mono nuclear intersticial difuso leve y focalmente perianexal.
184	30	TG joven	Hígado: algunos microgranulomas asociados a necrosis aislada de hepatocitos. Infiltrado inflamatorio mono nuclear leve alrededor de algunos conductos biliares. Riñón: engrosamiento de la cápsula de Bowman de algún glomérulo y membrana basal de algunos túbulos. Cilindros hialinos en algún túbulo. Glomeruloesclerosis focal. Gotas hialinas en células mesangiales extra glomerulares. Estomago glandular: infiltrado inflamatorio mixto focal sobretodo de la submucosa. Piel: infiltrado inflamatorio mono nuclear intersticial difuso leve con algunos mastocitos y focalmente perianexal.
184	31	TG joven	Riñón: engrosamiento de la cápsula de Bowman de algún glomérulo y membrana basal de algunos túbulos. Estomago: infiltrado inflamatorio mono nuclear difuso de la parte profunda de la lamina propia en la zona de transición entre el estomago glandular y el no glandular. Formas cristaloides hialinas en algunas células glandulares (Hialinosis). Piel: dermis con infiltrado inflamatorio mono nuclear difuso intersticial, focalmente perianexal y en el subcutis de la zona del cuello.
184	32	TG joven	Corazón: metaplasia condroide focal en la pared de la aorta. Hígado: algunos microgranulomas asociados a necrosis aislada de hepatocitos. Piel: infiltrado inflamatorio mono nuclear intersticial difuso y focalmente perianexal.
184	33	TG joven	Hígado: microgranulomas asociados a necrosis aislada de hepatocitos. Estomago glandular: infiltrado inflamatorio mixto difuso principalmente en la parte profunda de la lámina propia. Formas cristaloides hialinas en algunas células glandulares (hialinosis). Esófago: en la parte rostral, cúmulo focal de material granular basófilo en la lámina propia y túnica muscular. Piel: infiltrado inflamatorio mono nuclear y de mastocitos intersticial difuso, focalmente perianexal, también en el subcutis de la piel del cuello.
184	34	TG joven	Hígado: algunos microgranulomas asociados a necrosis aislada de hepatocitos. Estomago glandular: infiltrado inflamatorio mixto difuso en la parte profunda de la lámina propia y submucosa. Formas cristaloides hialinas en algunas células glandulares (hialinosis). Piel: en la zona inter escapular infiltrado inflamatorio mono nuclear intersticial difuso y focalmente perianexal.

184	35	TG joven	Hígado: leve infiltrado inflamatorio mono nuclear alrededor de algunos conductos biliares. Riñón: engrosamiento de la cápsula de Bowman y de algunos glomérulos y la membrana basal de algún túbulo. Estomago glandular: leve infiltrado inflamatorio mixto y difuso en la parte profunda de la lámina propia y submucosa. Piel inter escapular: infiltrado inflamatorio mono nuclear intersticial leve, focalmente subepidérmica.
221	36	TG joven	Hígado: microgranulomas asociados a necrosis aislada de hepatocitos. Infiltrado inflamatorio mono nuclear alrededor de algunos conductos biliares. Riñón: engrosamiento de la cápsula de Bowman de algún glomérulo y de la membrana basal de algunos túbulos. Piel: infiltrado inflamatorio mono nuclear intersticial difuso y focalmente perianexal. En la piel inter escapular se observa presencia de material granular basófilo en el endoneuro de algunos nervios cercanos, sobretodo de la musculatura.
221	37	TG joven	Piel ventral cuello: infiltrado mixto leve de intersticial a focal de la dermis superficial. Tejido conectivo subcutáneo muy laxo. Riñón: presencia de material granular ligeramente acidófilo, y cilindros hialinos en la luz de algunos túbulos renales. Infiltrado mono nuclear focal en el cortex. Vejiga: vacuolización de células superficiales del epitelio. Resto de órganos: SLA
221	38	TG joven	Hígado: infiltrado inflamatorio mono nuclear alrededor de algunos conductos biliares. Riñón: algunos glomérulos con engrosamiento de la cápsula de Bowman. Piel inter escapular: material granular basófilo en el endoneuro de algunos nervios cercanos, incluidos los de la musculatura. Infiltrado inflamatorio mono nuclear intersticial difuso y focalmente perianexal.
221	39	TG joven	SNC: presencia de material basófilo granular de forma leve bajo los ependimocitos, sobretodo del cuarto ventrículo, y en órganos subventriculares. Quiste epidermoide en el septo medial del cerebro. Corazón: dos focos de metaplasia condroide en la inserción de la válvula aórtica. Hígado: microgranulomas asociados a necrosis aislada de hepatocitos. Riñón: engrosamiento de la cápsula de Bowman de algún glomérulo y de la membrana basal de algún túbulo. Estomago glandular: foco de infiltrado inflamatorio mixto leve en la parte profunda de la mucosa y submucosa. Piel: en la zona inter escapular infiltrado inflamatorio mono nuclear intersticial difusa moderada en la dermis y focalmente en el subcutis con presencia de alguna célula gigante (multinucleada). En el cuello: infiltrado inflamatorio mono nuclear intersticial moderado y focalmente perianexal. Presencia de material basófilo granular en el endoneuro de algunos nervios y en la musculatura inter escapular.
221	***40***	WT adulto	SLA
221	***41***	WT adulto	SLA
194	***42***	WT adulto	SLA
172	***43***	WT adulto	Riñón: engrosamiento leve membranas en algún glomérulo, infiltrado intersticial mono nuclear leve. Cilindros hialinos en escasos túbulos. Dilatación tubular focal en medula.
172	***44***	WT adulto	Hígado: necrosis aislada de hepatocitos e infiltrado mixto asociado. Riñón: engrosamiento leve membrana en algún glomérulo y túbulo, infiltrado intersticial mono nuclear leve. Cilindros hialinos en escasos túbulos.
172	***45***	WT adulto	Hígado: necrosis aislada de hepatocitos e infiltrado mixto asociado. Riñón: engrosamiento leve membrana en algún glomérulo y túbulo. Cilindros hialinos en escasos túbulos.
172	***46***	WT	Riñón: engrosamiento leve membrana en algún glomérulo y túbulo.

		adulto	
172	***47***	WT adulto	Hígado: vacuolización irregular de hepatocitos distribución peri portal y media (zonas I, II). Piel dorso: tejido subcutáneo muy laxo.
172	***48***	WT adulto	Hígado: múltiples granulomas asociados a necrosis de hepatocitos, amplia afectación del parénquima; activación células. Kupffer. Bazo, placa de Peyer: hiperplasia linfoide. Riñón: infiltrado mono nuclear intersticial asociado a pérdida focal de túbulos y engrosamiento de la membrana basal de algún túbulo. Cilindros hialinos en escasos túbulos. Estómago: infiltrado intersticial mixto en la porción profunda de la mucosa y submucosa fúndica. Formas cristaloides hialinas en células. Glandulares (hialinosis). Piel: infiltrado intersticial mono nuclear con mastocitos y algunos PMNN, focalmente perianexal.
172	***49***	WT adulto	Pulmón: hemorragias focales perivasculars agudas. Hígado: necrosis aislada de hepatocitos e infiltrado mixto asociado - microgranulomas focales. Riñón: engrosamiento ligero de las membranas de glomérulos, focalmente esclerosante, y de algunos túbulo, con escasos cilindros hialinos. Infiltrado mono nuclear focal leve.
156	***50***	WT adulto	Riñón: escasos cilindros hialinos (perdida proteína) en algún túbulo renal. Engrosamiento membrana algún glomérulo. Hígado: microgranulomas asociados a necrosis aislada de hepatocitos. Piel: infiltrado intersticial mono nuclear con mastocitos dispersos Útero: mucosa de aspecto edematosa.
172	***51***	WT adulto	Miocardio: vacuolización peri nuclear de cardiocitos dispersos. Riñón: engrosamiento membranas algún glomérulo y túbulo; material acidófilo en el filtrado glomerular y en túbulos.
184	***52***	WT adulto	Tejido adiposo blanco y moreno: infiltrado linfocitario multifocal. Bazo: hiperplasia de la pulpa blanca. Hígado: microgranulomas asociados a necrosis aislada de hepatocitos. Estomago glandular: infiltrado inflamatorio mixto leve en la parte profunda de la lámina propia y submucosa. Formas cristaloides en algunas células glandulares (hialinosis). Piel del cuello: infiltrado intersticial leve mono nuclear con mastocitos, focalmente más intenso alrededor de dos folículos de pelo.
156	***53***	WT adulto	Hígado: microgranulomas asociados a necrosis aislada de hepatocitos. Infiltrado inflamatorio mono nuclear multifocal alrededor de algunos conductos biliares. Riñón: cilindros hialinos en algunos túbulos. Estomago glandular: leve infiltrado inflamatorio mixto en la submucosa. Formas cristaloides hialinas en algunas células glandulares (hialinosis). Esófago: en la parte craneal foco de material granular basófilo en la lámina propia.
156	***54***	WT adulto	Riñón: cilindros hialinos en algunos túbulos. Infiltrado inflamatorio mono nuclear asociado a algunos túbulos con membrana basal engrosada. Estomago glandular: formas cristaloides hialinas en algunas células glandulares (hialinosis).
156	***55***	WT adulto	Hígado: microgranulomas asociados a necrosis aislada de hepatocitos. Riñón: engrosamiento de la membrana basal de algún túbulo. Foco de infiltrado inflamatorio mono nuclear en el intersticio. Algún cilindro hialino.
156	***56***	WT adulto	Hígado: infiltrado inflamatorio mono nuclear alrededor de algunos conductos biliares. Estomago glandular: leve infiltrado inflamatorio mixto en la parte profunda de la lámina propia y submucosa.
156	***57***	WT adulto	Hígado: microgranulomas asociados a necrosis aislada de hepatocitos. Estomago glandular: leve infiltrado inflamatorio mixto en la parte profunda de la lámina propia y submucosa. Esófago: en la parte craneal, foco de material granular basófilo en la lámina propia.

221	***58***	WT adulto	Riñón: material en la luz de algún túbulo contorneado. Piel inter escapular: infiltrado intersticial de mastocitos y focal de linfocitos en la dermis. Resto de órganos SLA.
221	***59***	WT joven	SLA
221	***60***	WT joven	Estomago glandular e intestino delgado: infiltrado leve y disperso de polimorfo nucleares neutrofilos y eosinofilos en la lámina propia y focalmente en la submucosa gástrica. Ciego: presencia de parasito intestinal (nematodo). Resto de órganos normal.
194	***61***	WT joven	Piel: infiltrado inflamatorio mono nuclear intersticial difuso y focalmente perianexal leve.
194	***62***	WT joven	Hígado: microgranulomas asociados a necrosis aislada de hepatocitos. Estomago glandular: leve infiltrado inflamatorio mixto en la parte profunda de la mucosa y submucosa. Formas cristaloides hialinas en algunas células glandulares (hialinosis). Esófago: en la parte craneal foco de material granular basófilo en la lámina propia. Piel: infiltrado inflamatorio mono nuclear intersticial difuso leve.
194	***63***	WT joven	Riñón: engrosamiento de la cápsula de Bowman de algún glomérulo y de la lámina basal de algunos túbulos. Focalmente leve infiltrado inflamatorio mono nuclear alrededor de algunos vasos arcuatos. Estomago glandular: formas cristaloides hialinas en algunas células glandulares (hialinosis). Vejiga: vacuolización de las células superficiales del epitelio. Piel: en la zona del cuello, dermis con infiltrado inflamatorio mono nuclear intersticial difuso y focalmente perianexal al subcutis leve.
172	***64***	WT joven	Riñón: engrosamiento de la cápsula de Bowman de algún glomérulo. Gotas hialinas en algunas células mesangiales extra glomerulares.
172	***65***	WT joven	Corazón: metaplasia condroide en la pared de la aorta que se continua con la válvula atrio-ventricular. Riñón: engrosamiento de la cápsula de Bowman de algunos glomérulos con aumento del número de células. Engrosamiento de algunos túbulos. Vejiga: vacuolización de las células superficiales del epitelio. Piel: aspecto vacuolizado a nivel de la unión dermo-epitelial de distribución multifocal y asociado en ocasiones a material costroso después de la epidermis. En la dermis; de forma multifocal y asociado a las lesiones previamente descritas, hay infiltrado inflamatorio mono nuclear y fibrosis.
184	***66***	WT joven	Riñón: engrosamiento de la cápsula de Bowman de algún glomérulo y membrana basal de algún túbulo asociado a un leve infiltrado inflamatorio mono nuclear. Estomago: infiltrado inflamatorio mixto en la parte profunda de la lámina propia y submucosa sobretodo de la parte glandular. Formas cristaloides hialinas en algunas células glandulares (hialinosis). Útero: marcada laxitud del tejido conjuntivo del endometrio. Piel: infiltrado inflamatorio mono nuclear intersticial difuso y focalmente perianexal sobretodo en la zona inter escapular.
184	***67***	WT joven	Hígado: microgranulomas asociados a necrosis aislada de hepatocitos. Infiltrado inflamatorio mono nuclear leve alrededor de algunos conductos biliares. Riñón: engrosamiento de la membrana basal de algunos túbulos. Estomago: infiltrado inflamatorio mixto en la parte profunda de la lámina propia y submucosa. Formas cristaloides hialinas n algunas células glandulares (hialinosis). Esófago: en la parte rostral, cúmulo focal d material granular basófilo a la submucosa. Piel infiltrado inflamatorio mono nuclear intersticial difuso, focalmente afectando el subcutis a la piel inter escapular y focalmente perianexal en la zona del cuello.
184	***68***	WT joven	Hígado: microgranulomas asociados a necrosis aislada de hepatocitos. Riñón: engrosamiento de la cápsula de Bowman de algunos glomérulos y membrana basal de algunos túbulos asociados a infiltrados inflamatorios mono nucleares. Estomago glandular: infiltrado inflamatorio mixto en la parte profunda de la

			lámina propia y submucosa: Formas cristaloides hialinas en algunas células glandulares (Hialinosis).
156	***69***	WT joven	Riñón: engrosamiento de la cápsula de Bowman y membrana basal de algún glomérulo y túbulo. Pulmón sin cambios tisulares significativos. Piel: en la zona inter escapular, infiltrado inflamatorio mono nuclear perianexal focal.
156	***70***	WT joven	Hígado: infiltrado inflamatorio mono nuclear alrededor de algunos conductos biliares. Estomago glandular: infiltrado inflamatorio mixto en la parte profunda de la mucosa y submucosa. Formas cristaloides hialinas en algunas células glandulares (hialinosis). Útero: laxitud de la lamina propia del endometrio y escasas células
156	***71***	WT joven	Riñón: presencia de gotas hialinas en algunas células mesangiales extra glomerulares. Pulmón: hemorragia focal probablemente artefacto de manipulación.
156	***72***	WT joven	Pulmón: zona oscura por extravasación de sangre debido a la manipulación de la muestra. Hígado: foco superficial de necrosis asociada a infiltrado inflamatorio mixto. Riñón: cilindros hialinos en algunos túbulos, engrosamiento de la membrana basal de algunos túbulos dispersos con infiltrado inflamatorio mono nuclear asociado.
156	***73***	WT joven	Hígado: microgranulomas con necrosis aislada de hepatocitos. Corazón: foco de metaplasia condroide en la pared de la aorta. Útero sin cambios tisulares significativos. Esófago: en la parte craneal, cúmulo focal de material granular basófilo de la lámina propia.
156	***74***	WT joven	Corazón: metaplasia condroide focal de la válvula aortica. Hígado: microgranulomas asociados a necrosis aislada de hepatocitos. Estomago: infiltrado inflamatorio mono nuclear leve en la submucosa.
156	***75***	WT joven	Hígado: microgranulomas con necrosis aislada de hepatocitos. Leve infiltrado inflamatorio mono nuclear alrededor de algunos conductos biliares. Corazón: foco de metaplasia condroide en la pared de la aorta. Riñón: engrosamiento de la cápsula de Bowman de algunos glomérulos. Estomago glandular: infiltrado inflamatorio mixto y difuso leve en la parte profunda de la lámina propia y submucosa.
156	***76***	WT joven	Tráquea: cúmulo focal de material granular basófilo en la lamina propia. Riñón: engrosamiento de la cápsula de Bowman de algunos glomérulos focalmente asociado a infiltrado inflamatorio mono nuclear.
156	***77***	WT joven	Hígado: microgranulomas con necrosis aislada de hepatocitos. Foco hemorrágico asociado a necrosis de hepatocitos e infiltrado inflamatorio mixto.
156	***78***	WT joven	Estomago no glandular: infiltrado inflamatorio mixto y dilatación de vasos linfáticos en la parte profunda de la lámina propia.
156	***79***	WT joven	Hígado: microgranulomas con necrosis aislada de hepatocitos. Estomago glandular: leve infiltrado inflamatorio mixto focal en la parte profunda de la lámina propia y submucosa. Bazo: sin cambios tisulares significativos. Piel: dermis profunda del cuello con focos de infiltrado inflamatorio mixto.
156	***80***	WT joven	Hígado: microgranulomas asociados a necrosis aislada de hepatocitos. Estomago glandular: Infiltrado inflamatorio mixto difuso y leve en la submucosa. Esófago: en la parte craneal, cúmulos focales de material granular basófilo en la lámina propia.

Annex 7. Hematology report of mice in Study.

ID	Group	RBC (10^6 cells/µL) 7-10,1	measHGB (g/dL) 11,8-14,9	HCT(%) 36,7-46,8	MCV (fL) 42,2-59,2	MCH (pg) 13,8-18,4	MCHC (g/dL) 31-34,7	CHCM (g/dL) 30,7-34	RDW (%) 11,7-15,1	HDW (g/dL) 1,8-2,6	WBCP (10^3 cells/µL) 3,2-12,7	WBCB (10^3 cells/µL) 3,2-12,7	Neuts (10^3 cells/µL) 0,5-2	Lymphs (10^3 cells/µL) 3,8-8,9	Monos (10^3 cells/µL) 0-0,3	Eos (10^3 cells/µL) 0-0,4	Lucs (10^3 cells/µL) 0-0,3	Basos (10^3 cells/µL) 0-0,1	PLT (10^3 cells/µL) 766-1657
1	TG adulto	8,15	12	37,1	45,6	14,8	32,4	27,8	14,4	2,33	6,51	6,81	0,78	5,63	0,19	0,16	0,04	0,01	1526
2	TG adulto	8,29	12	36,3	43,9	14,5	33	28,5	14,1	2,34	8,46	8,44	0,34	7,69	0,19	0,15	0,05	0,01	1843
3	TG adulto	6,88	10,5	32,1	46,7	15,3	32,8	28,5	15,2	2,81	9,34	9,64	0,93	8,22	0,15	0,19	0,1	0,04	893
4	TG adulto	7,42	11,9	36	48,5	16	33	27,6	15,1	2,43	6,48	6,49	0,5	5,74	0,06	0,11	0,08	0,01	863
5	TG adulto	7,17	11,9	36,7	51,2	16,5	32,3	27	16,1	2,75	4,12	3,95	0,5	3,19	0,07	0,09	0,06	0,03	498
6	TG adulto	7,85	12,5	36,3	46,2	15,9	34,5	29,1	14,2	2,2	2,25	2,15	0,23	1,78	0,03	0,11	0,01	0	1022
7	TG adulto	8,29	12,6	41,7	50,3	15,2	30,3	24,4	14,9	2,27	1,24	1,1	0,08	0,93	0,02	0,05	0,01	0,01	793
8	TG adulto	8,15	12,4	36,5	44,8	15,2	34	29,1	14,6	2,45	1,78	1,74	0,24	1,39	0,02	0,08	0,01	0	1014
9	TG adulto	8,84	13,3	40,4	45,7	15	32,9	30,9	14,5	2,26	3,42	3,19	0,4	2,2	0,06	0,47	0,07	0	1009
10	TG adulto	7,8	12,3	36	46,2	15,8	34,2	29,9	14,5	2,46	1,63	1,54	0,22	1,25	0,03	0,04	0	0	1077
11	TG adulto	9,04	14,2	42,5	47	15,7	33,3	27,4	14,2	2,19	1,45	1,17	0,15	0,55	0,01	0,13	0,33	0,01	652
12	TG adulto	9,05	13,6	39,2	43,3	15	34,7	29,8	14,7	2,34	2,05	1,99	0,46	1,37	0,02	0,08	0,07	0	873
13	TG adulto	9,38	13,4	41,2	43,9	14,3	32,6	29,6	14,5	2,26	5,77	5,63	0,31	4,98	0,05	0,22	0,07	0	1372
14	TG adulto	8,56	12,5	37,2	43,5	14,6	33,7	29,6	15,5	2,58	7,2	7,2	0,84	5,9	0,15	0,11	0,19	0,01	1195
15	TG adulto	9,29	13,5	42,2	45,4	14,6	32	30,3	14,7	2,29	2,79	2,85	0,18	2,54	0,02	0,09	0,02	0	1087
16	TG adulto	7,99	11,8	36,4	45,5	14,8	32,4	28,7	16	3,07	2,81	2,95	0,43	2,27	0,06	0,14	0,05	0,01	576
17	TG adulto	9,42	13,5	41,6	44,2	14,3	32,3	28,8	15,3	3	5,68	5,97	0,56	5,03	0,07	0,26	0,03	0,01	914
18	TG adulto	6,79	10,9	30,7	45,2	16	35,5	33,7	15,4	2,62	2,45	2,49	0,37	1,99	0,05	0,08	0	0	896
19	TG joven	8,38	13,4	40,6	48,4	16	33,1	27,1	14,3	2,05	2,41	2,16	0,58	1,35	0,05	0,15	0,02	0,01	1828
20	TG joven	8,73	12,9	43,8	50,2	14,7	29,4	34,4	36,2	6,33	3,91	5,54	0,8	4,68	0,04	0	0,02	0	578
21	TG joven	9,17	13,7	48,5	53	15	28,3	33,2	34,7	6,05	3,37	3,59	0,24	2,91	0,02	0,18	0,02	0	1022
22	TG joven	8,16	12,5	37,2	45,6	15,3	33,6	31,4	16,5	2,24	4,72	4,86	0,4	4,17	0,06	0,17	0,05	0,01	1041
23	TG joven	8,51	12,5	38,8	45,6	14,6	32,1	31,2	17,3	2,13	5,31	5,2	0,47	4,29	0,12	0,28	0,03	0,01	1221

24	TG joven	8,45	12,8	39,1	46,3	15,1	32,7	29,7	16,9	2,06	2,07	1,95	0,15	1,53	0,03	0,18	0,04	0	1234
25	TG joven	8,52	12,9	39	45,8	15,1	32,9	29,1	16	2,06	2,64	2,59	0,22	2,03	0,07	0,24	0,02	0	1158
26	TG joven	8,08	12,8	36,7	45,4	15,8	34,9	30,4	16,4	2,14	3,31	3,3	0,29	2,79	0,05	0,16	0,01	0	1126
27	TG joven	9,86	14,9	44,3	45	15,1	33,6	32,7	17,1	2,19	11,38	11,76	0,87	10,13	0,28	0,37	0,08	0,03	715
28	TG joven	8,6	13,3	40,5	47,2	15,5	32,9	29,1	15,5	2,05	2,59	2,42	0,24	1,94	0,03	0,21	0	0	965
29	TG joven	8,56	13,6	39,7	46,4	15,9	34,2	29,3	16,4	2,09	1,93	1,43	0,15	0,92	0,02	0,34	0	0	758
30	TG joven	9,16	15	42,2	46,1	16,4	35,5	33,6	17,3	2,13	2,65	2,46	0,16	1,95	0,02	0,32	0	0	920
31	TG joven	9	15	41,5	46,2	16,7	36,2	31,9	16,7	2,22	6,13	6,38	0,38	5,69	0,18	0,09	0,02	0,01	1069
32	TG joven	7,98	13,3	42,4	53,1	16,7	31,4	28,2	14,9	1,86	3,92	4,1	0,24	3,66	0,04	0,09	0,06	0,01	751
33	TG joven	9,42	13,9	41,7	44,3	14,8	33,4	28,9	15,8	2,07	3,02	3,03	0,22	2,61	0,03	0,13	0,05	0	1021
34	TG joven	10	16,5	45,8	45,8	16,5	36	32	16,2	2,43	2,88	2,86	0,2	2,37	0,02	0,23	0,04	0	795
35	TG joven	8,99	13,7	41,8	46,4	15,2	32,7	29,8	15,7	2,06	2,22	1,85	0,2	1,33	0,02	0,28	0,01	0	981
36	TG joven	8,4	13,2	42,8	51	15,7	30,8	28,6	14,9	1,73	5,16	5,42	0,51	4,67	0,07	0,14	0,02	0,01	567
37	TG joven	8,19	13,1	40	48,8	16	32,8	31,2	16,2	2,18	5,91	5,84	0,58	4,81	0,12	0,24	0,08	0,01	559
38	TG joven	8,13	12,8	40,9	50,3	15,7	31,2	29,2	14,3	1,87	2,24	2,26	0,28	1,36	0,06	0,04	0,51	0,01	809
39	TG joven	8,31	13,4	38,5	46,3	16,2	34,9	32,2	17,5	2,19	4,77	5,14	0,27	4,61	0,06	0,15	0,03	0,01	1089
40	WT adulto	10,1	13,4	42,9	42,4	13,3	31,4	30	12,7	2,22	4,95	4,93	0,51	4,18	0,1	0,13	0,01	0	1172
41	WT adulto	10,12	13,9	45,7	45,2	13,7	30,4	28,8	13,6	2,14	2,45	2,56	0,29	2,06	0,01	0,19	0,01	0	913
42	WT adulto	8,77	14,7	39,7	45,3	16,7	36,9	32,5	13,5	2,38	4,87	5,36	0,71	4,11	0,17	0,32	0,04	0,01	563
43	WT adulto	8,55	13,2	41,2	48,2	15,4	31,9	28,9	13,8	2,24	1,54	1,56	0,2	1,24	0,02	0,05	0,04	0	1258
44	WT adulto	9,61	13,7	41,8	43,5	14,3	32,9	30,1	14	2,27	1,46	1,29	0,15	1,06	0,02	0,05	0,01	0	1161
45	WT adulto	9,06	13,3	41,5	45,8	14,7	32	29,3	13,4	2,15	0,88	0,87	0,08	0,72	0,02	0,05	0	0	949
46	WT adulto	8,49	12,6	37,9	44,7	14,9	33,3	30,1	14	2,4	2,9	2,84	0,45	2,22	0,09	0,05	0,03	0	1410
47	WT adulto	9,21	14,4	41,5	45,1	15,6	34,6	30,5	13,8	2,39	1,49	1,41	0,22	1,1	0,02	0,04	0,02	0	1346
48	WT adulto	8,72	13,4	38,7	44,4	15,4	34,7	30,5	15,5	2,61	1,4	1,28	0,11	1,01	0,02	0,1	0,03	0	1049
49	WT adulto	8,66	14	39,2	45,3	16,1	35,6	31	13,6	2,31	1,8	1,55	0,25	1,26	0,01	0,03	0,01	0	1278
50	WT adulto	8,73	14,1	41,4	47,4	16,1	34	28,4	14,5	2,27	1,98	2,05	0,32	1,58	0,04	0,06	0,05	0	885

51	WT adulto	8,97	14,3	42	46,8	15,9	34	28,6	13,6	2,12	2,57	2,44	0,18	2,13	0,03	0,05	0,04	0	937
52	WT adulto	7,86	12,1	35,4	45	15,3	34,1	29,6	16,1	2,68	2,55	2,46	0,28	2	0,03	0,09	0,05	0,01	1555
53	WT adulto	8,57	13,9	37,8	44,2	16,2	36,7	34,2	14,8	2,35	4,44	4,47	0,53	3,45	0,13	0,27	0,07	0	1446
54	WT adulto	8,49	13,4	38,2	45	15,8	35,2	32,7	13,4	2,29	7,69	7,13	0,43	5,87	0,18	0,62	0,02	0,01	1208
55	WT adulto	8,83	14	41,4	46,8	15,8	33,8	31,3	14,5	2,82	4,87	4,16	1,36	1,71	0,11	0,9	0,06	0,01	983
56	WT adulto	8,54	13,6	37,5	43,9	15,9	36,2	35	14,4	2,67	7,73	7,99	0,36	6,93	0,11	0,52	0,06	0,01	1059
57	WT adulto	8,73	14,4	38,8	44,4	16,5	37,1	35	14,1	2,77	6,48	6,39	0,33	5,39	0,09	0,52	0,04	0,01	1010
58	WT adulto	8,84	13,2	38,5	43,5	15	34,4	30,1	14,7	3,03	3,85	3,96	0,24	3,52	0,03	0,13	0,02	0,01	995
59	WT joven	8,63	13,5	42,1	48,8	15,6	32	26,9	16,1	2,01	5,37	4,24	0,82	2,83	0,07	0,5	0,03	0	1886
60	WT joven	8,56	13,6	46,2	54	15,9	29,4	32,4	34,9	5,94	7,27	7,52	0,55	6,4	0,08	0,14	0,09	0,01	814
61	WT joven	8,7	12,6	40,1	46	14,5	31,5	30,1	16,1	1,87	8,23	8,78	0,77	7,33	0,18	0,39	0,11	0	1349
62	WT joven	8,49	12,4	39,7	46,8	14,6	31,2	30	17,4	1,96	5,39	5,75	0,58	4,7	0,15	0,16	0,15	0	578
63	WT joven	8,89	13	41,3	46,5	14,6	31,4	29,8	15,6	1,78	5,62	5,8	0,45	4,81	0,13	0,34	0,07	0,01	1092
64	WT joven	8,17	12,7	37,7	46,2	15,5	33,5	30,1	15,5	2,03	3,24	3,37	0,44	2,64	0,11	0,14	0,03	0,01	1231
65	WT joven	7,98	1,7	37,7	47,3	2,2	4,6	29,6	17,5	2,03	6,08	6,27	0,29	5,67	0,06	0,13	0,12	0	917
66	WT joven	8,82	13,8	42,3	47,9	15,7	32,7	29,1	15,4	1,94	3,91	3,79	0,43	2,93	0,04	0,33	0,05	0,01	1042
67	WT joven	8,49	13,5	41,6	49	16	32,5	28,8	15,4	1,98	5,33	5,52	0,26	4,9	0,04	0,27	0,05	0	940
68	WT joven	9,56	15	44,3	46,3	15,7	33,8	29,2	15,2	2,06	3,04	2,95	0,26	2,36	0,03	0,28	0,03	0	941
69	WT joven	8,79	12,8	39,1	44,5	14,5	32,6	29,7	15,4	2,06	3,94	4,16	0,31	3,68	0,06	0,1	0,01	0	999
70	WT joven	8,37	13,3	40,3	48,1	15,8	32,9	28,9	17,1	2,38	6,13	6,13	0,32	5,51	0,07	0,17	0,06	0,01	954
71	WT joven	8,73	14,7	40,7	46,6	16,9	36,2	31,9	16,7	2,24	7,55	7,97	0,38	7,24	0,14	0,13	0,08	0,01	1001
72	WT joven	9,4	14,4	42,8	45,6	15,3	33,6	29,9	15,9	2,29	5,44	5,14	0,29	4,39	0,05	0,36	0,05	0,01	670
73	WT joven	8,52	13,7	39,6	46,5	16,1	34,5	32,1	17,4	2,27	2,16	2,17	0,13	1,92	0,03	0,06	0,03	0	963
74	WT joven	9,04	13,8	41,1	45,5	15,3	33,6	29,8	16,8	2,25	8,38	8,17	0,6	7,1	0,15	0,25	0,05	0,01	1206
75	WT joven	8,03	13,6	38,6	48,1	16,9	35,2	32,5	17	2,13	1,77	1,8	0,31	1,31	0,02	0,12	0,03	0,01	1121
76	WT joven	8,64	12,8	41,5	48	14,9	31	29,5	17,8	2,08	5,9	6,18	0,47	5,26	0,08	0,21	0,14	0,01	1104
77	WT joven	8,2	13,8	39	47,6	16,9	35,4	33,7	17,8	2,36	3,36	3,52	0,2	3,15	0,04	0,1	0,02	0,01	1022

78	WT joven	8,96	13,8	41,2	46	15,4	33,4	29,3	16,5	2,07	2,42	2,44	0,13	2,16	0,04	0,1	0,01	0	848
79	WT joven	7,9	13,1	37,3	47,2	16,6	35,1	32,1	15,8	2,21	6,12	6,26	0,27	5,78	0,1	0,08	0,02	0,01	945
80	WT joven	1,78	2,4	7,8	44	13,7	31,1	31	18,4	2,11	0,51	0,65	0,02	0,6	0,01	0,02	0	0	93

***Shaded cells indicate values outside normal range.**

Annex 8. List of genes in canine chromosomes 6 and 13.

	CAN FAM 2		CAN FAM 3					
CFA	**txStart**	**txEnd**	**txStart**	**txEnd**	**ENSEMBL version**	**GENE NAME**	**NAME**	**DISEASES**
chr6			37409925	37538007	ENSCAFG00000019251	CREBBP	CREB binding protein	Rubinstein-Taybi syndrome (RTS) , acute myeloid leukemia
chr6			37544899	37598729	ENSCAFG00000019262	TRAP1	TNF receptor-associated protein 1	Hereditary multiple exostoses, lupus nephritis
chr6			40352963	40389489	ENSCAFG00000019696	**NPRL3**	**Nitrogen permease regulator-like 3**	Secondary hypertrophic osteoarthropathy, myoblastoma. Human CAPS (Cryopyrin-associated periodic syndromes) producing direct inflammasome mutations that results in IL-1β release
chr6	40691672	40707467	37647781	37667850	ENSCAFG00000019268	SLX4	SLX4 structure-specific endonuclease subunit	Fanconi anemia complementation group P (FANCP) a disorder affecting all bone marrow elements and resulting in anemia, leukopenia and thrombopenia. It is associated with cardiac, renal and limb malformations, dermal pigmentary changes, and a predisposition to the development of malignancies
chr6	40727926	40744894	37686505	37703190	ENSCAFG00000019271	NLRC3	NLR family, CARD domain containing 3	Wegener's granulomatosis (type of vasculitis, or inflammation of the blood vessels. this limits the flow of blood to important organs, causing damage. it can affect any organ, but it mainly affects the sinuses, nose, trachea (windpipe), lungs and kidneys. Symptoms can vary in nature and severity, and may include sinus pain; discolored or bloody fluid from the nose; nasal ulcers; constant runny nose (rhinorrhea); joint pain; weakness; tiredness; and/or skin lesions) Another disease is Crohn's disease
chr6	40750597	40786952	37709194	37745356	ENSCAFG00000019274	CLUAP1	Clusterin Associated Protein 11	Colon cancer, osteosarcoma, thyroiditis, neuronitis, polycystic kidney disease and osteosarcoma
chr6	40803198	40810547	37761603	37769060	ENSCAFG00000019277	NAA60	N(alpha)-acetyltransferase 60, NatF catalytic subunit	Malaria
chr6	40835532	40839329	37793337	37803293	ENSCAFG00000032690	ZNF597	Zinc Finger Protein 5971	Russell-Silver syndrome which is a growth disorder characterized by slow growth before and after birth (failure to thrive)
chr6	40863432	40869834	37817603	37828238	ENSCAFG00000028614	ZNF174	Zinc Finger Protein 174	Prostatitis, endotheliitis and leukemia

chr6	40886307	40887619	37844712	37845650	ENSCAFG00000019302	**OR2C1**	**Olfactory receptor, family 2, subfamily C, member 1**	**Familial mediterranean fever** and neuronitis
chr6	40984686	40990209	37942782	37948607	ENSCAFG00000019292	ZNF263	Zinc Finger Protein 263	Prostatitis
chr6	41012203	41025333	37970548	37983737	ENSCAFG00000024473.2	**MEFV**	**Mediterranean Fever**	Familial mediterranean fever, serositis, hereditary periodic fever syndromes, muckle-wells syndrome, cold hypersensitivity, tumor necrosis factor receptor-associated periodic syndrome, renal amyloidosis, cinca syndrome, amyloidosis, brucellosis , psoriatic juvenile idiopathic arthritis , behcet's disease, idiopathic recurrent pericarditis, Intermittent hydrarthrosis, polyarteritis nodosa, erysipelas
chr6	41030049	41042812	37988373	38004294	ENSCAFG00000031888	**ZNF200**	**Zinc finger protein 200**	**Familial mediterranean fever**,Fanconi's anemia and prostatitis
chr6	41106459	41108818	38063599	38073992	ENSCAFG00000030711	**CASP16**	**Caspase 16, apoptosis-related cysteine peptidase**	**Familial mediterranean fever**
chr6	41113151	41133840	38085231	38093675	ENSCAFG00000023869	**ZNF205**	**Zinc finger protein 205**	**Familial mediterranean fever,** intrahepatic cholangiocarcinoma ,cholangiocarcinoma, ataxia
chr6	41153109	41156970	38111525	38115352	ENSCAFG00000019283	ZSCAN10	Zinc finger and SCAN domain containing 10	Neuronitis and neuroblastoma
chr6	41171697	41181080	38130092	38139965	ENSCAFG00000019309	MMP25	Matrix metallopeptidase 25	Weill-marchesani syndrome, encephalomyelitis, arthritis, cleft lip/palate, amelogenesis imperfecta,dentinogenesis imperfecta, cleft lip, dentin dysplasia, multiple sclerosis
chr6	41203080	41205788	38161582	38164186	ENSCAFG00000019317	THOC6	THO complex 6 homolog (Drosophila)	Kaposi's sarcoma sarcoma breast cancer
chr6	41208321	41209735	38166719	38168133	ENSCAFG00000023134	TNFRSF12A	Canis lupus familiaris tumor necrosis factor receptor superfamily, member 12A	Skeletal muscle regeneration, psoriatic arthritis, rheumatoid arthritis, multiple sclerosis , lupus nephritis kaposi's sarcoma, nephritis renal cell carcinoma, Multiple myeloma, prostate cancer, colon adenocarcinoma hepatitis b prostate cancer, atherosclerosis myeloma sarcoma hepatocellular carcinoma gingivitis ovarian cancer
chr6	41212209	41231698	38170607	38190010	ENSCAFG00000019337	CLDN6	Claudin 6	Hepatitis C, atypical teratoid, esophagitis ,hepatitis, rhabdoid tumors, esophageal squamous cell carcinoma, embryonal carcinoma, gastric adenocarcinoma, breast cancer, ovarian cancer, gastric cancer

chr6	41214151	41214805	38172549	38173203	ENSCAFG00000024263	CLDN9	Claudin 9	Hepatitis C, endolymphatic hydrops, hepatitis , gastric adenocarcinoma, gastric cancer adenocarcinoma, prostatitis
chr6	41248032	41252015	38206344	38210327	ENSCAFG00000019338	PKMYT1	Protein kinase, membrane associated tyrosine/threonine 1	Kaposi's sarcoma, skin cancer, sarcoma, melanoma
chr6	41253003	41255270	38211315	38213582	ENSCAFG00000019340	PAQR4	Progestin And AdipoQ Receptor Family Member IV	Malaria
chr6	41256911	41259987	38215223	38218299	ENSCAFG00000019341	KREMEN2	Kringle containing transmembrane protein 2	Myeloma
chr6	41337261	41351746	38295503	38309988	ENSCAFG00000019346	SRRM2	Serine/Arginine Repetitive Matrix 2	Acute myeloid leukemia, myeloid leukemia, parkinson's disease, leukemia, malaria
chr6	41352894	41356266	38311136	38314508	ENSCAFG00000019351	TCEB2	Transcription elongation factor B (SIII), polypeptide 2	Von hippel-lindau disease, renal clear cell carcinoma, hemangioma, *kidney disease,* parkinson's disease, pheochromocytoma, hepatocellular carcinoma, cervical cancer
chr6	41395062	41396678	38353438	38355054	ENSCAFG00000019354	ZG16B	Zymogen Granule Protein 16B	Adenocarcinoma, pancreatitis, Pancreatic ductal adenocarcinoma, ataxia
chr6	41412367	41415866	38370743	38374242	ENSCAFG00000023636	PRSS22	Protease, serine, 22	Psoriasis, thyroiditis, prostatitis
chr6	41435940	41441585	38394316	38399961	ENSCAFG00000019353	PRSS27	Protease, Serine 27	Peptic ulcer , cholecystitis, pancreatitis , psoriasis, carcinoma
chr6	41445953	41468159	38404329	38426544	ENSCAFG00000019357	KCTD5	Potassium Channel Tetramerisation Domain Containing	Rectal neoplasm, pterygium constipation
chr6	41561147	41566340	38519869	38525062	ENSCAFG00000019363	ATP6V0C	ATPase, H+ transporting, lysosomal 16kDa	Osteopetrosis, polycystic kidney disease, *rheumatoid arthritis,* cholera, twinning neurodegeneration , *arthritis* breast cancer, pneumonia, tuberculosis, malaria.
chr6	41577521	41582901	38536068	38541448	ENSCAFG00000019365	TBC1D24	novel gene TBC1 Domain Family, Member 24	Familial infantile myoclonic epilepsy, febrile convulsions, focal epilepsy, malaria, neuronitis
chr6	41600396	41602775	38558944	38561323	ENSCAFG00000019366	NTN3	Netrin 3	Tuberous sclerosis type 2 , mantle cell lymphoma, polycystic kidney disease, chronic lymphocytic leukemia, lymphocytic leukemia, neuronitis
chr6	41615699	41633262	38574247	38591810	ENSCAFG00000019372	CCNF	Cyclin F	Necrotizing fasciitis , polycystic kidney disease , lung adenocarcinoma , breast cancer, pancreatitis

chr6	41722897	41753512	38681454	38712112	ENSCAFG00000019379	ABCA3	ATP-Binding Cassette, Sub-Family A (ABC1), Member 3	pulmonary surfactant metabolism dysfunction, congenital ichthyosiform erythroderma , Pulmonary alveolar proteinosis, surfactant deficiency, b-cell lymphomas, interstitial lung disease, tangier disease, acute myeloid leukemia respiratory failure, myeloid leukemia, ichthyosis, pulmonary fibrosi, thyroid carcinoma, pharyngitis thyroiditis , leukemia, breast cancer , pneumonia
chr6	41761215	41962862	38719815	38921763	ENSCAFG00000019397	RNPS1	RNA Binding Protein S1, Serine-Rich Domain	Open-angle glaucoma , tuberous sclerosis, acinar cell carcinoma , *systemic lupus erythematosus* polycystic kidney diseasE, ataxia
chr6	41771559	41779591	38730159	38738200	ENSCAFG00000030058	ECI1	Enoyl-CoA Delta Isomerase 1	Tuberculosis, hepatitic C virus, mycobacterium tuberculosis
chr6	41784736	41793794	38743345	38752403	ENSCAFG00000019388	E4F1	E4F Transcription Factor 1	Type 2 tuberous sclerosis, polycystic kidney disease, hepatitis B
chr6	41797227	41798910	38755836	38757519	ENSCAFG00000019401	PGP	Phosphoglycolate Phosphatase	Tardive dyskinesia, polycystic kidney disease, acute myeloid leukemia, myeloid leukemia, pneumonia, tuberculosis malaria, mycobacterium tuberculosis
chr6	41803412	41806297	38762021	38764906	ENSCAFG00000019407	MLST8	MTOR Associated Protein, LST8 Homolog (S. Cerevisiae)	Human t-cell leukemia virus type 1 , tuberous sclerosis, embryonal carcinoma, alzheimer's disease, colon cancer neuroblastoma, retinitis, pancreatitis, hepatitis, neuronitis
chr6	41829835	41839559	38788453	38798177	ENSCAFG00000019418	TRAF7	TNF Receptor-Associated Factor 7, E3 Ubiquitin Protein Ligase	Familial cylindromatosis
chr6	41848951	41853761	38807569	38812379	RAB26	RAB26	ensembl: uncharacterized protein RAB26, Member RAS Oncogene Family	polycystic kidney disease, transitional cell carcinoma , neuronitis
chr6	41940525	41945811	38899143	38904429	ENSCAFG00000019439	NTHL1	Nth Endonuclease III-Like 1 (E. Coli)	Graft versus host disease, sclerosing cholangitis, chronic lymphocytic leukemia, colorectal cancer, tuberculosis malaria
chr6	41947149	41956182	38905767	38915074	ENSCAFG00000019449	SLC9A3R2	Na(+)/H(+) exchange regulatory cofactor NHERF2; Uncharacterized protein	

chr6	41990582	41992340	38949483	38951241	ENSCAFG00000019461	GFER	Growth Factor, Augmenter Of Liver Regeneration	Polycystic kidney disease, hepatitis, nodular regenerative hyperplasia, congenital cataracts, cataract myopathy viral hepatitis, liver cirrhosis, hepatoblastoma, hepatocellular carcinoma, t-cell leukemia, twinning leukemia, neuroblastoma, tuberculosis, carcinoma, malaria, mycobacterium tuberculosis
chr6	41997326	42003297	38956227	38962198		TBL3	Transducin (Beta)-Like 3	polycystic kidney disease kidney disease thyroiditis malaria
chr6	42009840	42012268	38968900	38971099	ENSCAFG00000019476.3	NDUFB10	NADH Dehydrogenase (Ubiquinone) 1 Beta Subcomplex, 10, 22kDa	huntington's disease parkinson's disease
chr6	42043017	42043626	39001861	39002470	ENSCAFG00000024261	*HS3ST6*	Heparan Sulfate (Glucosamine) 3-O-Sulfotransferase 6	*Sly syndrome* and *morquio syndrome b*
chr6	42125683	42146748	39084527	39105592	ENSCAFG00000019490	**HAGH**	**Hydroxyacylglutathione Hydrolase**	Glyoxalase ii deficiency , **familial mediterranean fever,** muscular dystrophy, thrombocytosis, bladder carcinoma, hepatitis b, hyperglycemia,, prostate cancer, breast cancer, hepatitis , prostatitis
chr6	42157963	42159808	39116807	39118652	ENSCAFG00000019493	IGFALS	Insulin-Like Growth Factor Binding Protein, Acid Labile Subunit	Precocious puberty, testicular germ cell tumor, acromegaly, breast cancer , pulmonary disease, prostate cancer atherosclerosis, prostatitis
chr6	42160490	42162593	39119334	39121437	ENSCAFG00000019494	NUBP2	Nucleotide Binding Protein 2	Pulmonary disease , tuberculosis, malaria, mycobacterium tuberculosis
chr6	42163989	42168199	39122833	39127052	ENSCAFG00000019495	SPSB3	SplA/Ryanodine Receptor Domain And SOCS Box Containing 3	Scabies, brucellosis, obesity
chr6	42172986	42173783	39131839	39132636	ENSCAFG00000019497	NME3	NME/NM23 Nucleoside Diphosphate Kinase 3	Squamous cell carcinoma, ataxia , neuroblastoma, tuberculosis, malaria , mycobacterium tuberculosis
chr6	42175236	42221867	39134089	39180729	ENSCAFG00000019513	MAPK8IP3	Mitogen-Activated Protein Kinase 8 Interacting Protein 3	fibrous histiocytoma, neuronitis.
chr6	42226790	42243028	39185652	39201890	ENSCAFG00000019540	HN1L	Hematological And Neurological Expressed 1-Like	Cramps, squamous cell carcinoma, lung cancer , prostatitis
chr6	42246900	42280111	39205762	39238973	ENSCAFG00000014270	CRAMP1L	Crm, Cramped-Like (Drosophila)	cramps
chr6	42316501	42330840	39275372	39289711	ENSCAFG00000019547	TMEM204	uncharacterized protein	Peritonitis hypoxia

chr6	42350545	42360411	39309416	39319282	ENSCAFG00000019549	TELO2	TEL2, Telomere Maintenance 2, Homolog (S. Cerevisiae)	macular degeneration fanconi's anemia anemia ataxia
chr6	42372298	42396246	39331169	39355117	ENSCAFG00000019565	CLCN7	Chloride Channel, Voltage-Sensitive 7	Osteopetrosis ,lysosomal storage disease, bartter disease, dent disease, optic atrophy, nephrocalcinosis nephrolithiasis, neurodegeneration, osteoporosis, neuronitis
chr6	42446932	42459781	39405808	39418657	ENSCAFG00000019583	GNPTG	N-Acetylglucosamine-1-Phosphate Transferase, Gamma Subunit	Mucolipidosis iiic , mucolipidosis iii gamma, mucolipidosis ii , short stature, dysostosis , scoliosis, parkinson's disease ovarian carcinoma, retinitis, carcinoma
chr6	42463239	42471893	39422124	39430778	ENSCAFG00000019589	BAIAP3	BAI1-Associated Protein 3	Desmoplastic small round cell tumor
chr6	42650140	42653130	39609034	39612024	ENSCAFG00000019600	SSTR5	Somatostatin Receptor 5	Resistance to growth hormone, secreting pituitary adenoma, oncogenic osteomalacia, glucagonoma , anorexia nervosa, prolactinoma, fetal adenoma, pancreatic endocrine tumors, pituitary tumor , acromegaly atopic dermatiti, insulinoma, carcinoid tumors, cushing's syndrome
chr6	42710336	42713740	39669234	39672638	ENSCAFG00000019601	SOX8	SRY (Sex Determining Region Y)-Box 8	Testicular germ cell tumor, campomelic dysplasia, germ cell tumor, alpha thalassemia, myoblastoma , retinitis
chr6	42723354	42803813	39682252	39762711	ENSCAFG00000019603	LMF1	Lipase Maturation Factor 1	Lipase deficiency combined, familial hypertriglyceridemia, lipodystrophy hepatoblastoma, tuberculosis, hepatitis malaria, mycobacterium tuberculosis
chr6	42869147	42871206	39828088	39830147	ENSCAFG00000019616	MSLN	Mesothelin	Squamous cell carcinoma , Ovarian cancer , malignant biphasic mesothelioma, bile duct adenoma, gastrointestinal stromal tumor, renal clear cell carcinoma , epithelioid sarcoma , benign mesothelioma, pancreatic ductal adenocarcinoma, asbestosis, thymic carcinoma , acute myeloid leukemia, myeloid leukemia , thoracic cancer pancreatitis
chr6	42887929	42894351	39846870	39853292	ENSCAFG00000019618	NARFL	nuclear prelamin A recognition factor-like	Acute closed-angle glaucoma , scrapie, pertussis hypoxia
chr6	42895038	42897442	39853979	39856383	ENSCAFG00000019606	HAGHL	Hydroxyacylglutathione Hydrolase-Like	Hepatitis B
chr6	42898864	42902380	39857805	39861321	ENSCAFG00000019621	CCDC78	Coiled-Coil Domain Containing 78	Hepatitis B

chr6	42934548	42936125	39893489	39895066	ENSCAFG00000031099	STUB1	STIP1 homology and U-box containing protein 1, E3 ubiquitin protein ligase	Colon cancer, multiple endocrine neoplasia, amyotrophic lateral sclerosis, lateral sclerosis, tauopathy, lafora disease, chronic lymphocytic leukemia, neurodegenerative disease, chronic myeloid leukemia, intrahepatic cholangiocarcinoma, cystic fibrosis, prostate cancer
chr6	42941946	42946909	39900887	39905850	ENSCAFG00000019647	RHOT2	Ras Homolog Family Member T2	Hypoxia
chr6	42947466	42962048	39906407	39920989	ENSCAFG00000019654	WDR90	WD Repeat Domain 90	Malaria
chr6	42975229	42977465	39934170	39936406	ENSCAFG00000019660	WFIKKN1	WAP, Follistatin/Kazal, Immunoglobulin, Kunitz And Netrin Domain Containing	Pancreatitis
chr6	43063055	43085404	40021996	40044291	ENSCAFG00000019670	RAB11FIP3	RAB11 family interacting protein 3 (class II)	Large cell medulloblastoma, breast cancer, thyroiditis
chr6	43152456	43156955	40111214	40115713	ENSCAFG00000019675	DECR2	2,4-Dienoyl CoA Reductase 2, Peroxisomal	Tuberculosis
chr6	43179688	43186846	40137824	40144954	ENSCAFG00000019680	TMEM8A	Transmembrane Protein 8	Tonsilitis
chr6	43187961	43189915	40146070	40148024	ENSCAFG00000019682	MRPL28	Mitochondrial Ribosomal Protein L28	Melanoma, placental abruption, non-hodgkin lymphoma, hodgkin's lymphoma, hepatitis b, inflammatory bowel disease, acute lymphoblastic leukemia, hepatitis c,, acute myeloid leukemia , bronchitis , rheumatoid arthritis influenza , esophageal carcinoma, hepatocellular carcinoma, esophagitis
chr6	43200533	43260469	40158325	40217747	ENSCAFG00000019684	AXIN1	Axin 1	Hepatocellular carcinoma, hepatoblastoma, adenocarcinoma, familial adenomatous polyposis , somatic adenoid cystic carcinoma, oral squamous cell carcinoma, cerebellar medulloblastoma, merkel cell carcinoma , basal cell carcinoma, embryonal sarcoma, medulloblastoma, pituitary adenoma, adenoiditis, Wilms tumor
chr6	43261385	43264649	40218663	40221797	ENSCAFG00000015429	PDIA2	Protein Disulfide Isomerase Family A, Member 2	Pancreatitis, diphtheria, neurodegenerative disease, insulin resistance, brain ischemia, hyperglycemia , hypoxia immunodeficiency, Cardiomyopathy, adenocarcinoma , neuronitis
chr6	43269587	43277256	40225981	40233303	ENSCAFG00000023874	RGS11	Regulator Of G-Protein Signaling 11	Night blindness, retinoschisis, squamous cell carcinoma, pharyngitis, esophagitis, adenocarcinoma .

chr6	43318146	43353718	40274401	40309875	ENSCAFG00000019689	LUC7L	LUC7-Like (S. Cerevisiae)	Hhuntington's disease malaria
chr6			40326459	40329857	ENSCAFG00000029904	HBA	Hemoglobin subunit alpha	Alpha-thalassemia, Heinz body anemias.
chr6			40330683	40332438	ENSCAFG00000029224	HBM	Hemoglobin, mu	Hyperostosis corticalis and *diffuse cutaneous mastocytosis.*
chr6			40352963	40389489	ENSCAFG00000019696	NPRL3	Nitrogen permease regulator-like 3	Secondary hypertrophic osteoarthropathy, myoblastoma.
chr6			40389096	40394808	ENSCAFG00000019700	MPG	N-methylpurine-DNA glycosylase	Lutembacher's syndrome and tricuspid valve stenosis.
chr6	43478169	43481373	40417065	40420269	ENSCAFG00000019715	POLR3K	polymerase (RNA) III (DNA directed) polypeptide K, 12.3 kDa	DNA topoisomerase , *systemic lupus erythematosus,* Sjogren's syndrome, hepatitis b, *scleroderma,* hepatocellular carcinoma , microphthalmia , retinoblastoma, carcinoma, immunodeficiency, malaria, neuronitis
chr6			40613728	40625949	ENSCAFG00000019738	ATP5F1	ATP synthase, H+ transporting, mitochondrial Fo complex, subunit B1	Myeloid leukemia, huntington's disease, parkinson's disease, hermaphroditism, colon cancer, leukemia, prostatitis, neuronitis
chr6	43815305	43826991	40754909	40766595	ENSCAFG00000019759	CHIA	Chitinase, Acidic	Churg-strauss syndrome, asthma , Gaucher's disease, multiple sclerosis, eosinophilia, *uveitis,* conjunctivitis
chr6	43882301	43896338	40821986	40836023	ENSCAFG00000019764	DENND2D	DENN/MADD domain containing 2D	lung squamous cell carcinoma and squamous cell carcinoma
chr6	44084104	44100162	41023786	41039844	ENSCAFG00000019770	LRIF1	Ligand Dependent Nuclear Receptor Interacting Factor 1	huntington's disease
chr6	44131233	44149634	41070933	41089334	ENSCAFG00000019772	CD53	CD53 Molecule	Phagocyte bactericidal dysfunction , immunodeficiency, eczema, *rheumatoid arthritis,* Hepatitis b ,*arthritis,* melanoma
chr6	44403897	44405202	41343606	41344911	ENSCAFG00000023296	KCNA3	potassium voltage-gated channel, shaker-related subfamily, member 3	Breast adenocarcinoma, autoimmune pancreatitis
chr6	44555784	44557391	41495647	41497254	ENSCAFG00000019778	KCNA10	Potassium voltage-gated channel, shaker-related subfamily, member 10	Long qt syndrome, breast and colorectal cancer
chr6	44606301	44611021	41546164	41550884	ENSCAFG00000019786	PROK1	Prokineticin 1	Osteonecrosis, endometritis.
chr6	44666896	44700447	41606768	41640319	ENSCAFG00000019788	SLC16A4	Solute carrier family 16, member 4	embryonal rhabdomyosarcoma, rhabdomyosarcoma

chr6	44706951	44713170	41646823	41653042	ENSCAFG00000019789	RBM15	RNA binding motif protein 15	pancreatic cystadenoma, megakaryocytic leukemia
chr6	44837039	44866500	41776844	41806332	ENSCAFG00000019791	SLC6A17	Solute carrier family 6 (neutral amino acid transporter), member 17	malaria, cerebritis
chr6	44958717	44967186	41898582	41906963	ENSCAFG00000019795	ALX3	Proline-Rich Transcription Factor ALX3	frontonasal dysplasia 1, and basal encephalocele
chr6	44973808	44990593	41913585	41930370	ENSCAFG00000019793	FAM40A	striatin interacting protein 1	cerebral cavernous malformations 3, and cavernous malformation
chr6	45007287	45020769	41947425	41960907	ENSCAFG00000019796	AHCYL1	Adenosylhomocysteinase-like 1	xeroderma pigmentosum, and tonsillitis
chr6	45094023	45105247	42034161	42045409	ENSCAFG00000019798	CSF1	Colony stimulating factor 1 (macrophage)	acute non lymphoblastic leukemia, and sharp syndrome
chr6	45224263	45235916	42164425	42176078	ENSCAFG00000019805	EPS8L3	EPS8-like 3	hypotrichosis, hereditary, marie unna type, 1, and hypotrichosis
chr6	45248276	45251112	42188438	42191274	ENSCAFG00000019809	GSTM3	Glutathione S-transferase mu 3 (brain)	bronchogenic carcinoma, and oral cancer
chr6	45300129	45310193	42240529	42250593	ENSCAFG00000019815	AMPD2	Adenosine monophosphate deaminase 2	pontocerebellar hypoplasia type 9 major depressive disorder tonsillitis aterosclerosis hepatocellular carcinoma hiv-1 malaria cerebritis
chr6	45319301	45327682	42259701	42268082	ENSCAFG00000019823	GNAT2	Guanine nucleotide binding protein (G protein), alpha transducing activity polypeptide 2	pertussis, retinoblastoma, retinal degeneration, blindness, huntington's disease, retinitis, multiple myeloma
chr6	45411070	45412664	42351959	42353553	ENSCAFG00000019827	AMIGO1	Adhesion molecule with Ig-like domain 1	pthirus pubis infestation, kidney disease, cerebritis, neuronitis
chr6	45422866	45424591	42363755	42365480	ENSCAFG00000019828	CYB561D1	Cytochrome b561 family, member D1	kidney disease, obesity
chr6	45427221	45435077	42368110	42375966	ENSCAFG00000019829	ATXN7L2	Ataxin 7-like 2	kidney disease, ataxia
chr6	45439254	45445030	42380143	42385919	ENSCAFG00000019831	SYPL2	Synaptophysin-like 2	kidney disease, tetanus
chr6	45484825	45509186	42425714	42450075	ENSCAFG00000019833	PSMA5	Proteasome (prosome, macropain) subunit, alpha type, 5	wolfram syndrome lactic acidosis fanconi's anemia down syndrome, huntington's disease kidney disease
chr6	45535448	45575999	42476346	42516897	ENSCAFG00000019835	SORT1	Sortilin 1	geniculate ganglionitis, and cerebral artery occlusion
chr6	45600916	45603225	42541795	42544104	ENSCAFG00000019839	PSRC1	Proline/serine-rich coiled-coil 1	gigantism, and hypertriglyceridemia

chr6	45608406	45632528	42549285	42573407	ENSCAFG00000019841	CELSR2	Cadherin, EGF LAG seven-pass G-type receptor 2	Pulmonary embolism strabismus protein s deficiency coronary heart disease
chr6	45643913	45664235	42584792	42605114	ENSCAFG00000019847	SARS	Seryl-tRNA synthetase	hyperuricemia, pulmonary hypertension, renal failure, lkalosis, hyperuricemia, appendicitis, *contact dermatitiS,* tonsillitis thyroiditis cerebritis
chr6	45672879	45706270	42613758	42647149	ENSCAFG00000019851	KIAA1324	KIAA1324	endometrial carcinoma intrahepatic cholangiocarcinoma cholangiocarcinoma breast and colorectal cancer
chr6	45810851	45858186	42751867	42799202	ENSCAFG00000019867	WDR47	WD Repeat-Containing Protein 47	lissencephaly neuronitis tonsillitis thyroiditis
chr6	45866455	45886716	42807471	42827732	ENSCAFG00000019871	CLCC1	Chloride channel CLIC-like 1	nephrocalcinosis tonsillitis retinitis thyroiditis
chr6	45889643	45927422	42830659	42868438	ENSCAFG00000019880	GPSM2	G-protein signaling modulator 2	Hydrocephalus malaria hodgkin's lymphoma hypertension pancreatic cancer pancreatitis breast cancer multiple myeloma
chr6	46007169	46057144	42948235	42998210	ENSCAFG00000019913	STXBP3	Syntaxin binding protein 3	polycystic ovary syndrome insulin resistance obesity pancreatitis endotheliitis neuronitis
chr6	46106452	46113487	43045517	43052552	ENSCAFG00000029761	PRPF38B	Pre-mRNA processing factor 38B	sarcoma colon adenocarcinoma adenocarcinoma malaria
chr6	46501468	46536045	43440462	43475039	ENSCAFG00000019940	SLC25A24	Solute carrier family 25 (mitochondrial carrier; phosphate carrier), member 24	blindness graves' disease thyroiditis
chr6	46857489	47061401	43796483	44000395	ENSCAFG00000019951	VAV3	Vav 3 guanine nucleotide exchange factor	primary angle-closure glaucoma osteopetrosis primary open angle glaucoma open-angle glaucoma anaplastic large cell lymphoma glaucoma b-cell chronic lymphocytic leukemia chronic lymphocytic leukemia hypothyroidism prostate cancer spasticity prostatitis pancreatic cancer pancreatitis leukemia endotheliitis breast cancer neuronitis
chr6	47460554	47476230	44397257	44412933	ENSCAFG00000019958	NTNG1	netrin G1	epileptic encephalopathy, early infantile, 2 atypical rett syndrome rett syndrome systemic lupus erythematosus endotheliitis neuronitis
chr6	47540329	47541457	44477032	44478160	ENSCAFG00000023098	PRMT6	Protein arginine methyltransferase 6	glycogen storage disease ii wolff-parkinson-white syndrome glycogen storage disease

chr6	50072549	50098045	47018744	47044240	ENSCAFG00000019972	RNPC3	RNA-binding region (RNP1, RRM) containing 3	mixed connective tissue disease rubella connective tissue disease crimean-congo hemorrhagic fever, rift valley fever rheumatic disease hemorrhagic fever *collagen disease*
chr6	50501419	50674308	47447672	47620611	ENSCAFG00000019985	COL11A1	Collagen, type XI, alpha 1	stickler syndrome, type iv snowflake vitreoretinal degeneration wagner syndrome dihydropyrimidine dehydrogenase deficiency pierre robin sequence macroglossia multiple epiphyseal dysplasia primary angle-closure glaucoma spinal stenosis chorioretinitis
chr13	5987517	5993814	2969982	2976279	ENSCAFG00000000584	ZNF706	Zinc finger protein 706	laryngeal squamous cell carcinoma
chr13	6387104	6404305	3369569	3386770	ENSCAFG00000030111	NCALD	Neurocalcin delta	diabetic nephropathy neuronitis retinitis cervicitis pancreatitis endotheliitis
chr13	6818666	6857203	3799130	3837667	ENSCAFG00000000602	RRM2B	Ribonucleotide reductase M2 B	mitochondrial dna depletion syndrome 1 ophthalmoplegia axonal neuropathy colon adenocarcinoma lactic acidosis hypotonia hypogonadism esophageal squamous cell carcinoma oral cancer transitional cell carcinoma
chr13	6914599	7000390	3895063	3980859	ENSCAFG00000000619	UBR5	Ubiquitin protein ligase E3 component n-recognin 5	mantle cell lymphoma brain cancer colon adenocarcinoma *dermatitis* adenocarcinoma ovarian cancer hiv-1 breast cancer malaria
chr13	7156317	7165616	4137256	4146555	ENSCAFG00000030644	ODF1	Outer dense fiber of sperm tails 1	epididymitis infertility
chr13	7237028	7242522	4218083	4223577	ENSCAFG00000000638	KLF10	Kruppel-like factor 10	inferior myocardial infarction frasier syndrome goldenhar syndrome denys-drash síndrome brain cancer pallister-hall síndrome borjeson-forssman-lehmann syndrome nephroblastoma pancreatic cancer hemoglobinopathy renal clear cell carcinoma pancreatitis osteosarcoma osteoporosis hypertrophic cardiomyopathymyocardial infarction periodontitis lymphoblastic leukemia type 1 diabetes aterosclerosis
chr13	23348772	23364912	20311698	20327838	ENSCAFG00000029394	**HAS2**	**Hyaluronan synthase 2**	**Periodic Fever Syndrome** lipoblastoma arthropathy rheumatoid arthritis osteosarcoma morquio syndrome arthritis sly syndrome eye disease mucopolysaccharidoses osteoarthritis prostate adenocarcinoma fibrosarcoma hyperglycemia multiple myeloma *atopic dermatitis* diabetic

								nephropathy peritonitis endometrial carcinoma atherosclerosis
chr13	24413969	24416486	21377315	21379832	ENSCAFG00000000967	ZHX2	Zinc fingers and homeoboxes 2	usher syndrome smallpox neurofibromatosis thalassemia nephrotic syndrome pertussis hodgkin's lymphoma ataxia neuroblastoma prostate cancer prostatitis
chr13	24462062	24488975	21425408	21452321	ENSCAFG00000000974	DERL1	Derlin 1	neuronal ceroid lipofuscinosis hemangioma cholera epididymitis lateral sclerosis amyotrophic lateral sclerosis tonsillitis neuronitis endotheliitis adenocarcinoma thyroiditis malaria lung cancer hepatitis
chr13	24602924	24626533	21566379	21589976	ENSCAFG00000000997	FAM83A	Family with sequence similarity 83, member A	prostatitis lung cancer breast cancer
chr13	24704384	24769491	21667832	21732939	ENSCAFG00000000992	ATAD2	ATPase family, AAA domain containing 2	cholangiocarcinoma osteosarcoma lung adenocarcinoma prostate cancer breast cancer
chr13	24778808	24795471	21742256	21758919	ENSCAFG00000001004	WDYHV1	WDYHV motif containing 1	Ataxia, malaria
chr13	24846286	24874667	21809734	21838115	ENSCAFG00000001007	FBXO32	F-box protein 32	hyperthyroidism lynch syndrome inclusion body myositis myopathy myositis muscular atrophy muscular dystrophy lateral sclerosis amyotrophic lateral sclerosis sepsis cystic fibrosis kidney disease
chr13	25077140	25113296	22040589	22076745	ENSCAFG00000001027	FAM91A1	Family with sequence similarity 91, member A1	pancreatic cancer pancreatitis malaria
chr13	25580588	25582095	22544046	22545553	ENSCAFG00000001040	TRMT12	TRNA methyltransferase 12 homolog	noma, breast cancer
chr13	25596545	25608850	22560003	22572308	ENSCAFG00000029985	RNF139	Ring finger protein 139 [	familial renal cell carcinoma clear cell renal cell carcinoma collecting duct carcinoma thyroid cancer chromophobe renal cell carcinoma papillary renal cell carcinoma dysgerminoma thyroiditis encephalitis malaria multiple myeloma myeloma
chr13	25609780	25645778	22573238	22609236	ENSCAFG00000001044	TATDN1	TatD DNase domain containing 1	pheochromocytoma pneumonia malaria

chr13	25671781	25808705	22635239	22772163		MTSS1	metastasis suppressor 1	wiskott-aldrich syndrome kidney cancer huntington's disease hepatocellular carcinoma squamous cell carcinoma prostate cancer prostatitis colorectal cancer breast cancer endotheliitis neuronitis
chr13	26019412	26020798	22982879	22984265	ENSCAFG00000030125	ZNF572	Zinc finger protein 572	breast and colorectal cancer
chr13	26031070	26054661	22994537	23018128	ENSCAFG00000001056	SQLE	Squalene epoxidase	lung squamous cell carcinoma hypercholesterolemia
chr13	26056311	26109274	23019778	23072741	ENSCAFG00000001070	KIAA0196	KIAA0196	optic atrophy ulcerative colitis cervicitis prostate cancer prostatitis multiple myeloma
chr13	26376524	26382740	23338080	23344316	ENSCAFG00000001077	TRIB1	Tribbles pseudokinase 1	ischemic heart disease megakaryocytic leukemia familial hypercholesterolemia crohn's disease hypercholesterolemia hypertriglyceridemia coronary heart disease coronary artery disease acute leukemia inflammatory bowel disease thyroiditis obesity